X-622-67-500

NASA TM X-55974

AN ATLAS OF TOTAL OUTGOING LONG-WAVE RADIATION AND OF SHORT-WAVE REFLECTANCES FROM NIMBUS II OBSERVATIONS

MUSA PASTERNAK

OCTOBER 1967

GODDARD SPACE FLIGHT CENTER
GREENBELT, MARYLAND

X-622-67-500

AN ATLAS OF TOTAL OUTGOING LONG-WAVE RADIATION AND OF SHORT-WAVE REFLECTANCES FROM NIMBUS II OBSERVATIONS

Musa Pasternak

October 1967

GODDARD SPACE FLIGHT CENTER
Greenbelt, Maryland

AN ATLAS OF TOTAL OUTGOING LONG-WAVE

RADIATION AND OF SHORT-WAVE REFLECTANCES

FROM NIMBUS II OBSERVATIONS

Musa Pasternak

ABSTRACT

An atlas of total outgoing long-wave radiation and of short-wave reflectances derived from measurements of the Nimbus II Medium Resolution (Infrared) Radiometer (MRIR) during its lifetime from 15 May to 27 July 1966 is presented. The outgoing long-wave radiation has been derived from measurements of the 5-30 micron channel whereas the short-wave reflectances have been derived from measurements of the 0.2-4.0 micron channel. Weekly averages of the data over the entire globe are presented in mapped form, utilizing Mercator and polar stereographic projections.

CONTENTS

ILLUSTRATIONS

AN ATLAS OF TOTAL OUTGOING LONG-WAVE RADIATION AND OF SHORT-WAVE REFLECTANCES FROM NIMBUS II OBSERVATIONS

INTRODUCTION

Nimbus II, launched on 15 May 1966, was equipped with a Medium Resolution Radiometer. This radiometer, which received data from launch until 27 July 1966, contained a 5-30 μ channel which measured the outgoing long-wave radiation and a 0.2-4.0 μ channel which measured the reflected solar radiation. Weekly averages of the long-wave flux and of the reflectance from the measurements of these two channels were displayed on Mercator and polar stereographic maps. The purpose of this atlas is to make available the data in this form generally to workers in the field. It is hoped that they may find these data useful, either for correlative purposes or in their own right, in studies of large-scale meteorological phenomena such as the radiation balance, cloud cover, and the general circulation.

NIMBUS II MRIR EXPERIMENT

The Nimbus II satellite moved in a nearly circular orbit with an inclination of 100.311 degrees at a mean height of 1140 km. Because the orbit was nearly sun-synchronous, the ascending nodes of all orbits occurred at 32 minutes before noon local mean solar time during the lifetime of the MRIR. The satellite saw the sunlit portion of the earth when it was northbound and the nighttime portion when it was southbound. The acquisition of data from all of the orbits would give daily global coverage. However, data were not acquired from all orbits and no data were received from any orbit in the vicinity of a Data Acquisition Facility. Two Data Acquisition Facilities existed, one at Fairbanks, Alaska and the other at Rosman, North Carolina.

Each channel of the MRIR measured the electromagnetic radiation emitted or reflected from the earth and its atmosphere in a selected wavelength interval. These five wavelength regions were 6.4-6.9 μ, 10-11 μ, 14-16 μ, 5-30 μ, and 0.2-4.0 μ.

The radiometer essentially measured the effective radiance within an instantaneous field of view of about 2.8°. The effective radiance $\bar{N}$ to which the radiometer responds can be expressed by

$$\bar{N} = \int_0^\infty N_\lambda \phi_\lambda \, d\lambda \qquad (1)$$

where

N_λ is the spectral radiance in the direction of the satellite from the earth and its atmosphere

ϕ_λ is the effective spectral response of the instrument

λ is the wavelength.

For the four infrared channels, $\bar{N}$ can also be expressed by

$$\bar{N} = \int_0^\infty B_\lambda \left(T_{BB}\right) \phi_\lambda \, d\lambda \tag{2}$$

where

B_λ is the Planck radiance, a function of the equivalent temperature T_{BB} of a blackbody filling the field of view of the channel.

Thus from the above equations the radiometer measurements can be expressed in terms of $\bar{N}$ or T_{BB}. In the Nimbus Meteorological Radiation Tapes (NMRT's) the measurements of each of the four infrared channels are given in terms of the equivalent blackbody temperature T_{BB}. The measurements of the 0.2-4.0 μ channel are expressed directly in terms of the effective radiance $\bar{N}$.

A blackbody target whose temperature was telemetered from the satellite afforded an on-board calibration capability for the infrared channels. There was no comparable on-board calibration for the 0.2-4.0 μ channel, but its data did not show any significant deterioration during the orbital lifetime of the MRIR. More detailed information about the radiometer and its calibration is given in the Nimbus II Users Guide.[1]

This report is only concerned with data from the two radiometer channels which measure energy in the 5-30 μ and the 0.2-4.0 μ wavelength intervals. The 5-30 μ channel measured long-wave emission from which the total outgoing long-wave radiation could be inferred, and the 0.2-4.0 μ channel measured the radiance of reflected solar radiation from which reflectance values could be determined.

DATA CHARACTERISTICS AND CALCULATIONS

Calculation of the Total Outgoing Long-Wave Flux

The outgoing long-wave flux was calculated from the 5-30 μ equivalent blackbody temperatures using a method developed by Wark, Yamamoto, and Lienesch.[2] The equations used were[3]

$$\overline{W} = 2.137 \times 10^{-5} T_{BB}^3 - 2.794 \times 10^{-3} T_{BB}^2 - .2166 T_{BB} + 37.54 \tag{3}$$

$$F = 0.9233 \left\{ \left[0.0439 + 1.729 \times 10^{-3} \overline{W} + 1.038 \times 10^{-6} \overline{W}^2 + \theta^3 \left(1.36 \times 10^{-8} - 2.523 \times 10^{-10} \overline{W} + 1.164 \times 10^{-12} \overline{W}^2\right)\right] \Big/ \left[- 7.807 \times 10^{-9} \theta^4 + 6.149 \times 10^{-7} \theta^3 - 4.247 \times 10^{-5} \theta^2 + 1.933 \times 10^{-4} \theta + 1.0 \right] \right\} \tag{4}$$

where

$\overline{W} = \pi \overline{N}$ is the effective radiant emittance in watts/meter^2

T_{BB} is the equivalent blackbody temperature of the 5-30 μ channel in °K

F is the total outgoing long-wave flux in langleys/min.

θ is the zenith angle of the satellite measured from the instantaneous intersection of the radiometer optical axis with the earth's surface in degrees.

The flux-T_{BB} relationships for different zenith angles are shown in Figure 1. The global flux averages derived from measurements constrained by scan nadir angle limits of 0°-25° and 25°-45° were virtually identical, showing that these flux calculations adequately compensate for limb darkening.

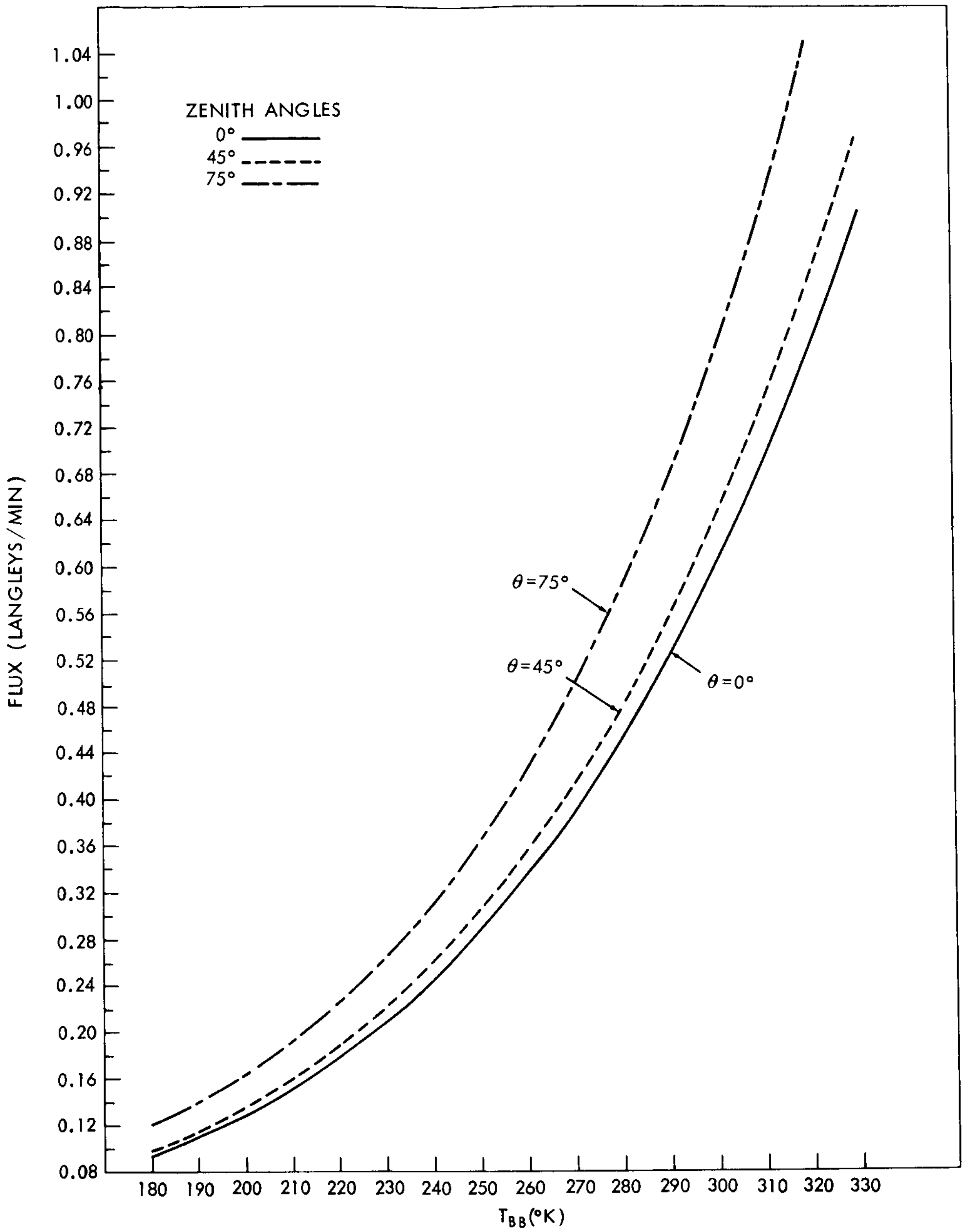

Figure 1. Total Outgoing Infrared Flux versus Equivalent Blackbody Temperature, Nimbus II Channel 4 (5-30 μ)

Calculation of the Short-Wave Reflectance

The reflectance was calculated from the measured effective radiance $\bar{N}$ by

$$R = \frac{\pi \bar{N} \, r_0^2}{\bar{H}^* \cos \zeta} \tag{5}$$

where

R is the reflectance

$\bar{N}$ is the measured effective radiance

ζ is the solar zenith angle

$\bar{H}^*$ is the effective solar irradiance at the "top" of the atmosphere

r_0 is the ratio of the actual earth-sun distance to the mean earth-sun distance

$$\bar{H}^* = \int_0^\infty H_\lambda^* \phi_\lambda \, d\lambda$$

where

H_λ^* is the spectral solar irradiance given by Johnson.[4]

The reflectance given by Equation (5) assumes that the solar radiation is reflected isotropically. It is known that the reflection of solar radiation by the earth-atmosphere system is actually anisotropic, especially under large solar zenith angle conditions, but at the time these data were processed an adequate model considering the anisotropy had not been developed. Subsequently such a model was developed and was used in a study of the global radiation balance by Raschke and Pasternak.[5]

MAPPING PROCEDURES

In order to present the data, two different map bases were used: (1) a polar stereographic map base extending from latitude 40° to the pole in each hemisphere, and (2) a Mercator map base extending from latitude 60°N to 60°S. Thus, there is overlapping coverage in the zones 40°-60° North and South between the two types of maps. The long-wave flux and short-wave reflectance data were gathered on a rectangular grid of equispaced points, each grid point being assigned the average value of all observations falling within its square of influence. The relationship of the polar stereographic projection to the rectangular array was such that longitude 80°W in either hemisphere lay over the middle column of grid points in the bottom half of the projection and latitude 60° was at a distance of 12.5 mesh intervals (i.e. the distance between adjacent grid points in a row or column) from the pole. The relationship of the Mercator projection to the rectangular array was such that each column of grid points was identified with a specific longitude and was 5° in longitude apart from adjacent columns. According to the rules governing the Mercator projection, then, the spacing between adjacent rows of grid points was about 5° of latitude at the Equator and about 2.5° of latitude at latitude 60°. The map scales in terms of the number of grid mesh intervals per unit distance on the earth were approximately the same for both types of maps at latitude 60°, and varied at other latitudes in accordance with the rules governing the two map projections. Representative numbers of individual measurements making up the initial grid point averages for the weekly long-wave maps were 200 to 1700, although for certain "limited data" regions there were few or no measurements at all. Corresponding numbers for the short-wave maps were about 50% as large.

Due to temporal discontinuities in the coverage, a 3 x 3 smoothing function was used to obtain new grid values through which the isolines were drawn. Each initial grid point average $R_{m,n}$ on row m and column n was replaced by a smoothed grid point average $A_{m,n}$ determined by

$$
\begin{aligned}
A_{m,n} = {} & \frac{1}{24} R_{m-1,n-1} + \frac{1}{12} R_{m-1,n} + \frac{1}{24} R_{m-1,n+1} \\
& + \frac{1}{12} R_{m,n-1} + \frac{1}{2} R_{m,n} + \frac{1}{12} R_{m,n+1} \\
& + \frac{1}{24} R_{m+1,n-1} + \frac{1}{12} R_{m+1,n} + \frac{1}{24} R_{m+1,n+1} \qquad (6)
\end{aligned}
$$

Isolines of long-wave flux having a contour interval of 0.03 ly $\min^{-1}$ and isolines of reflectance having a contour interval of 5% were used in analyzing the maps. The isolines were drawn by means of an electronic plotter. A "limited data" region was defined as one in which the initial grid point values were averages from less than 40 individual measurements, and no isolines were drawn in such a "limited data" region.

SEVEN-DAY MEAN MAPS

Long-wave and reflectance maps were constructed for each week of Nimbus II data covering the period 15 May — 27 July, 1966. All of the maps, except those for the final four-day period, 24-27 July, consisted of seven-day means of data. To eliminate space contamination and limb effects, the radiation maps used only measurements whose associated scan nadir angles were less than 45°. In addition, for greater accuracy the reflectance maps only used local daytime measurements whose associated solar zenith angles were less than 70°.

For each time period, a Mercator map and polar stereographic maps for both Northern and Southern Hemispheres depict the total outgoing long-wave radiation; a Mercator map and a polar stereographic map for only the Northern Hemisphere depict the short-wave reflectances. The solar declination minimum of 18.7° during the lifetime of the MRIR and the 70° solar zenith angle maximum eliminated all reflectance measurements south of latitude 51.3°S; hence, a polar stereographic map for the Southern Hemisphere was not required. In presenting the data for each period, corresponding long-wave and reflectance maps are displayed on facing pages. The fifth map then, showing long-wave radiation from the Southern Hemisphere on a polar stereographic map base, alternates between the first and last position in each period, depending upon whether the sequence begins on an odd or even numbered page respectively.

Data regions in which the initial grid point values were averaged from less than 40 measurements are indicated by shading on the maps. All of the reflectance maps have shaded regions south of 51.3°S due to the lack of reflectance data meeting the aforementioned criteria. Also the reflectance maps have data gaps extending from pole to pole and spanning some 30° in longitude, including Eastern Australia and Japan. These gaps resulted from the locations of the two Data Acquisition Facilities and from the design of the MRIR which employs a continuous-loop tape recorder making it impossible to store data for more than one orbit.[1]

ACKNOWLEDGMENTS

This project was conducted under the guidance and supervision of Mr. William Bandeen, Head of the Planetary Radiations Branch, Goddard Space Flight Center. The treatment of the vast amount of data was facilitated by Mr. Robert T. Hite, Head, and other members of the Branch Mathematics and Computing Section. In particular, I should like to thank Mr. Allen Simmons and Mr. Ray Sears for writing the mapping program and Mr. Paul Heil for preparing the maps.

REFERENCES

1. Nimbus Project, Nimbus II Users' Guide, Goddard Space Flight Center, Greenbelt, Md. 1966.

2. Wark, D. Q., Yamamoto, G., and Lienesch, J. H., "Methods of Estimating Infrared Flux and Surface Temperature from Meteorological Satellites," J. Atmos. Sci., 19, 369-384, 1962.

3. Lienesch, J. H., personal communication, July 1966.

4. Johnson, Frances, "Solar Radiation," in Satellite Environment Handbook, Stanford University Press, 1961.

5. Raschke, E., and Pasternak, M., "The Global Radiation Balance of the Earth-Atmosphere System Obtained from Radiation Data of the Meteorological Satellite Nimbus II," Document X-622-67-383, NASA Goddard Space Flight Center, August 1967.

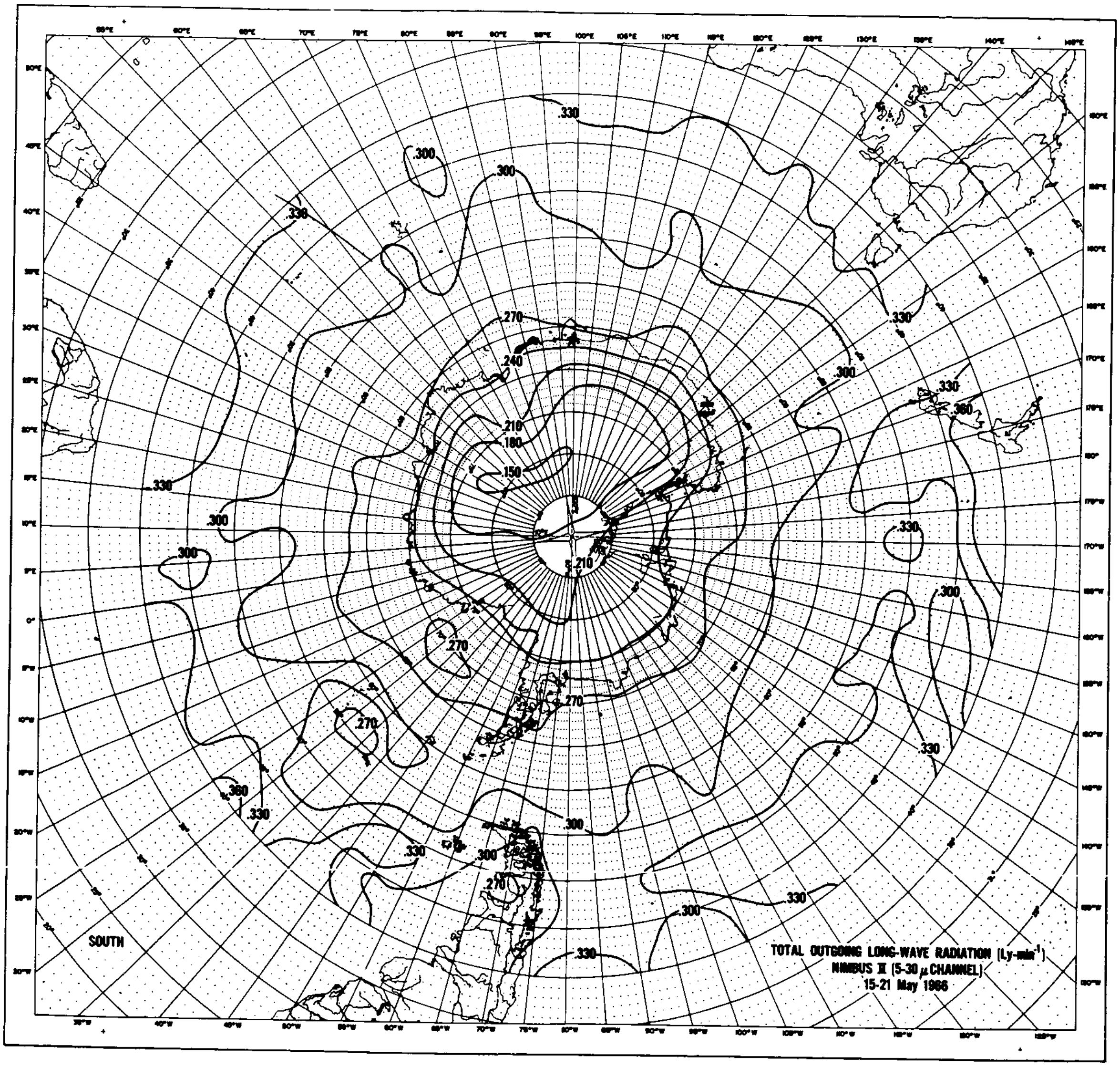

SOUTH
TOTAL OUTGOING LONG-WAVE RADIATION (Ly-min⁻¹)
NIMBUS II (5-30 μ CHANNEL)
15-21 May 1966

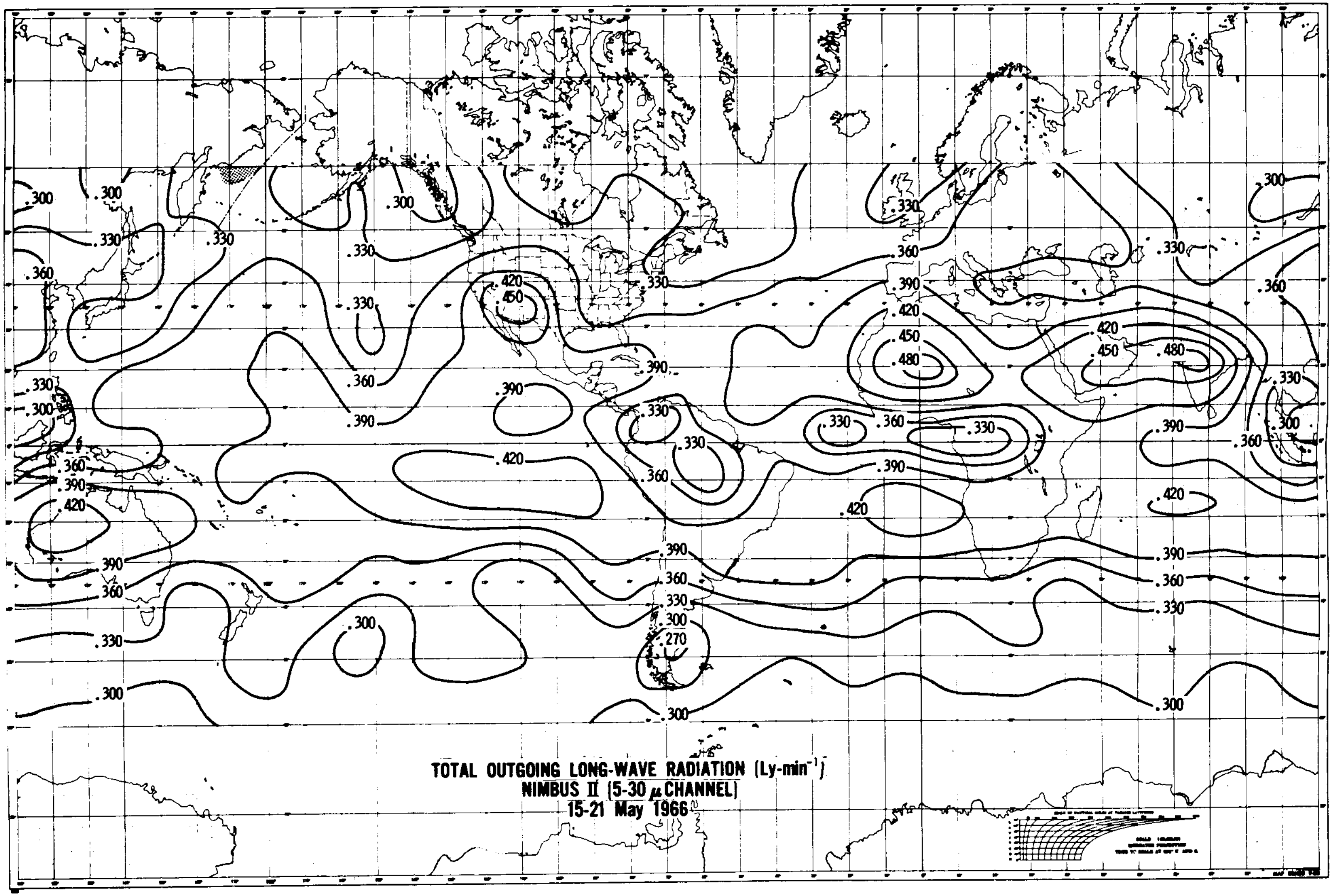

TOTAL OUTGOING LONG-WAVE RADIATION (Ly-min^{-1})
NIMBUS II (5-30 μ CHANNEL)
15-21 May 1966

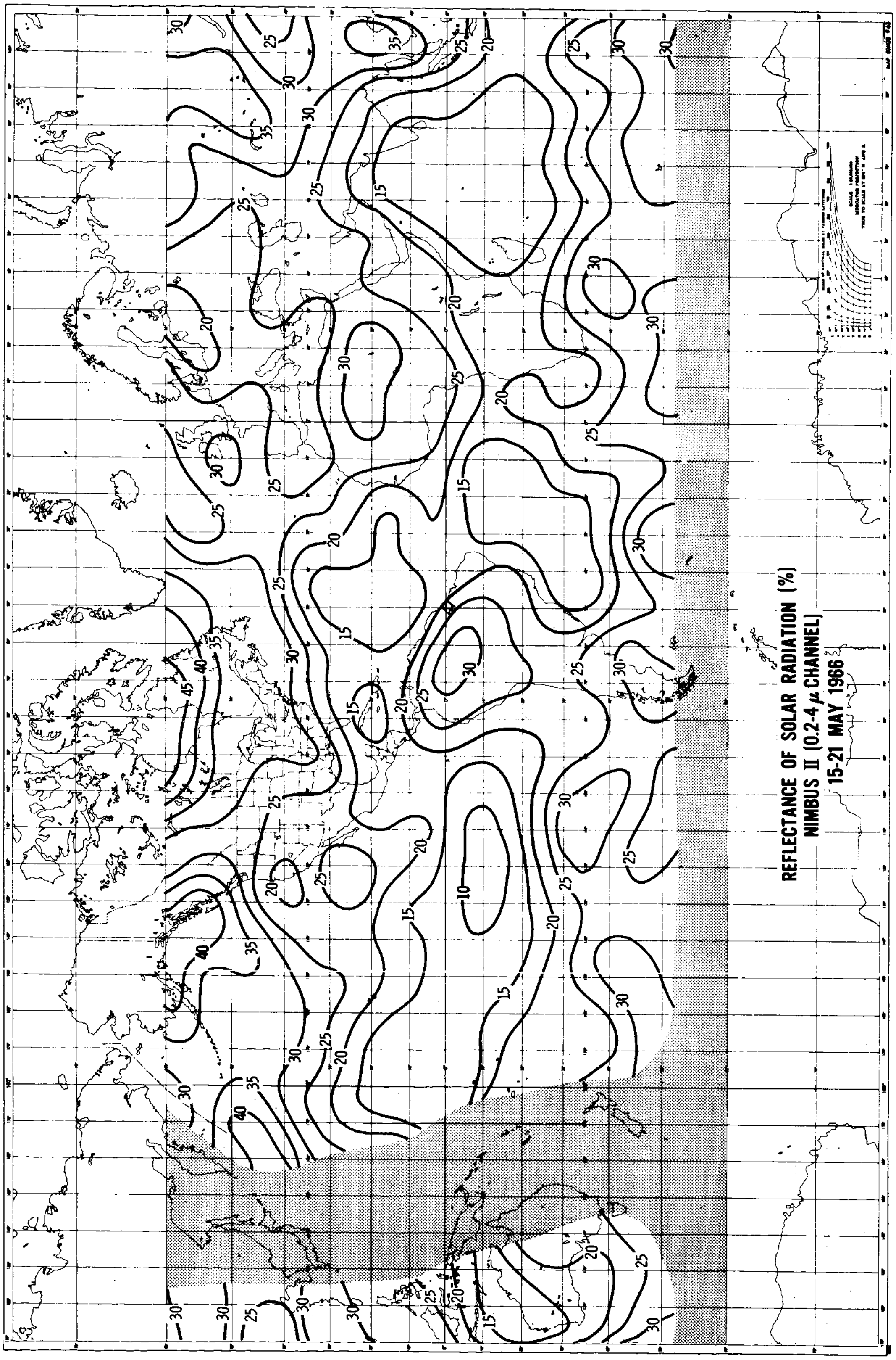

REFLECTANCE OF SOLAR RADIATION (%)
NIMBUS II (0.2-4 μ CHANNEL)
15-21 MAY 1966

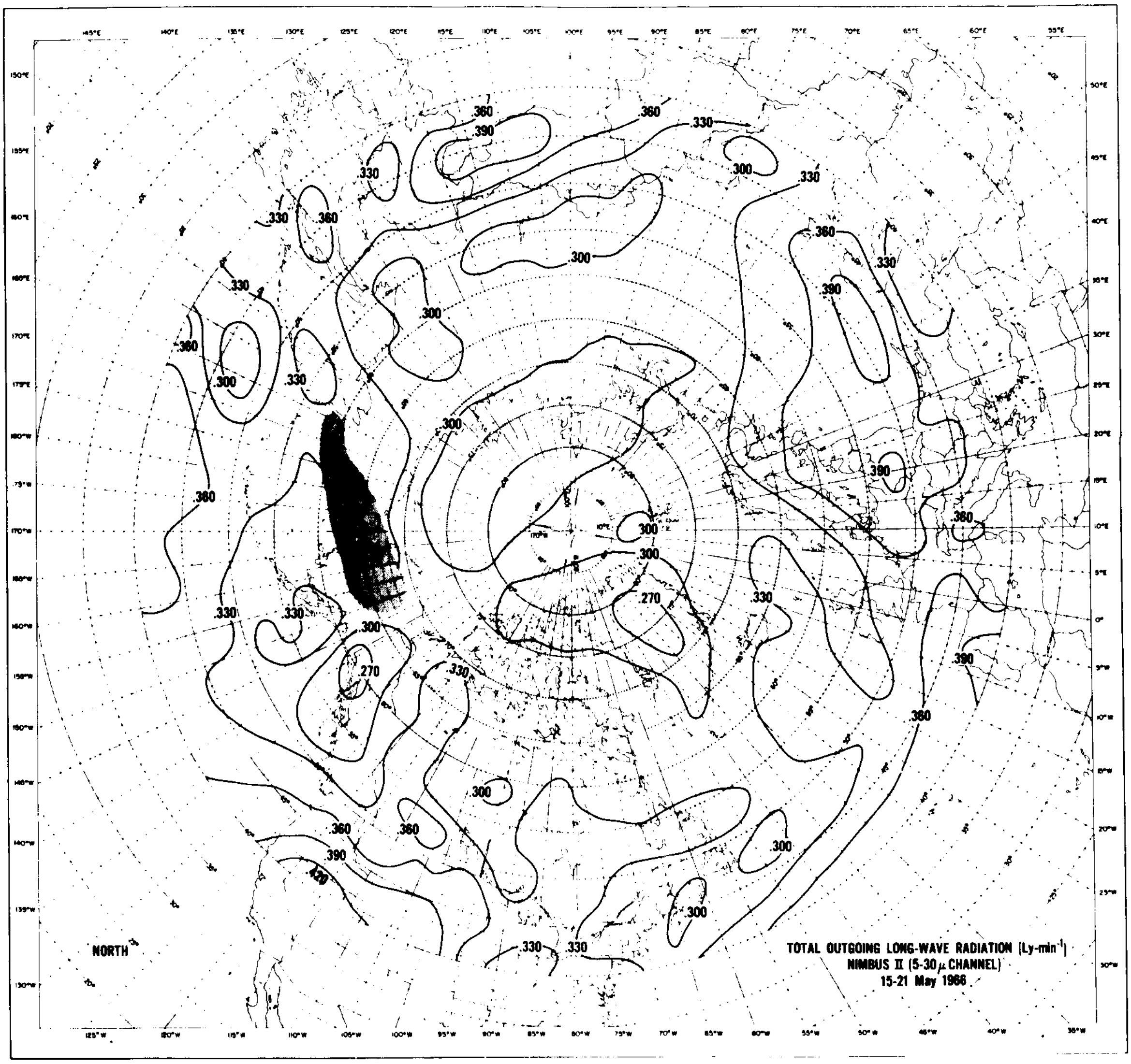
NORTH
TOTAL OUTGOING LONG-WAVE RADIATION (Ly-min^{-1})
NIMBUS II (5-30 μ CHANNEL)
15-21 May 1966
.270
.300
.330
.360
.390
.420

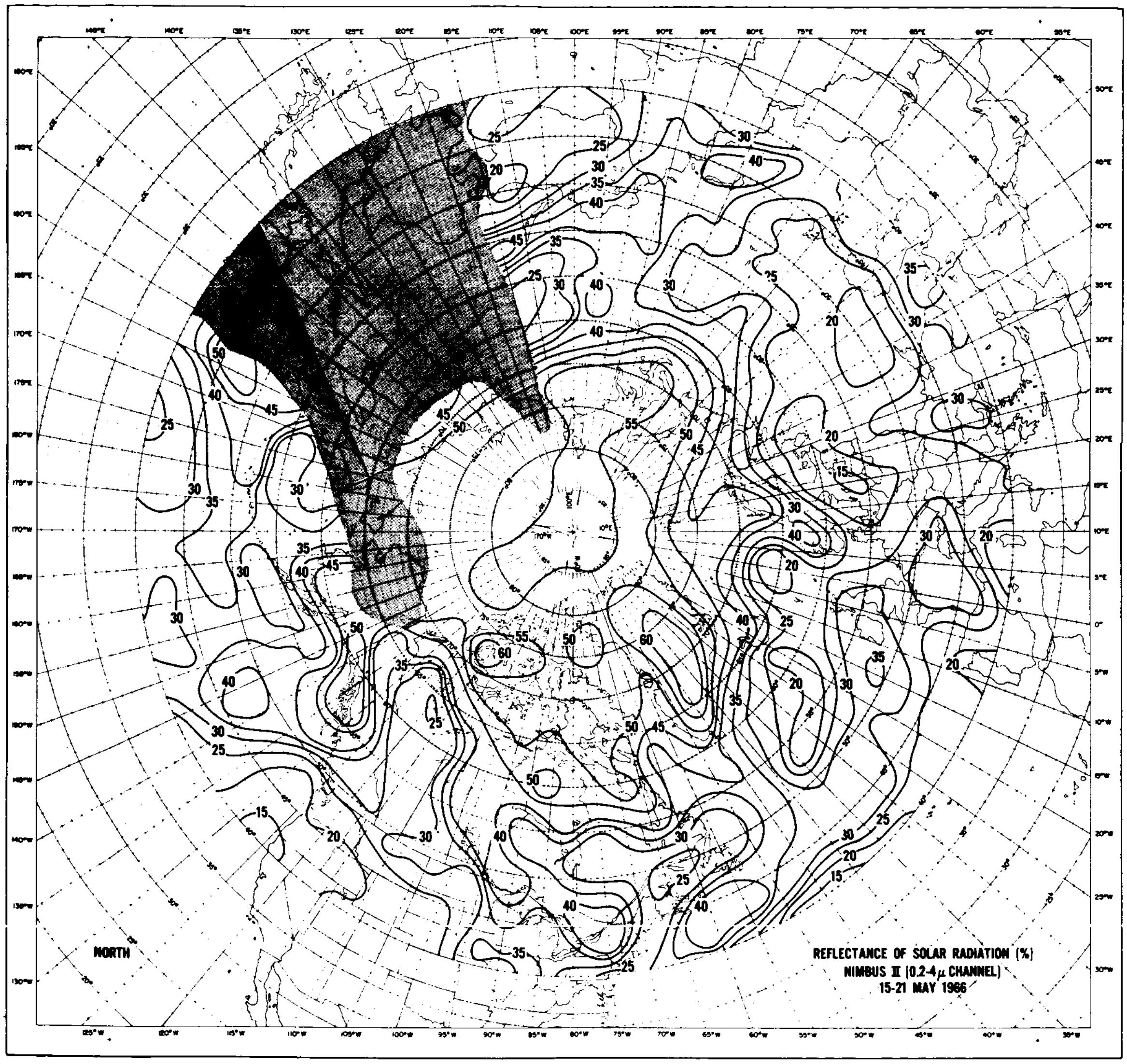
NORTH
REFLECTANCE OF SOLAR RADIATION (%)
NIMBUS II (0.2-4μ CHANNEL)
15-21 MAY 1966

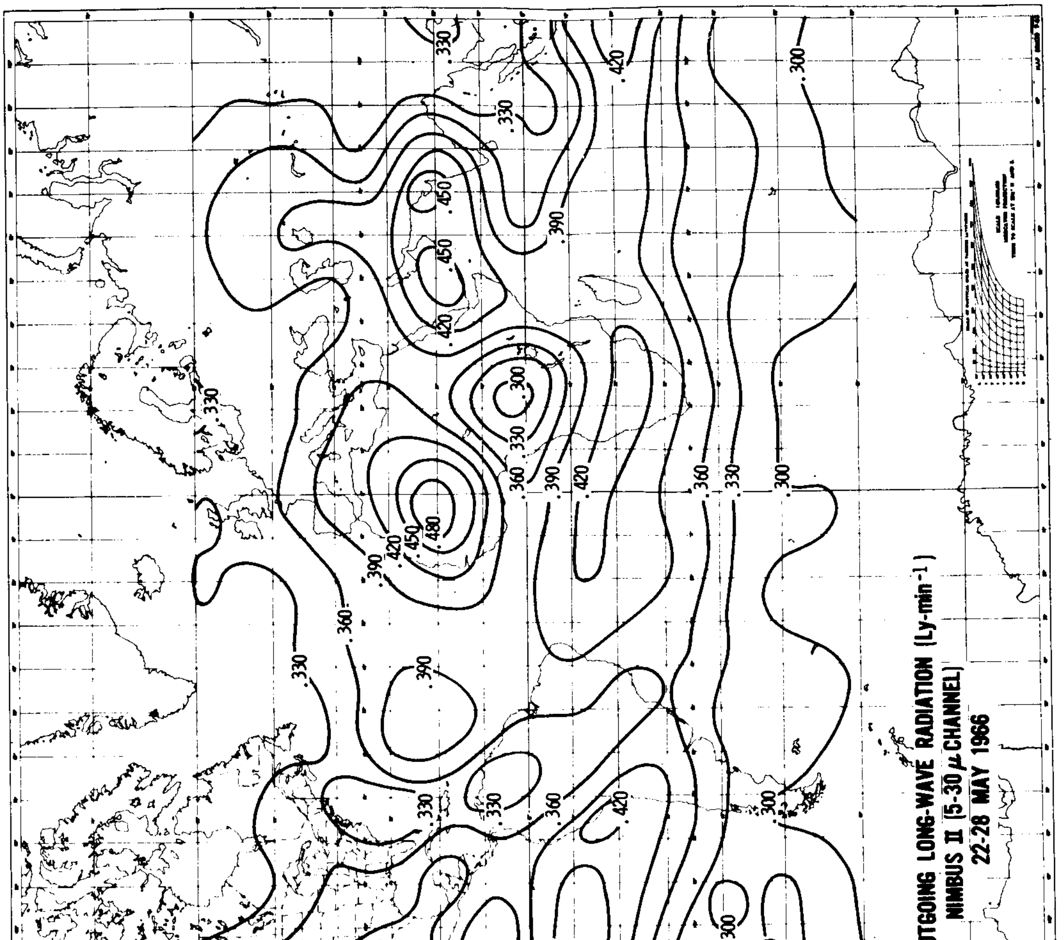

TOTAL OUTGOING LONG-WAVE RADIATION (Ly-min^{-1})
NIMBUS II (5-30 μ CHANNEL)
22-28 MAY 1966

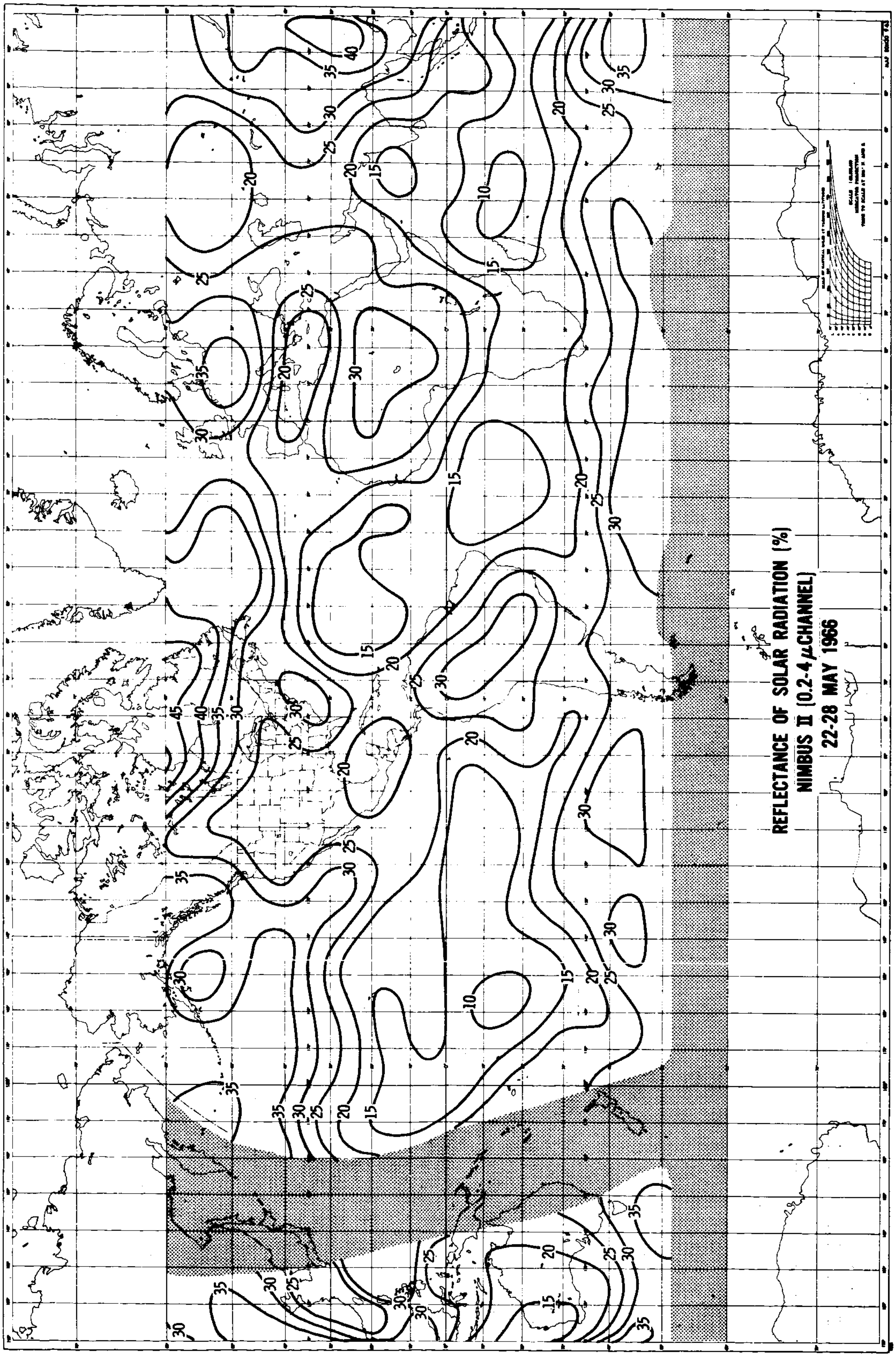
REFLECTANCE OF SOLAR RADIATION (%)
NIMBUS II (0.2-4 μ CHANNEL)
22-28 MAY 1966

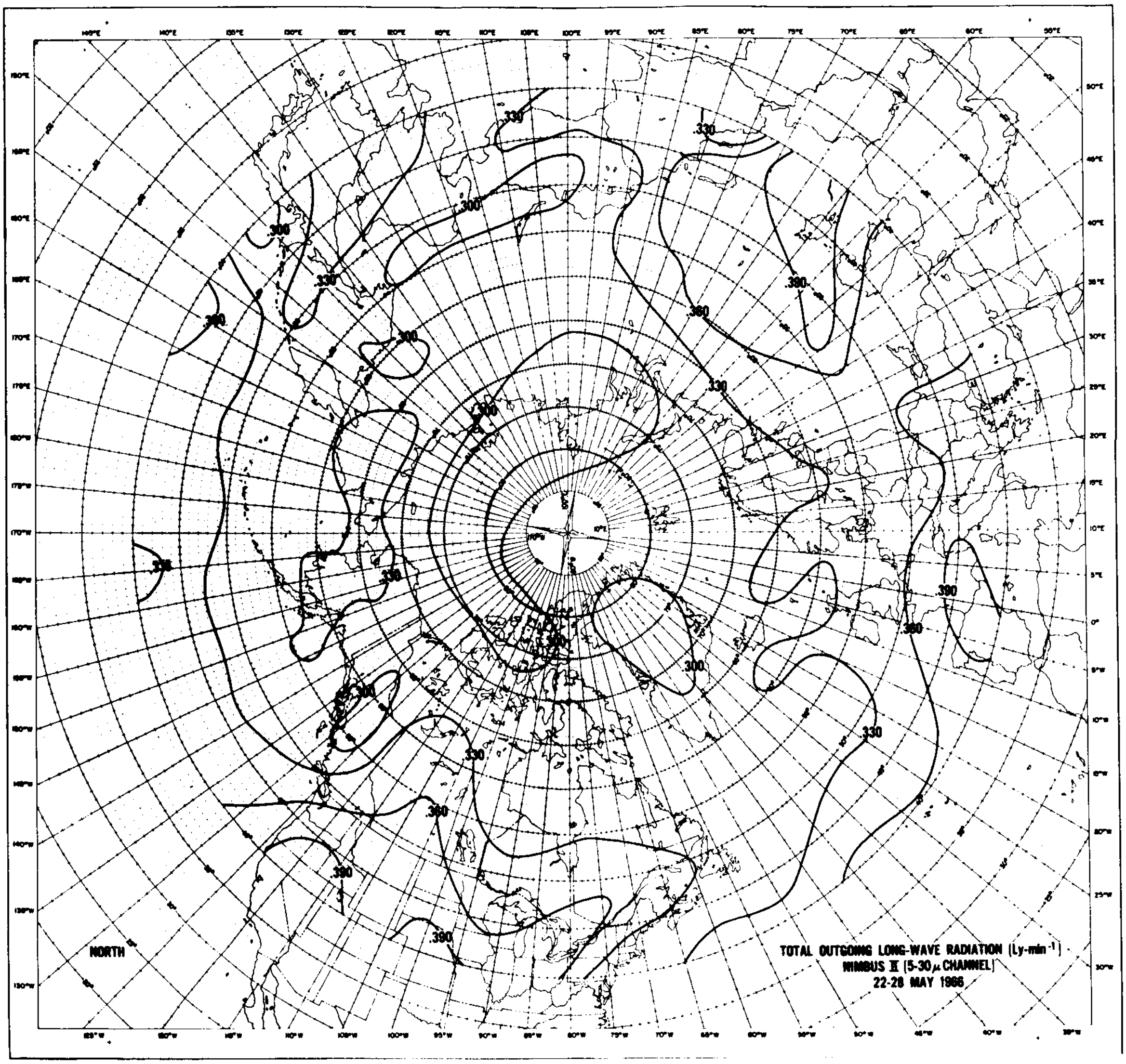

NORTH
TOTAL OUTGOING LONG-WAVE RADIATION (Ly-min⁻¹)
NIMBUS II (5-30μ CHANNEL)
22-28 MAY 1966
.300
.330
.360
.390

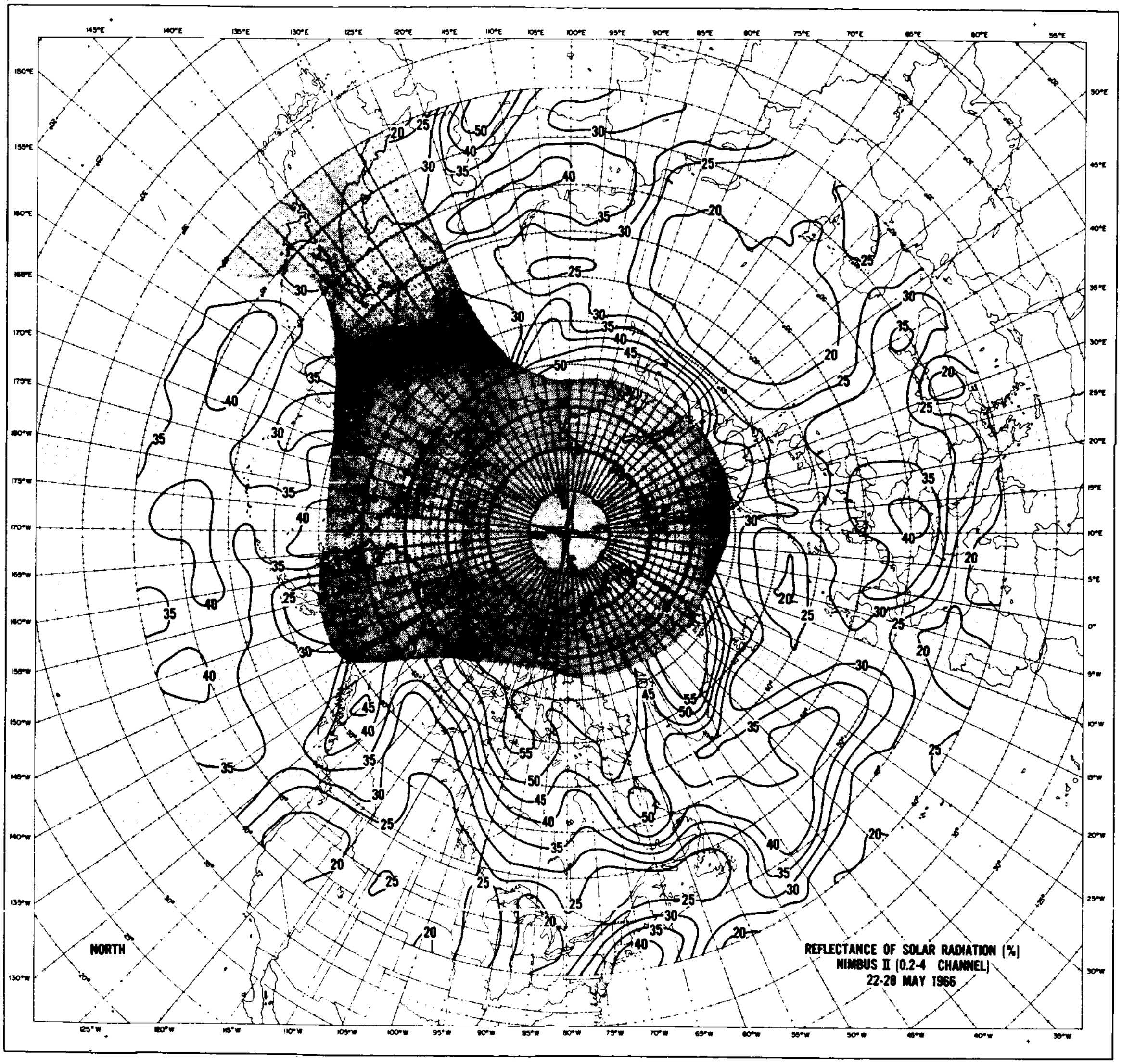
NORTH
REFLECTANCE OF SOLAR RADIATION (%)
NIMBUS II (0.2-4 CHANNEL)
22-28 MAY 1966

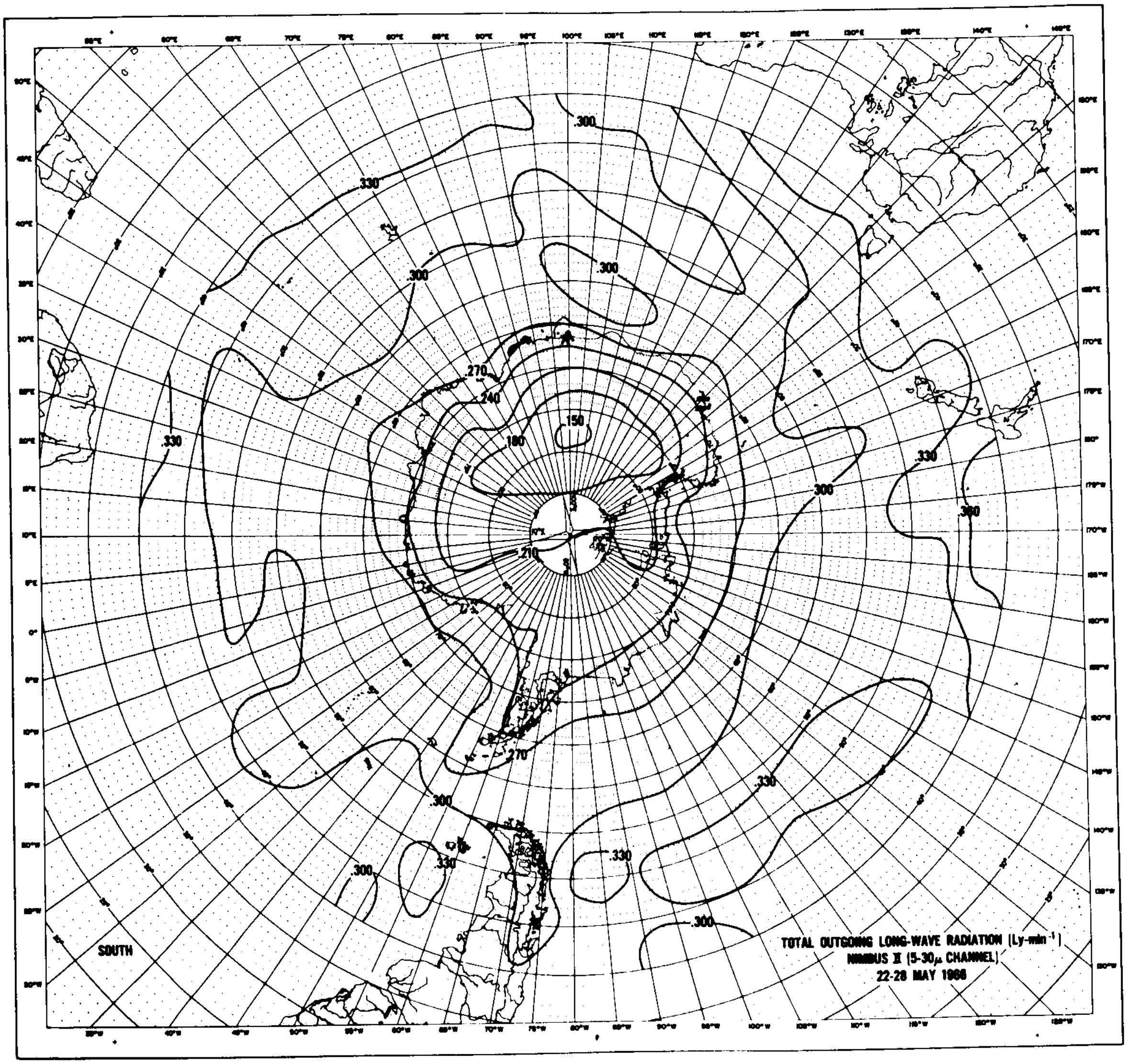

.300
.330
.300
.300
.270
.240
.150
.180
.210
.330
.330
.300
.380
.270
.300
.330
.300
.330
.330
.300
SOUTH
TOTAL OUTGOING LONG-WAVE RADIATION (Ly-min⁻¹)
NIMBUS II (5-30μ CHANNEL)
22-28 MAY 1966

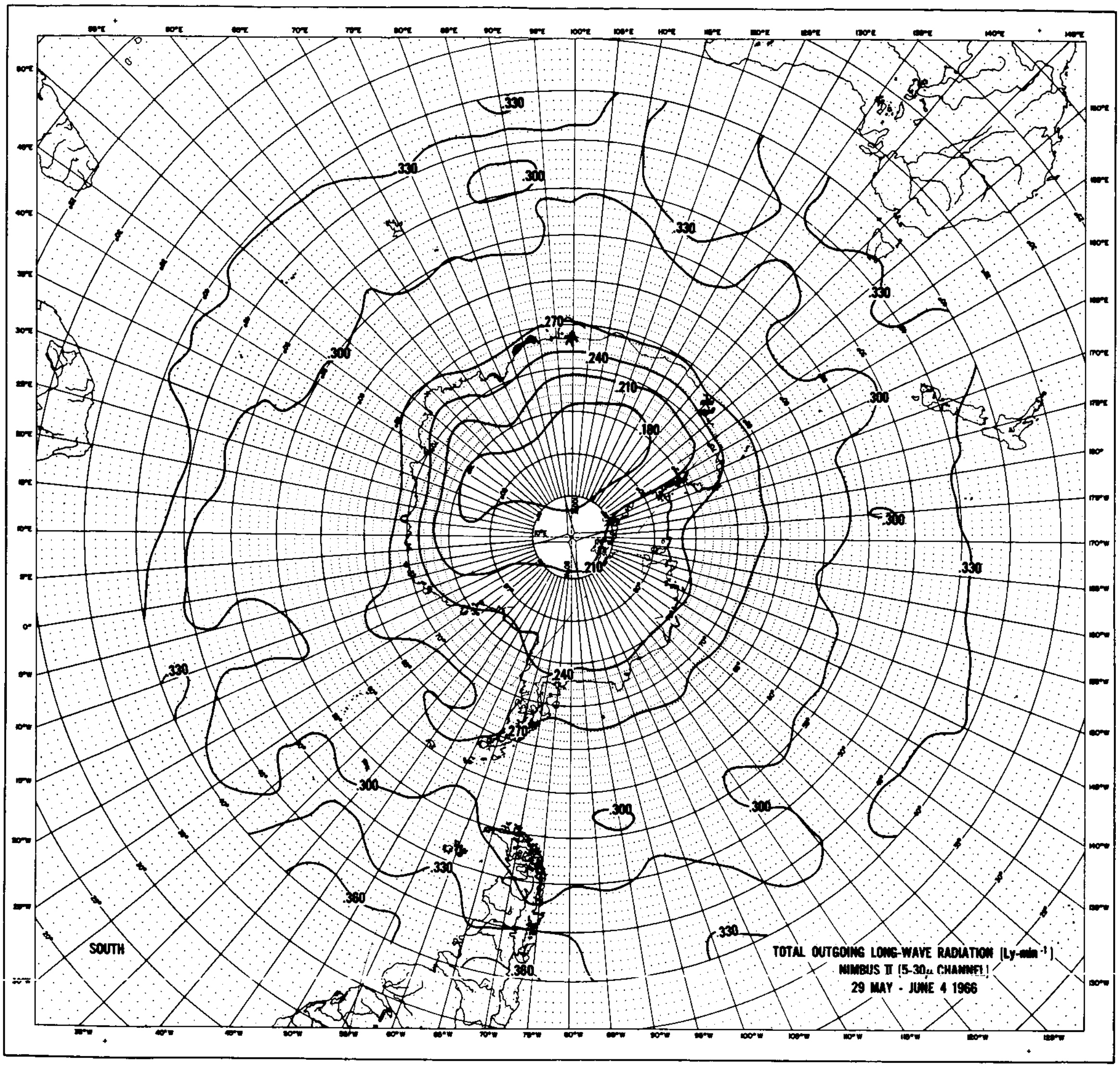

TOTAL OUTGOING LONG-WAVE RADIATION (Ly-min^{-1})
NIMBUS II (5-30μ CHANNEL)
29 MAY - JUNE 4 1966

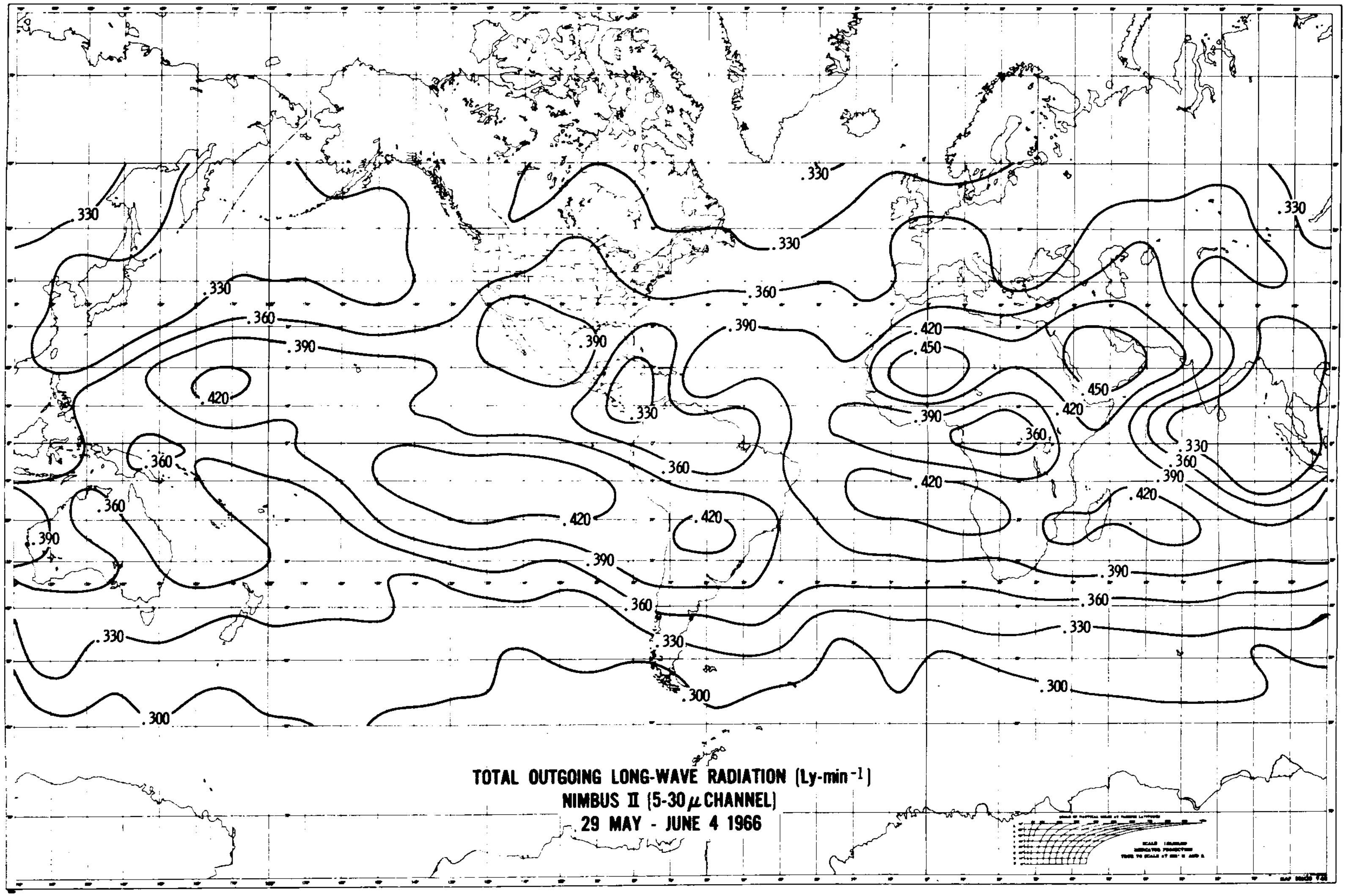

TOTAL OUTGOING LONG-WAVE RADIATION (Ly-min^{-1})
NIMBUS II (5-30 μ CHANNEL)
29 MAY - JUNE 4 1966

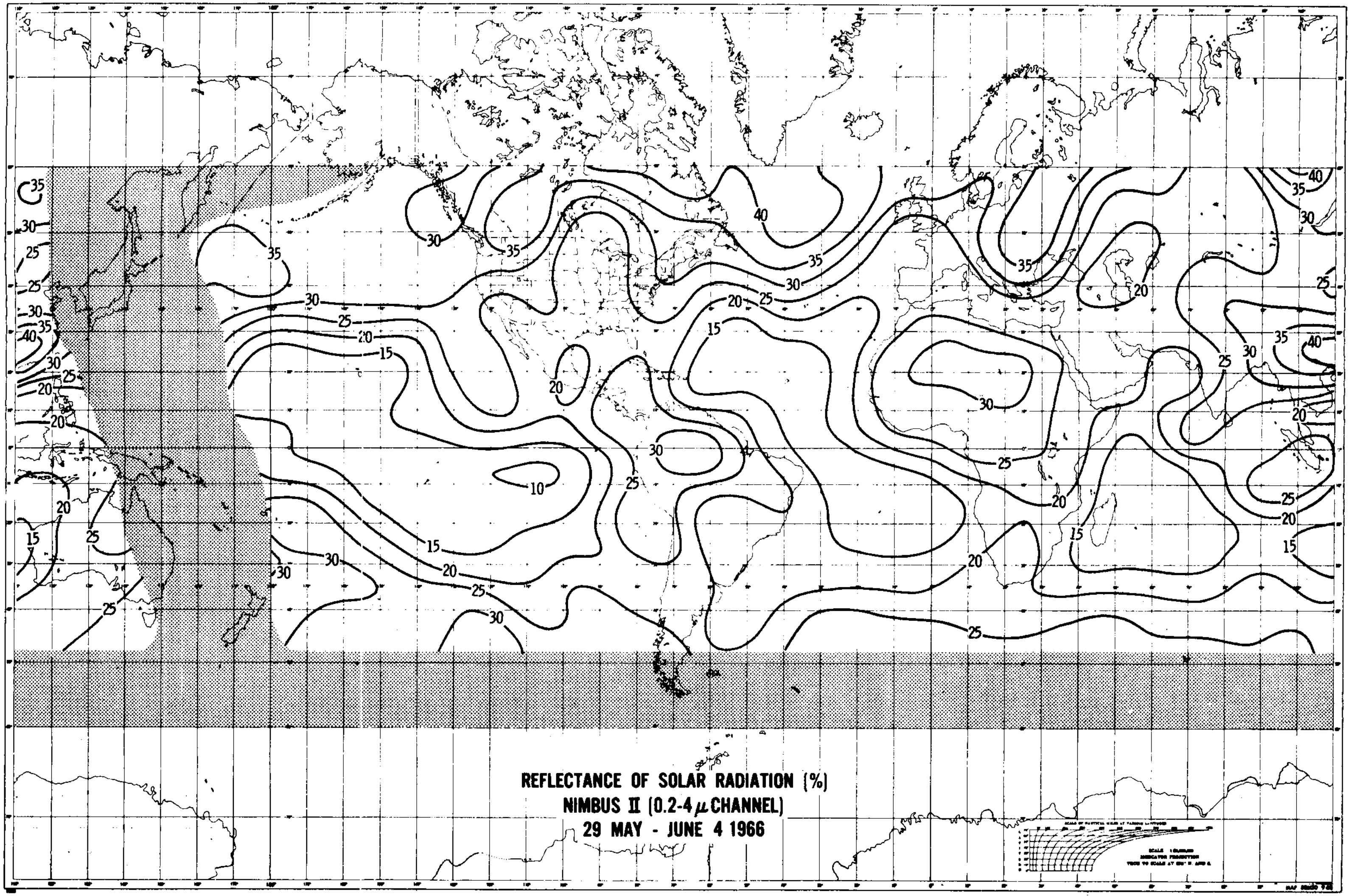

REFLECTANCE OF SOLAR RADIATION (%)
NIMBUS II (0.2-4 μ CHANNEL)
29 MAY - JUNE 4 1966

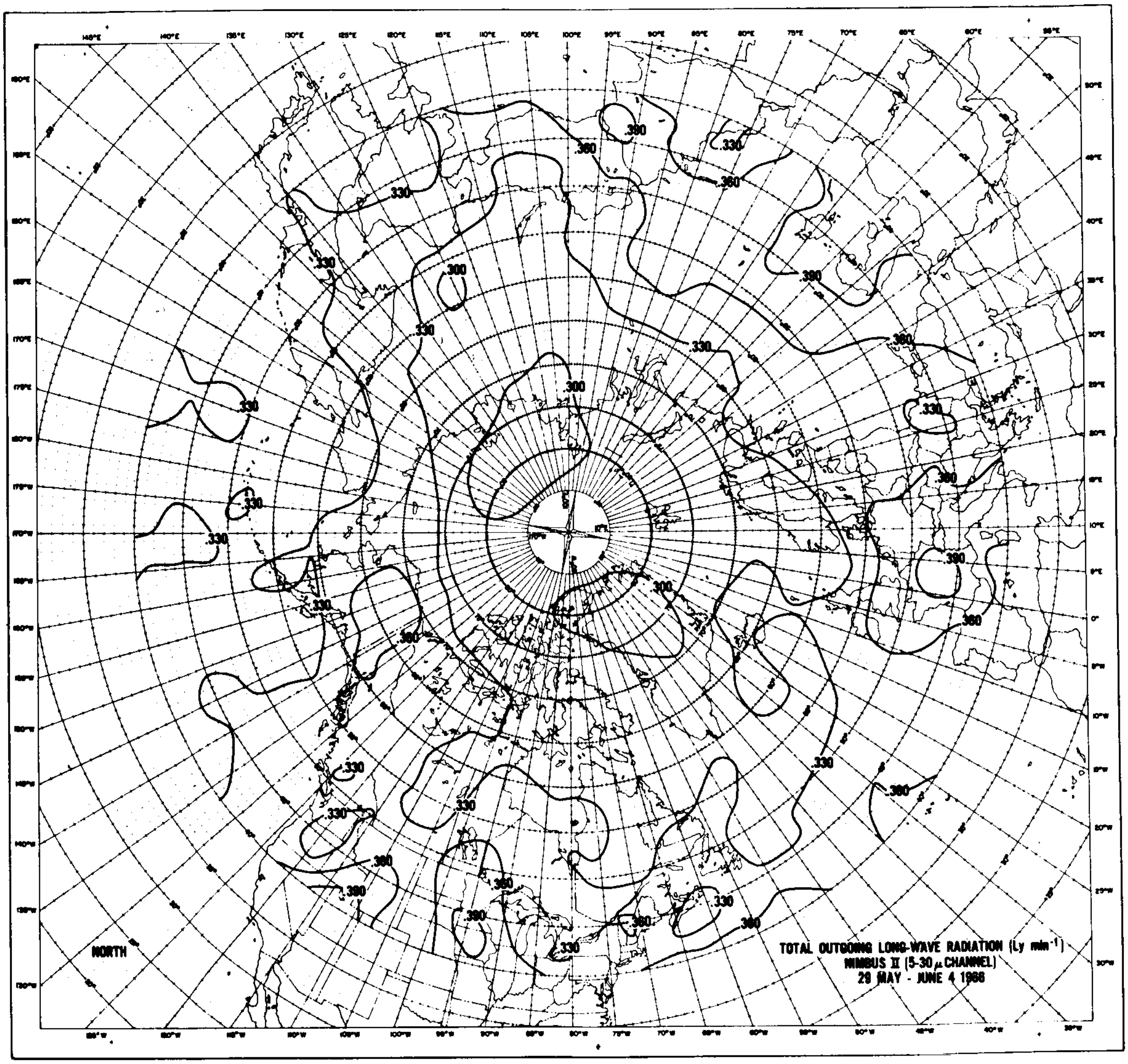
TOTAL OUTGOING LONG-WAVE RADIATION (Ly min⁻¹)
NIMBUS II (5-30 μ CHANNEL)
29 MAY - JUNE 4 1966
NORTH

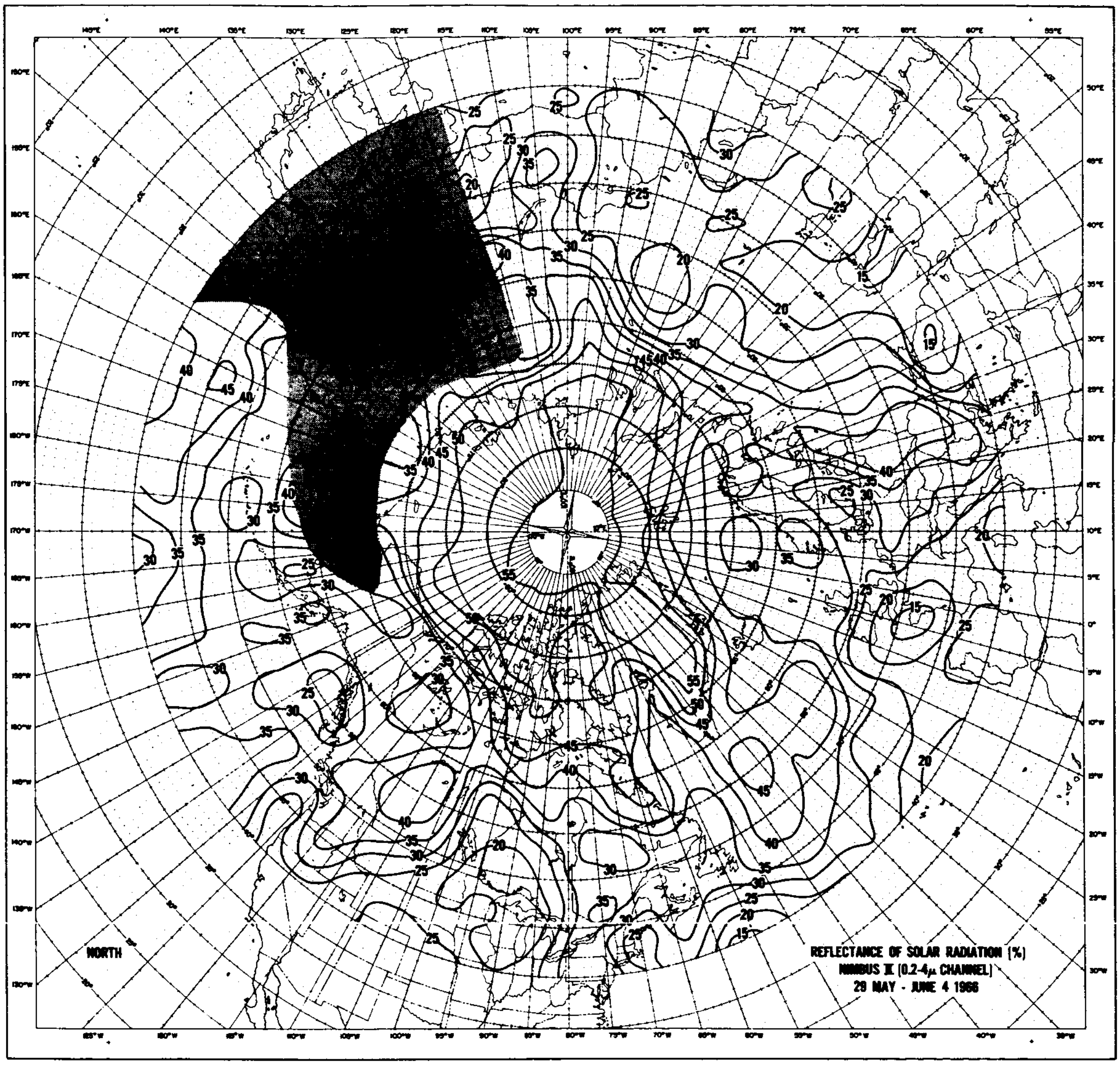
NORTH
REFLECTANCE OF SOLAR RADIATION (%)
NIMBUS II (0.2-4μ CHANNEL)
29 MAY - JUNE 4 1966

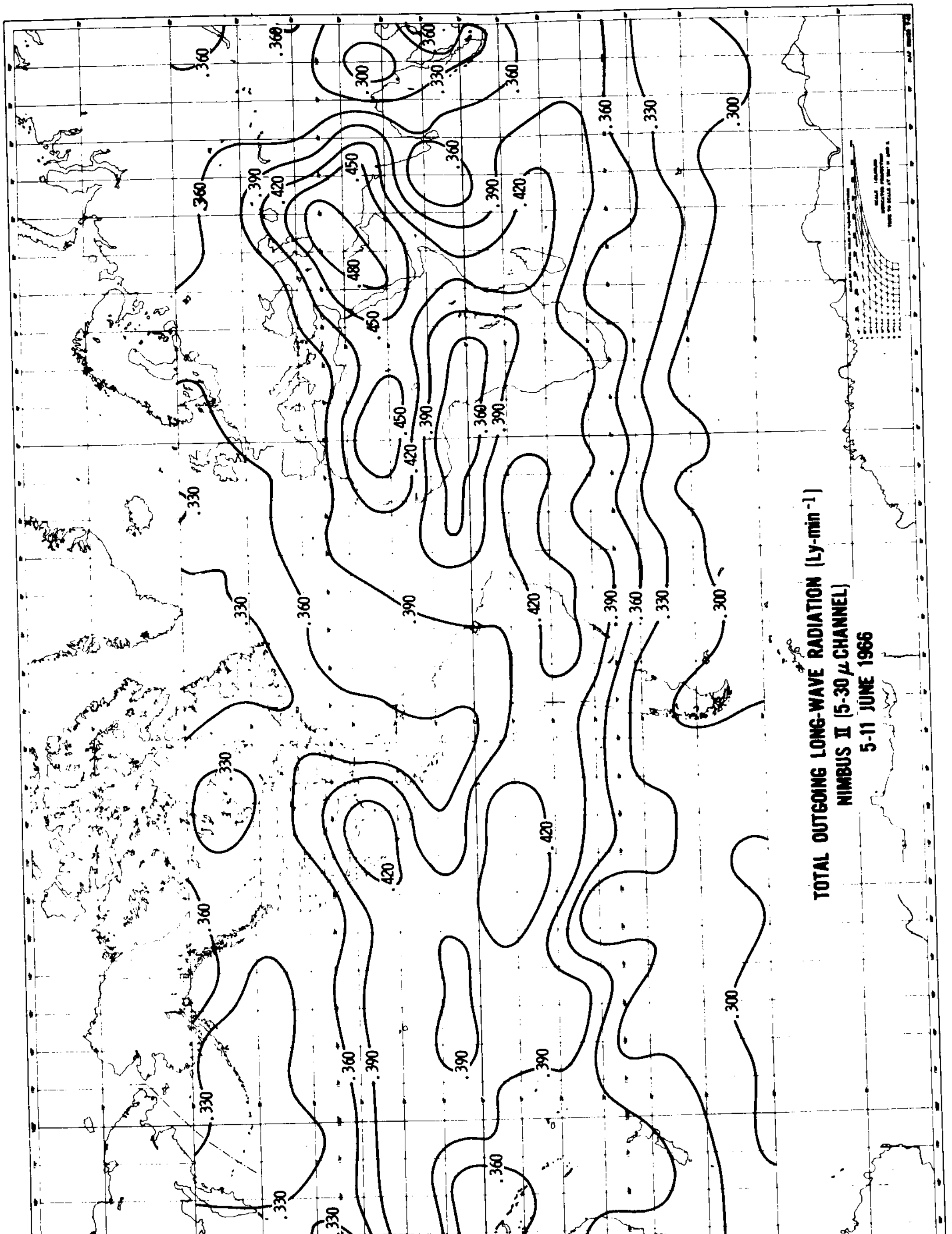

TOTAL OUTGOING LONG-WAVE RADIATION (Ly-min^{-1})
NIMBUS II (5-30 μ CHANNEL)
5-11 JUNE 1966

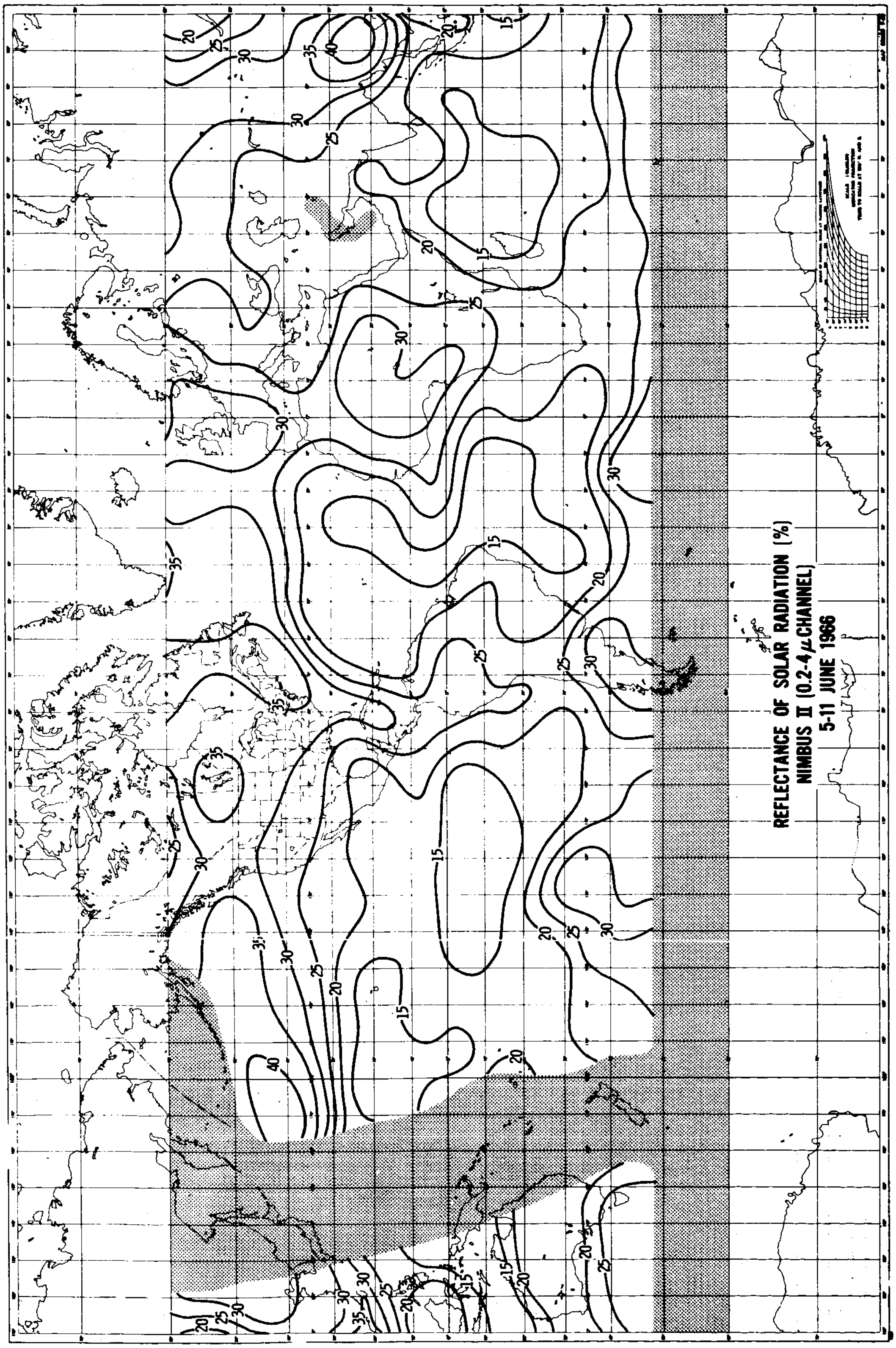

REFLECTANCE OF SOLAR RADIATION (%)
NIMBUS II (0.2-4 μ CHANNEL)
5-11 JUNE 1966

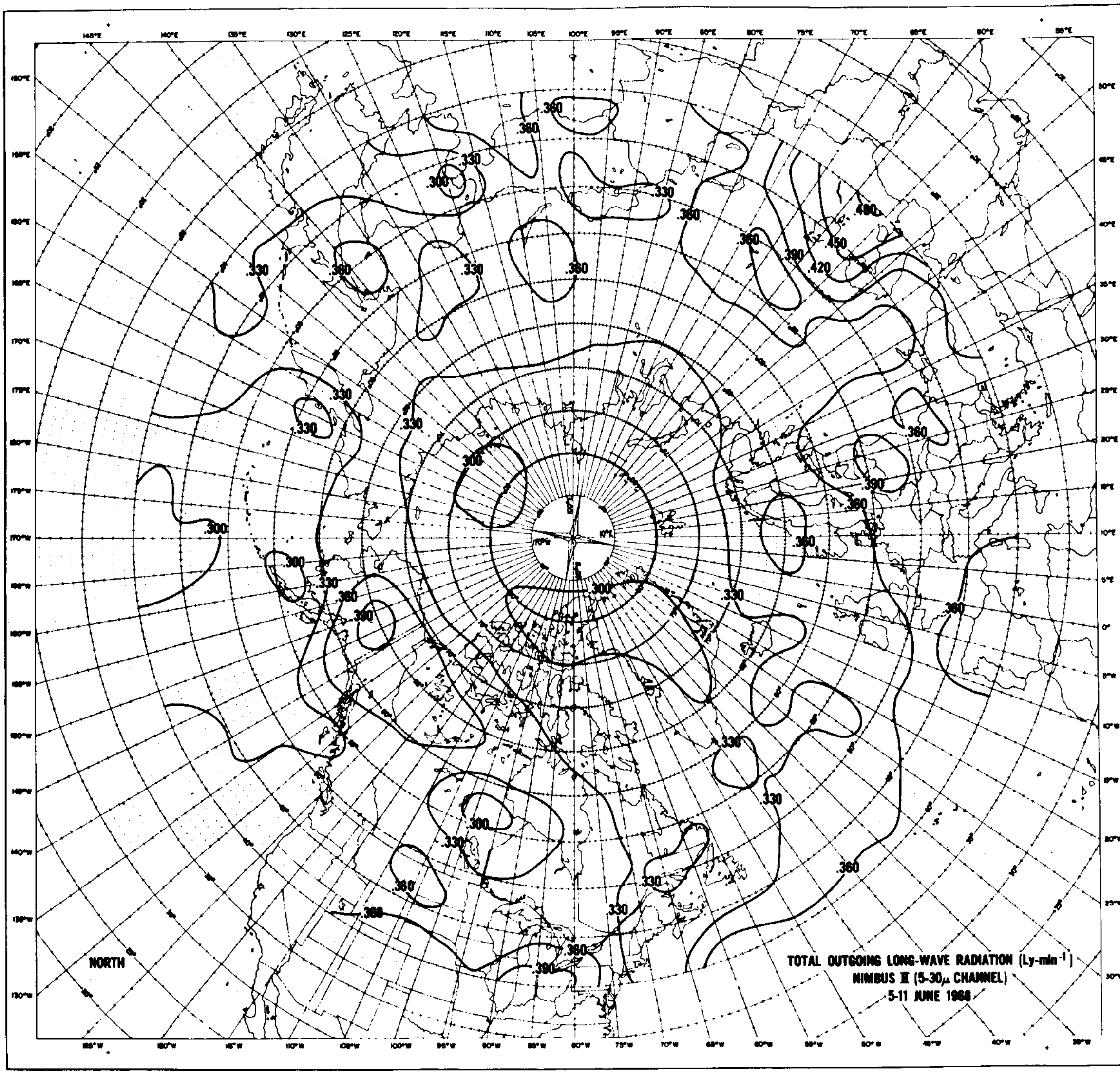
NORTH
TOTAL OUTGOING LONG-WAVE RADIATION (Ly-min^{-1})
NIMBUS II (5-30μ CHANNEL)
5-11 JUNE 1966

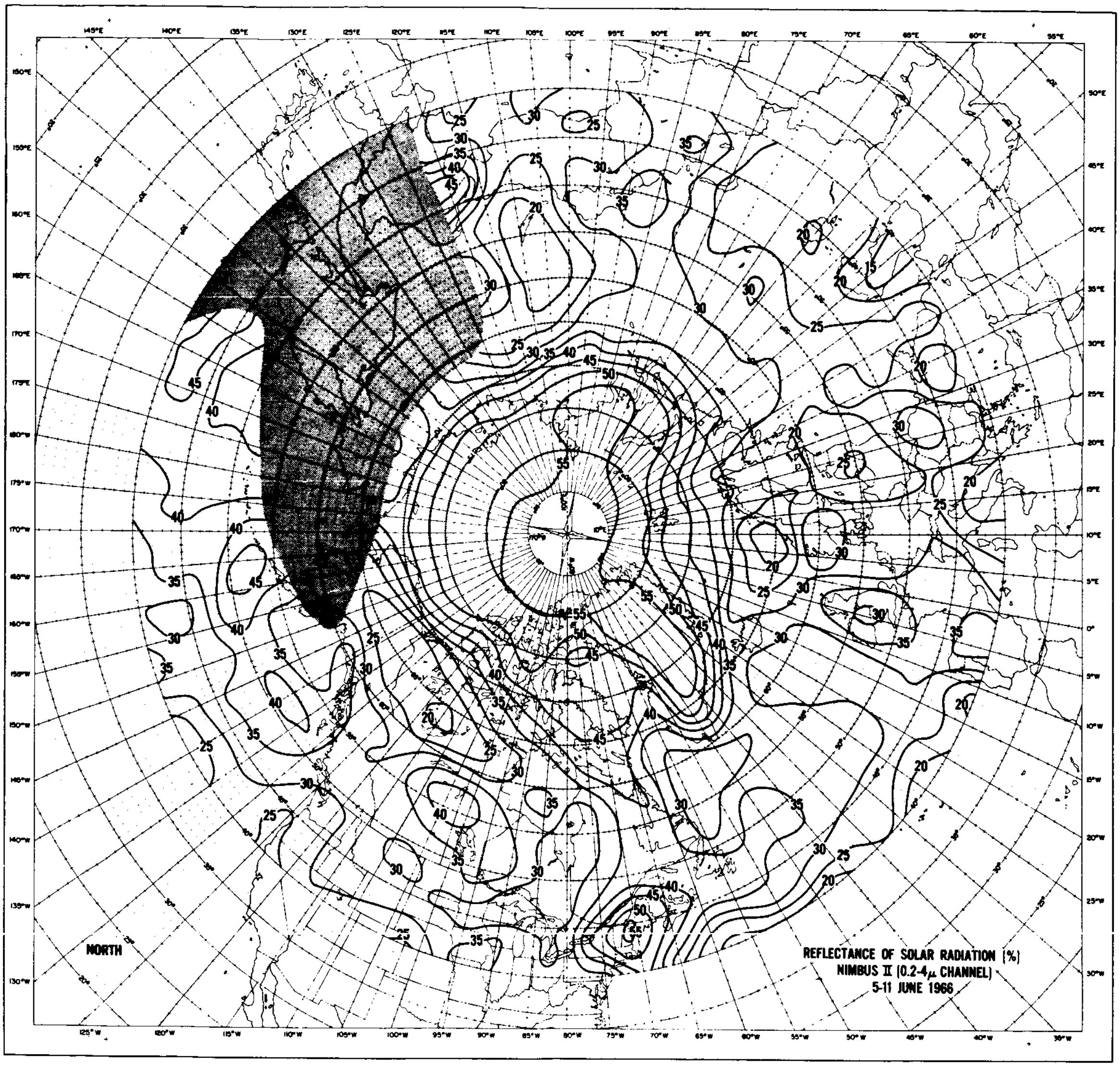
REFLECTANCE OF SOLAR RADIATION (%)
NIMBUS II (0.2-4μ CHANNEL)
5-11 JUNE 1966
NORTH

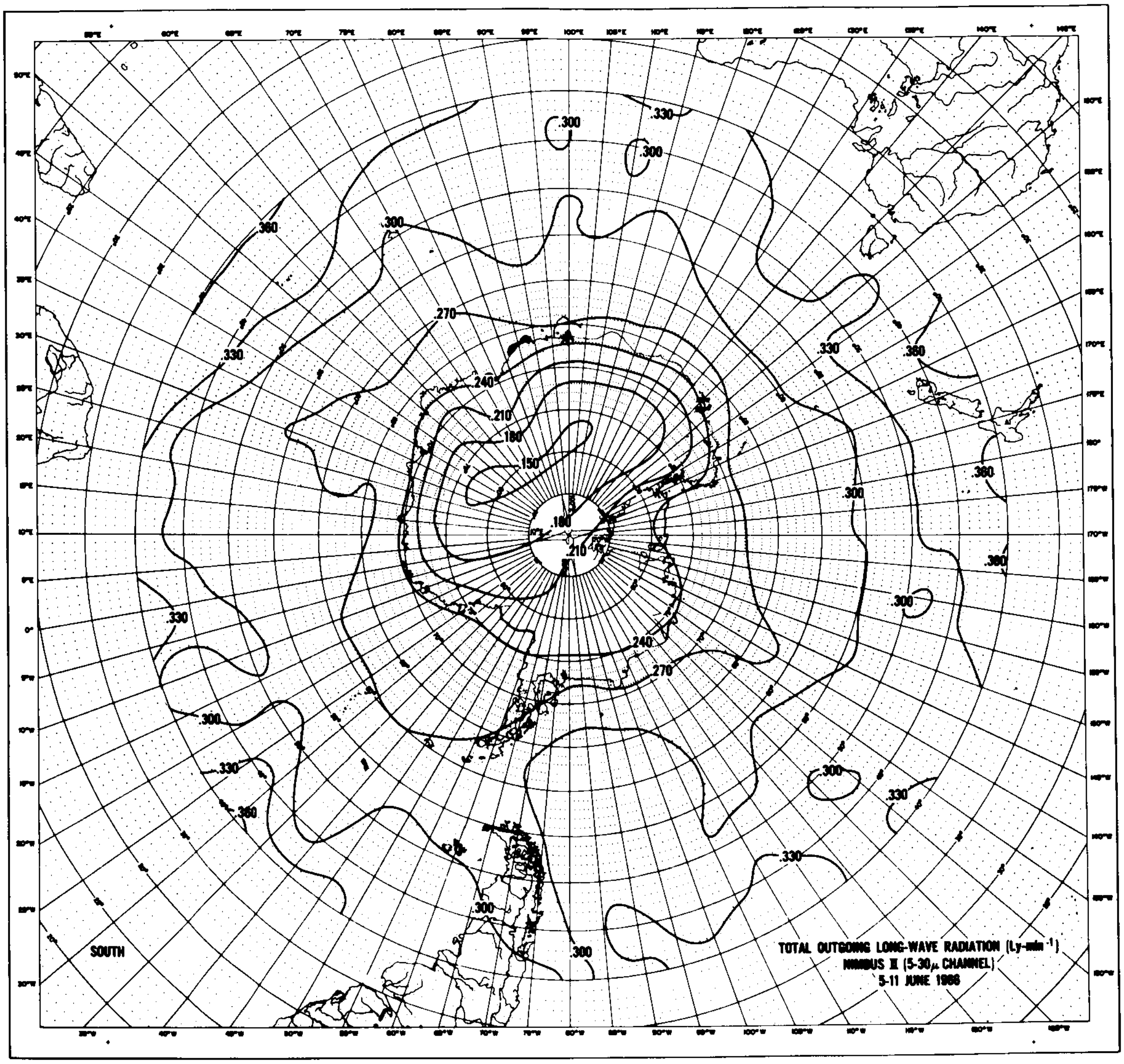
SOUTH
TOTAL OUTGOING LONG-WAVE RADIATION (Ly-min⁻¹)
NIMBUS II (5-30μ CHANNEL)
5-11 JUNE 1966
.150
.180
.210
.240
.270
.300
.330
.360

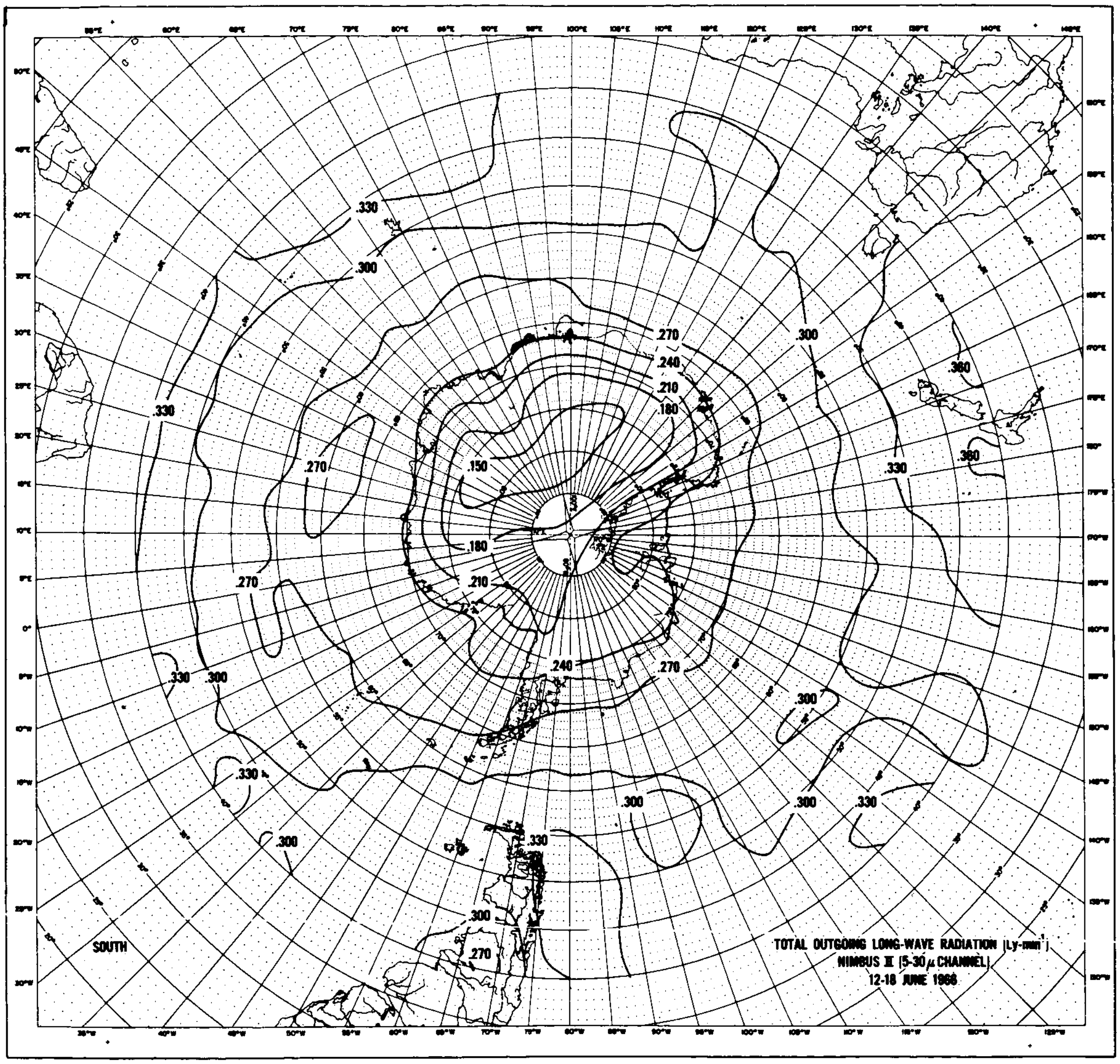

TOTAL OUTGOING LONG-WAVE RADIATION (Ly-min⁻¹)
NIMBUS II (5-30 μ CHANNEL)
12-18 JUNE 1966
SOUTH
.330
.300
.270
.240
.210
.180
.150
.360

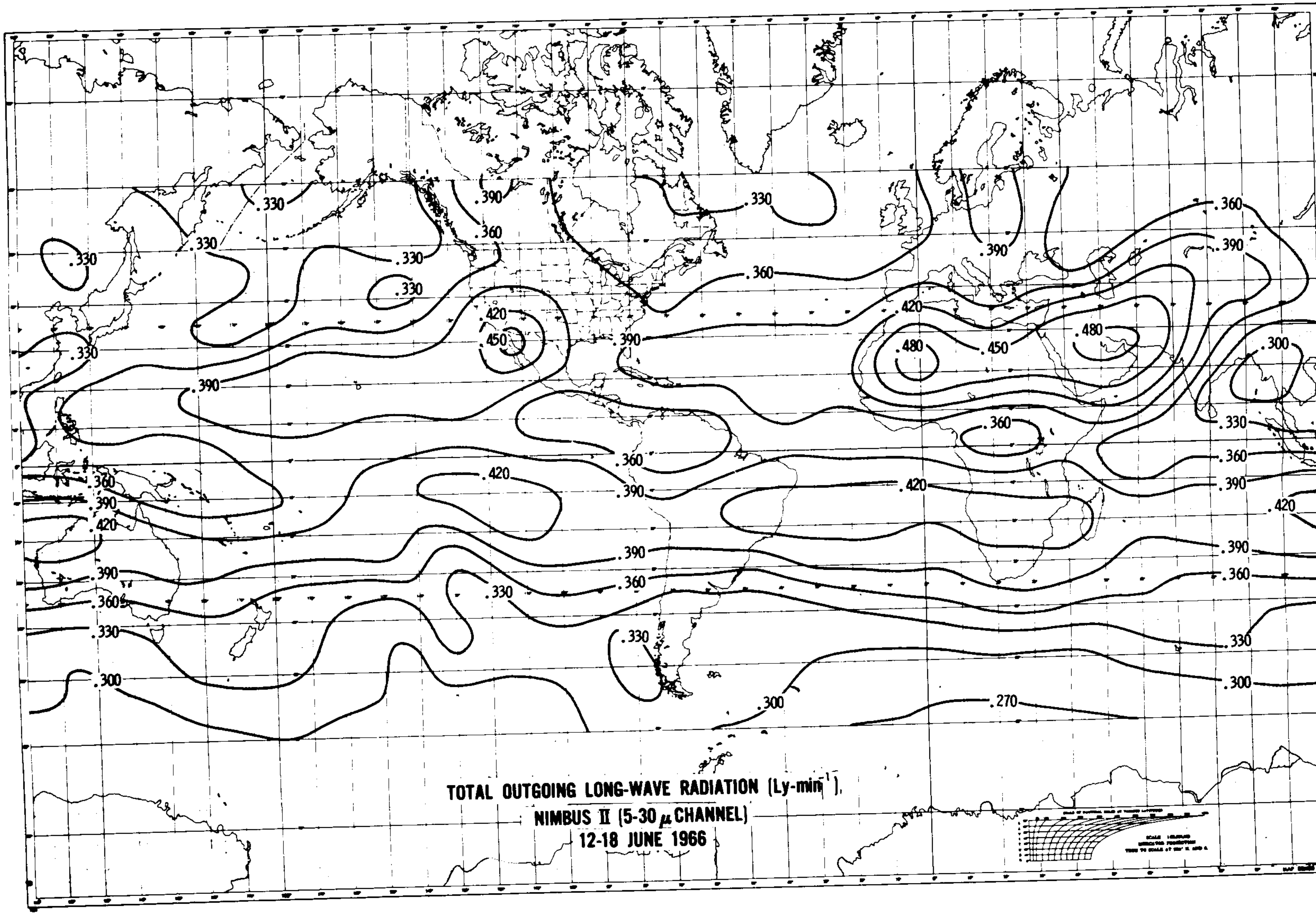

TOTAL OUTGOING LONG-WAVE RADIATION ($Ly\text{-}min^{-1}$)
NIMBUS II (5-30 μ CHANNEL)
12-18 JUNE 1966

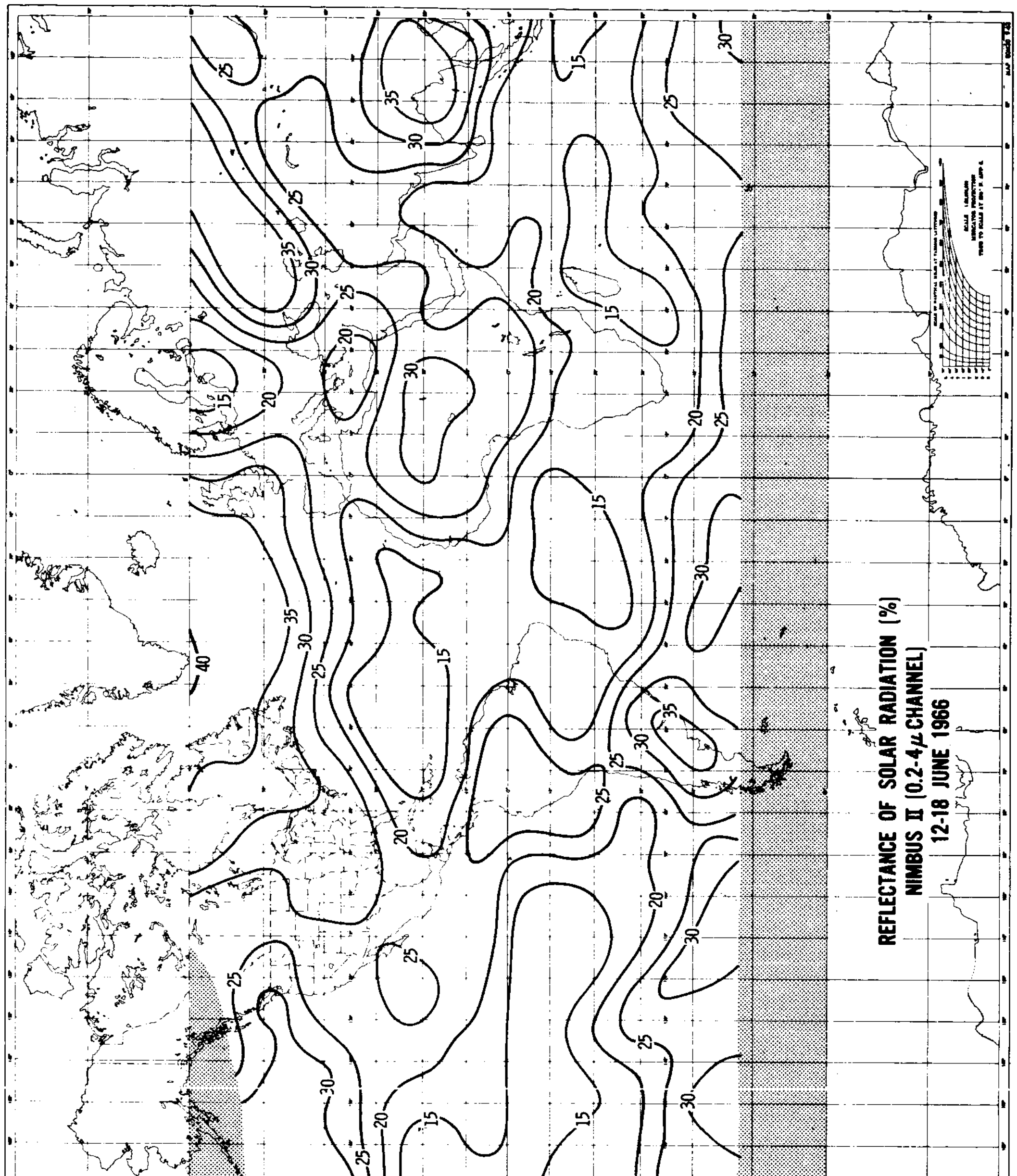

REFLECTANCE OF SOLAR RADIATION (%)
NIMBUS II (0.2-4 μ CHANNEL)
12-18 JUNE 1966

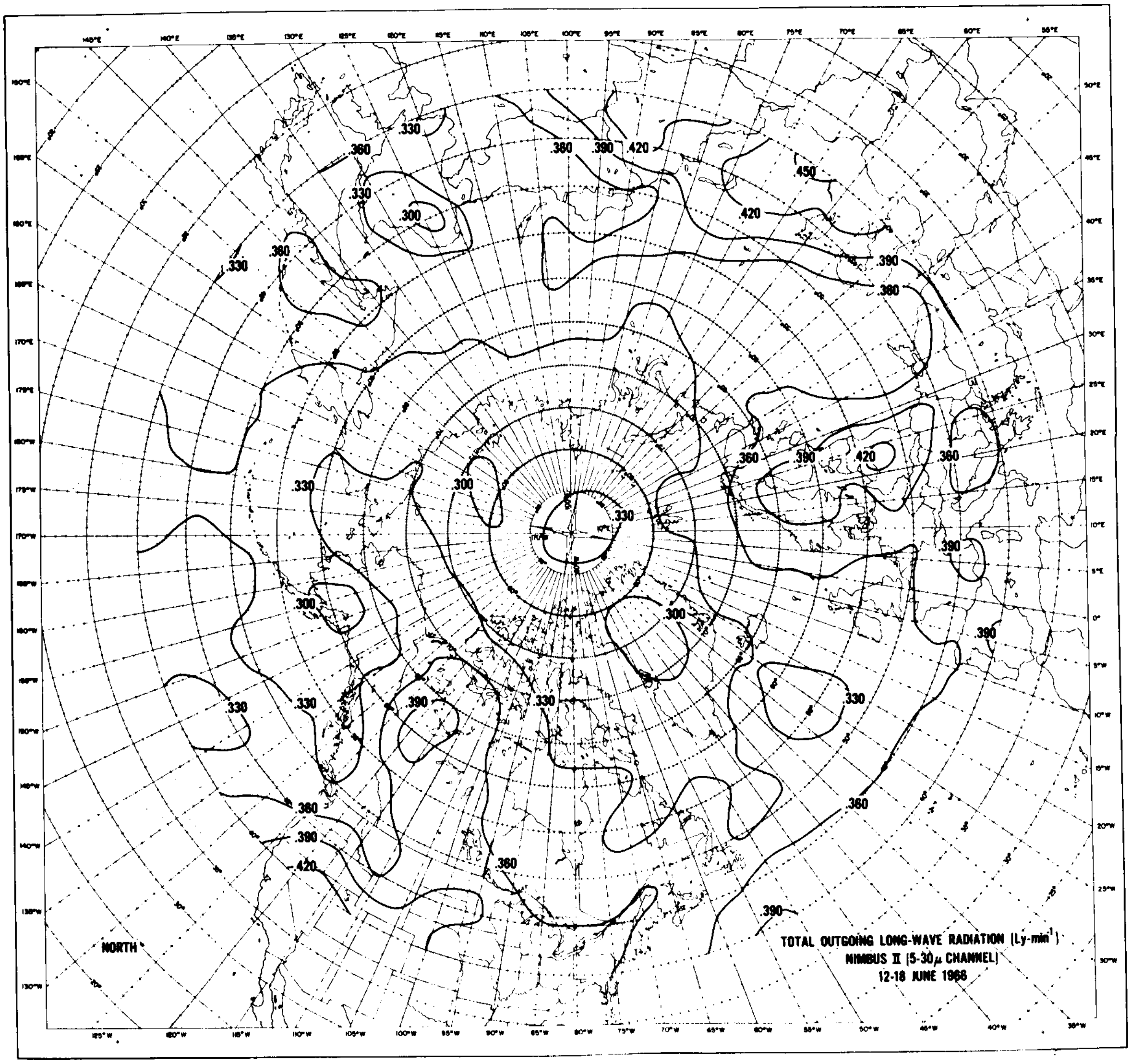
TOTAL OUTGOING LONG-WAVE RADIATION (Ly-min⁻¹)
NIMBUS II (5-30μ CHANNEL)
12-18 JUNE 1966
NORTH

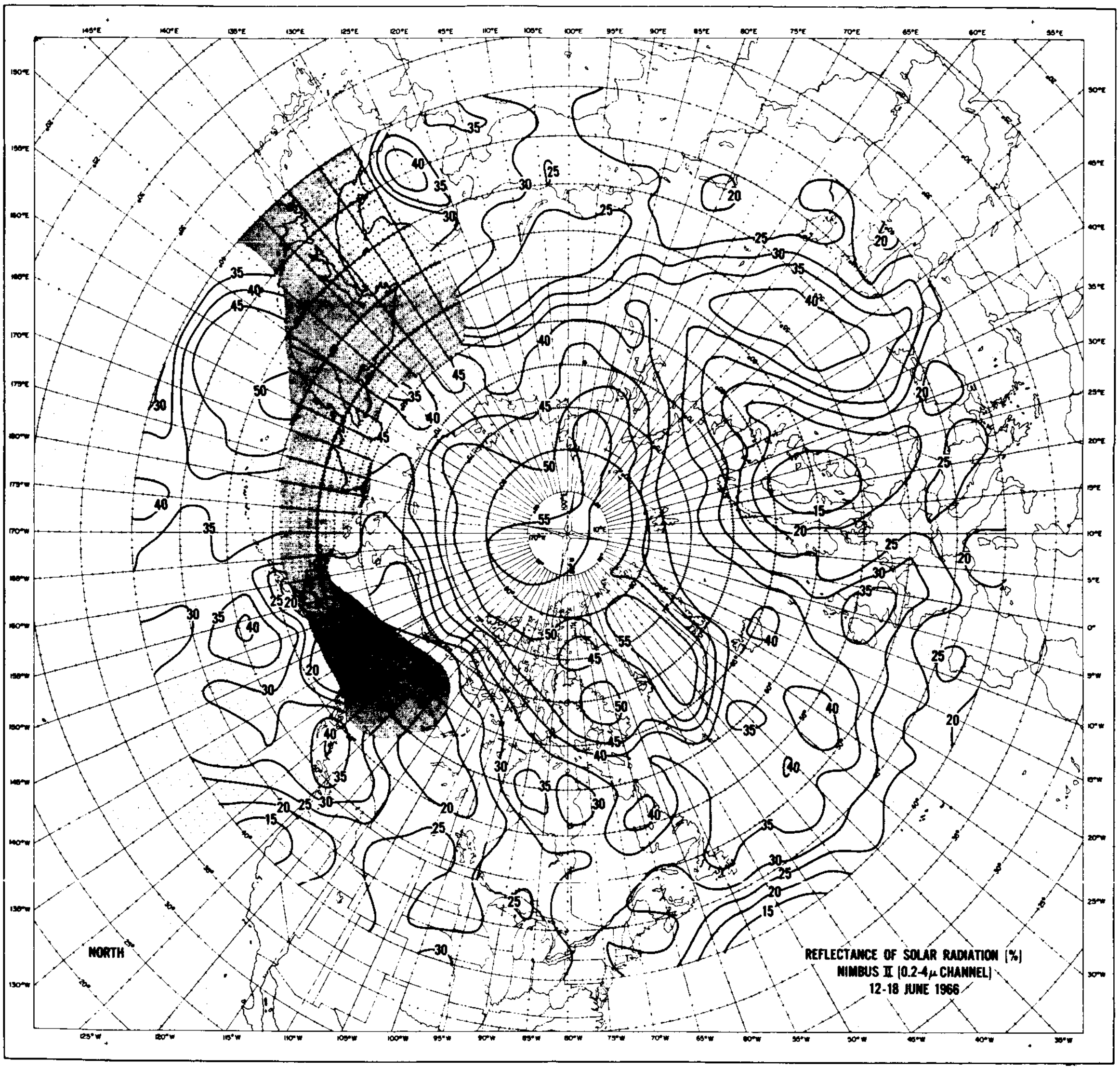
REFLECTANCE OF SOLAR RADIATION (%)
NIMBUS II (0.2-4μ CHANNEL)
12-18 JUNE 1966
NORTH

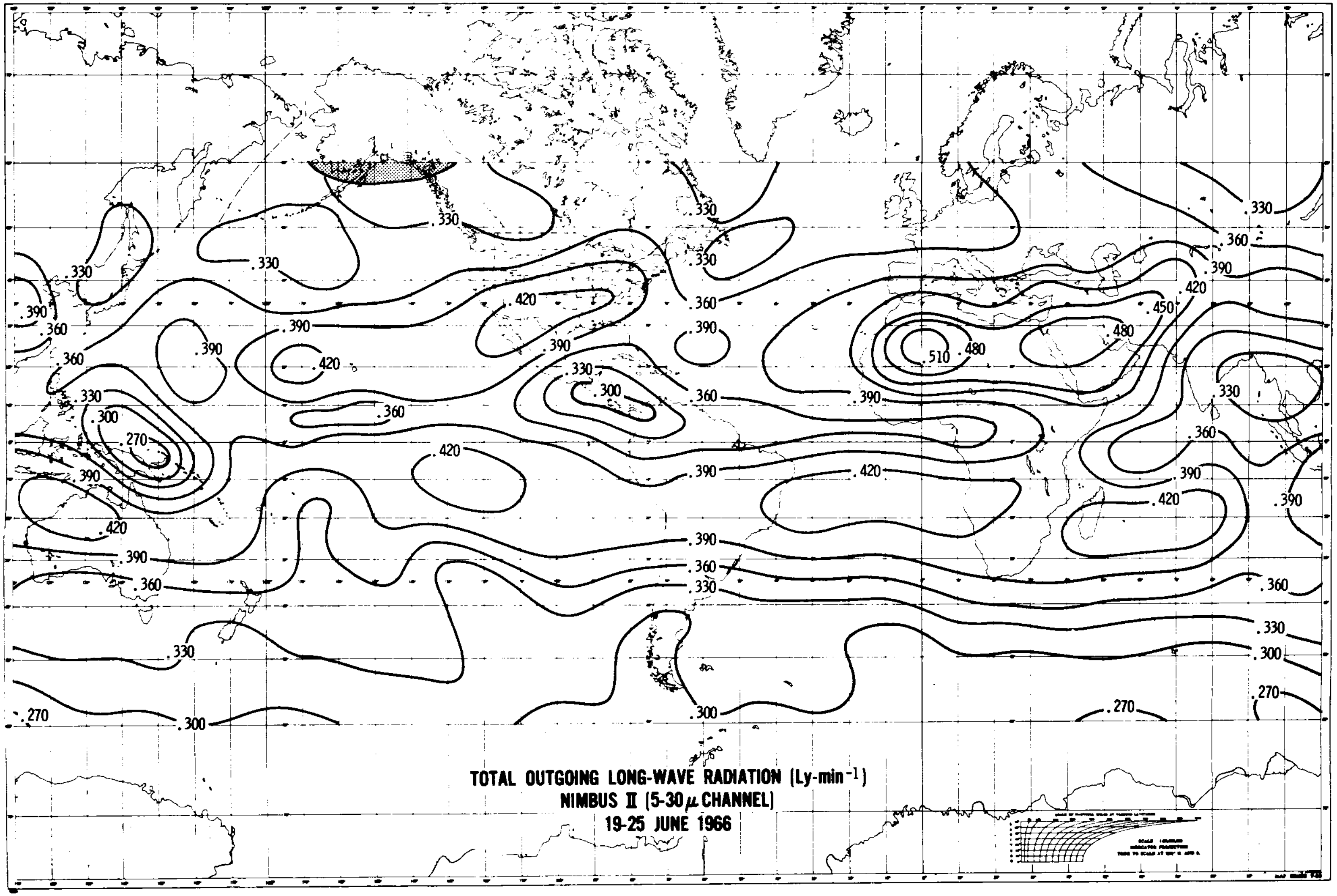

TOTAL OUTGOING LONG-WAVE RADIATION (Ly-min^{-1})
NIMBUS II (5-30μ CHANNEL)
19-25 JUNE 1966

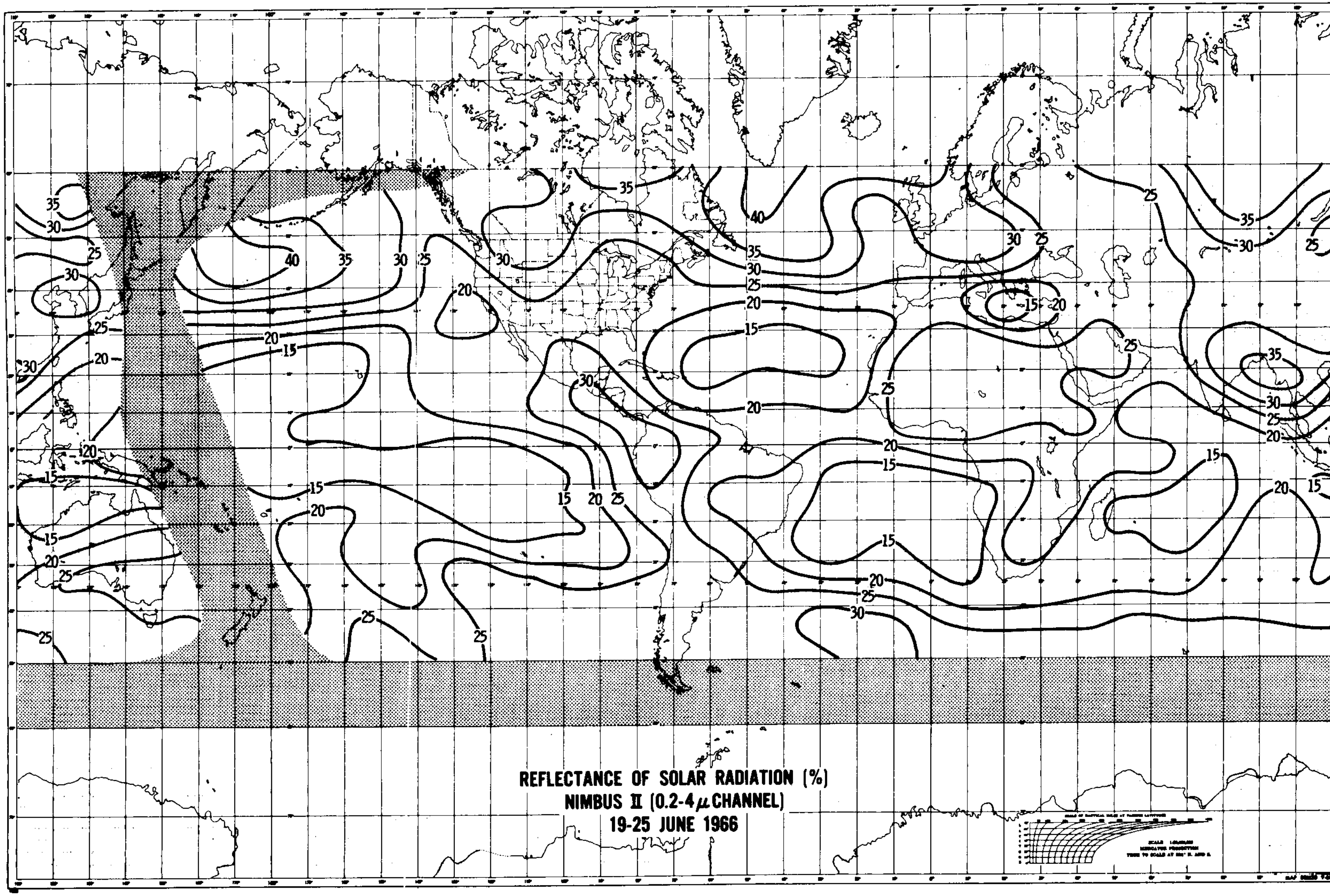
REFLECTANCE OF SOLAR RADIATION (%)
NIMBUS II (0.2-4 μ CHANNEL)
19-25 JUNE 1966

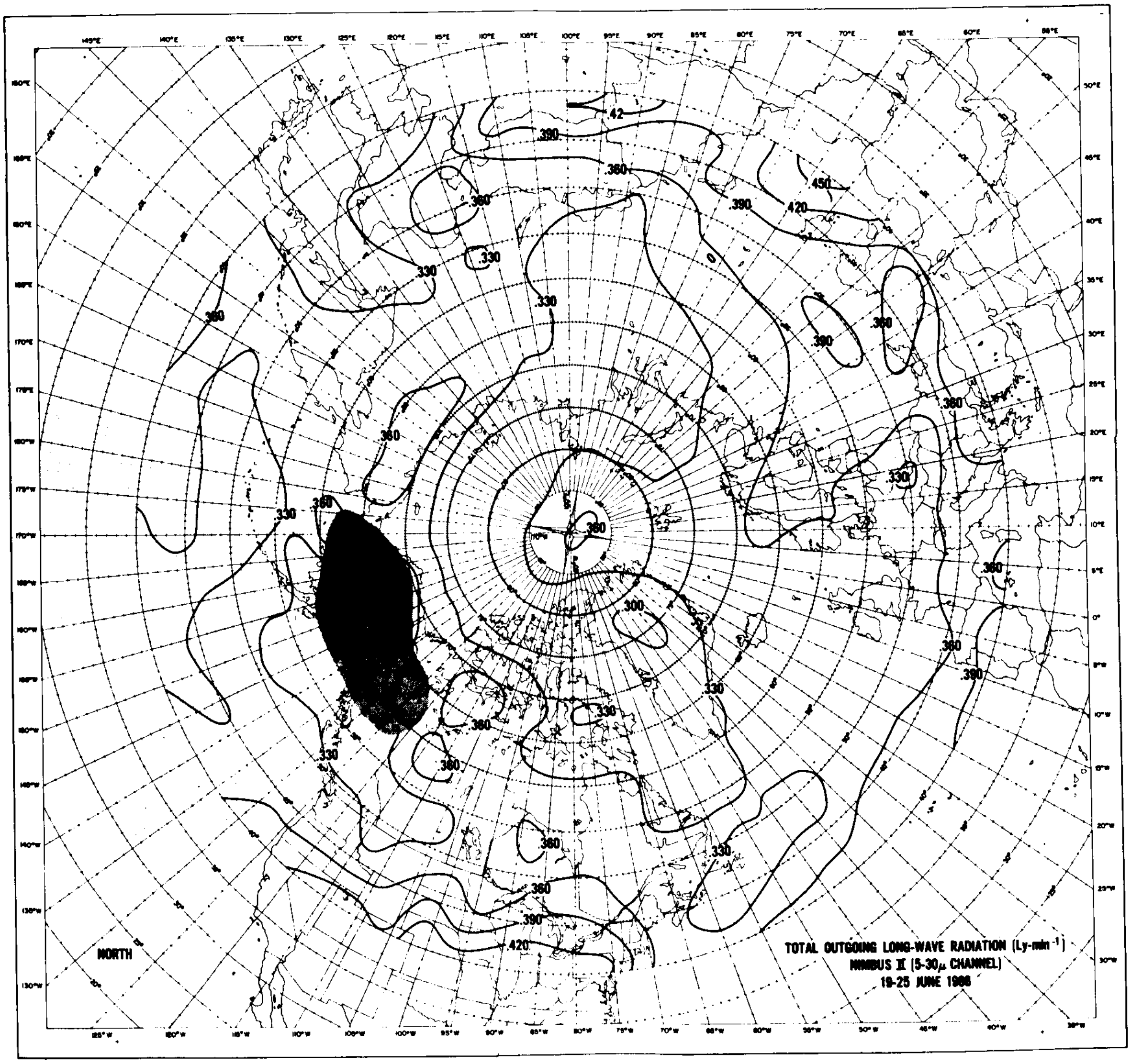

TOTAL OUTGOING LONG-WAVE RADIATION (Ly-min^{-1})
NIMBUS II (5-30μ CHANNEL)
19-25 JUNE 1966
NORTH
.420
.390
.360
.330
.300
.450

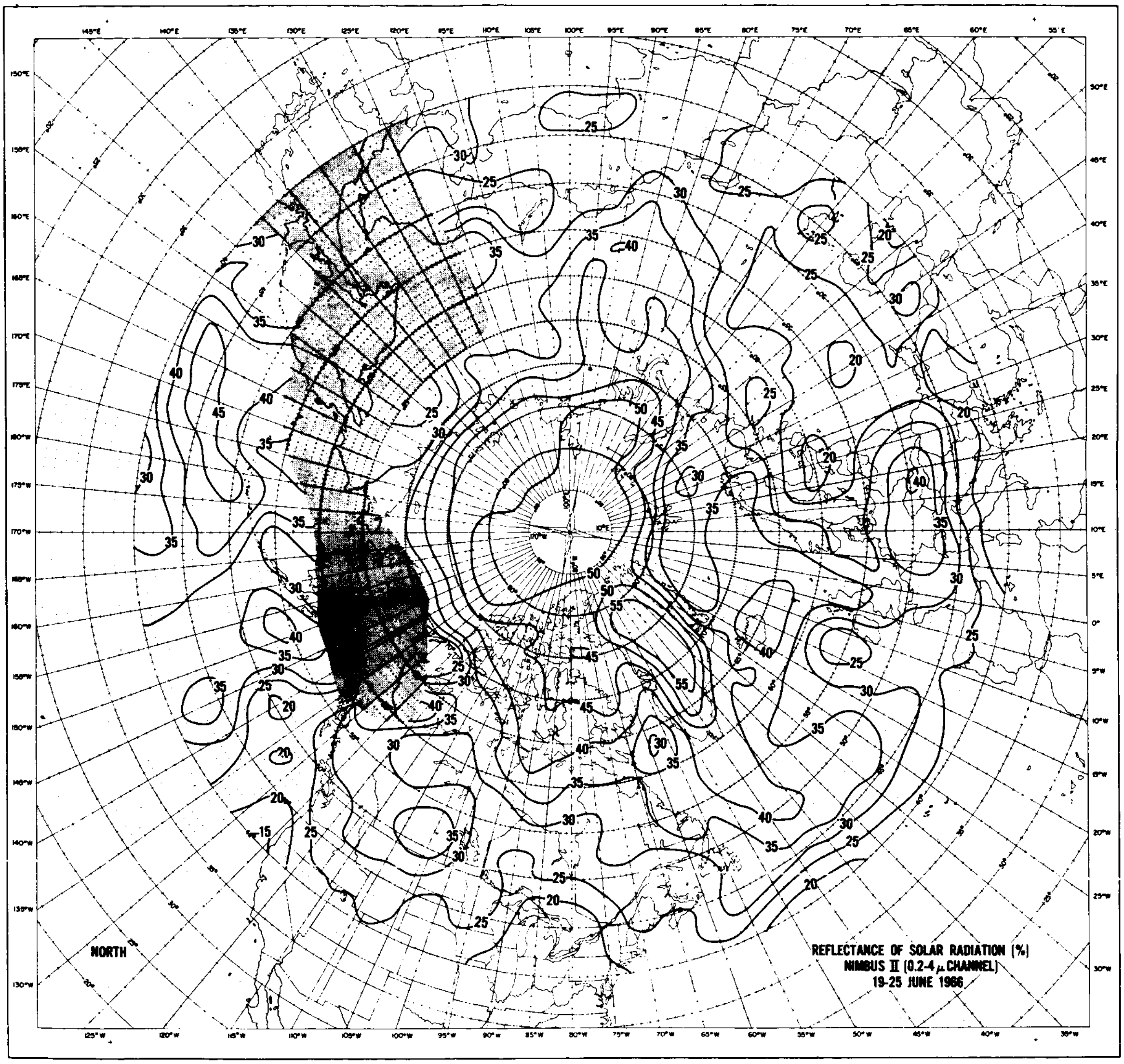
NORTH
REFLECTANCE OF SOLAR RADIATION (%)
NIMBUS II (0.2-4 μ CHANNEL)
19-25 JUNE 1966

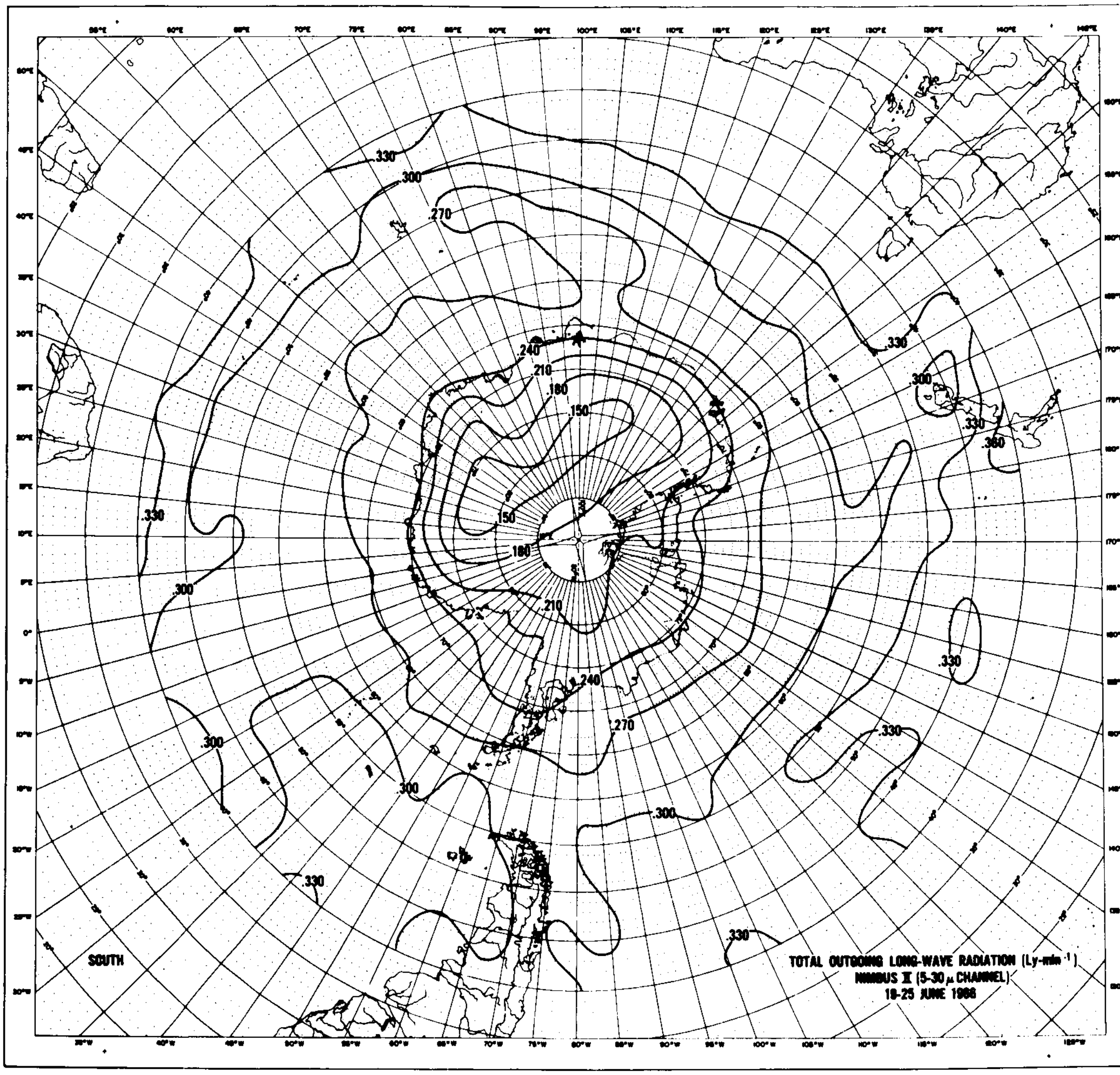
.330
.300
.270
.240
.210
.180
.150
.360
SOUTH
TOTAL OUTGOING LONG-WAVE RADIATION (Ly-min⁻¹)
NIMBUS II (5-30 μ CHANNEL)
18-25 JUNE 1966

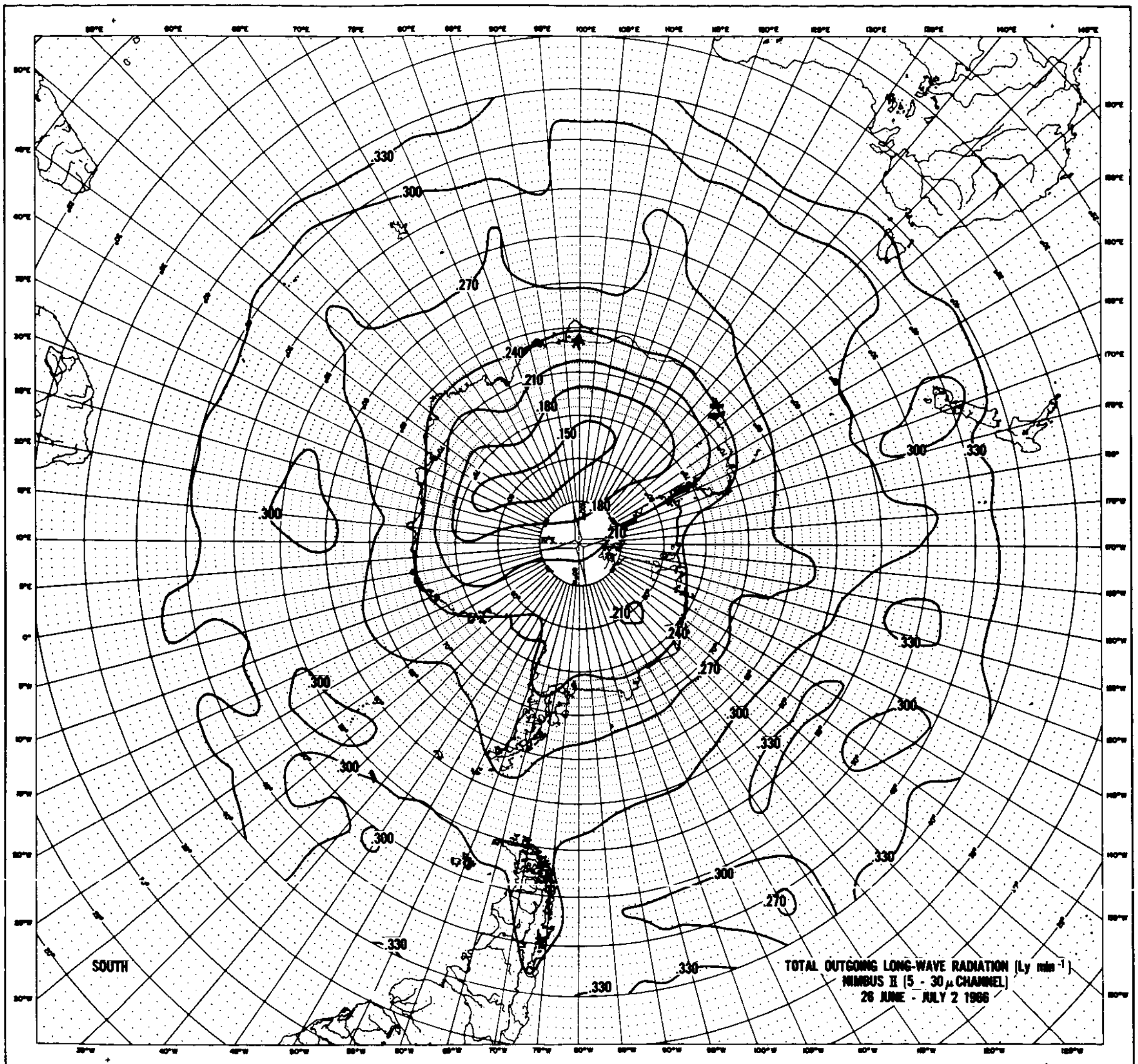
.330
.300
.270
.240
.210
.180
.150
SOUTH
TOTAL OUTGOING LONG-WAVE RADIATION (Ly min⁻¹)
NIMBUS II (5 - 30 μ CHANNEL)
26 JUNE - JULY 2 1966

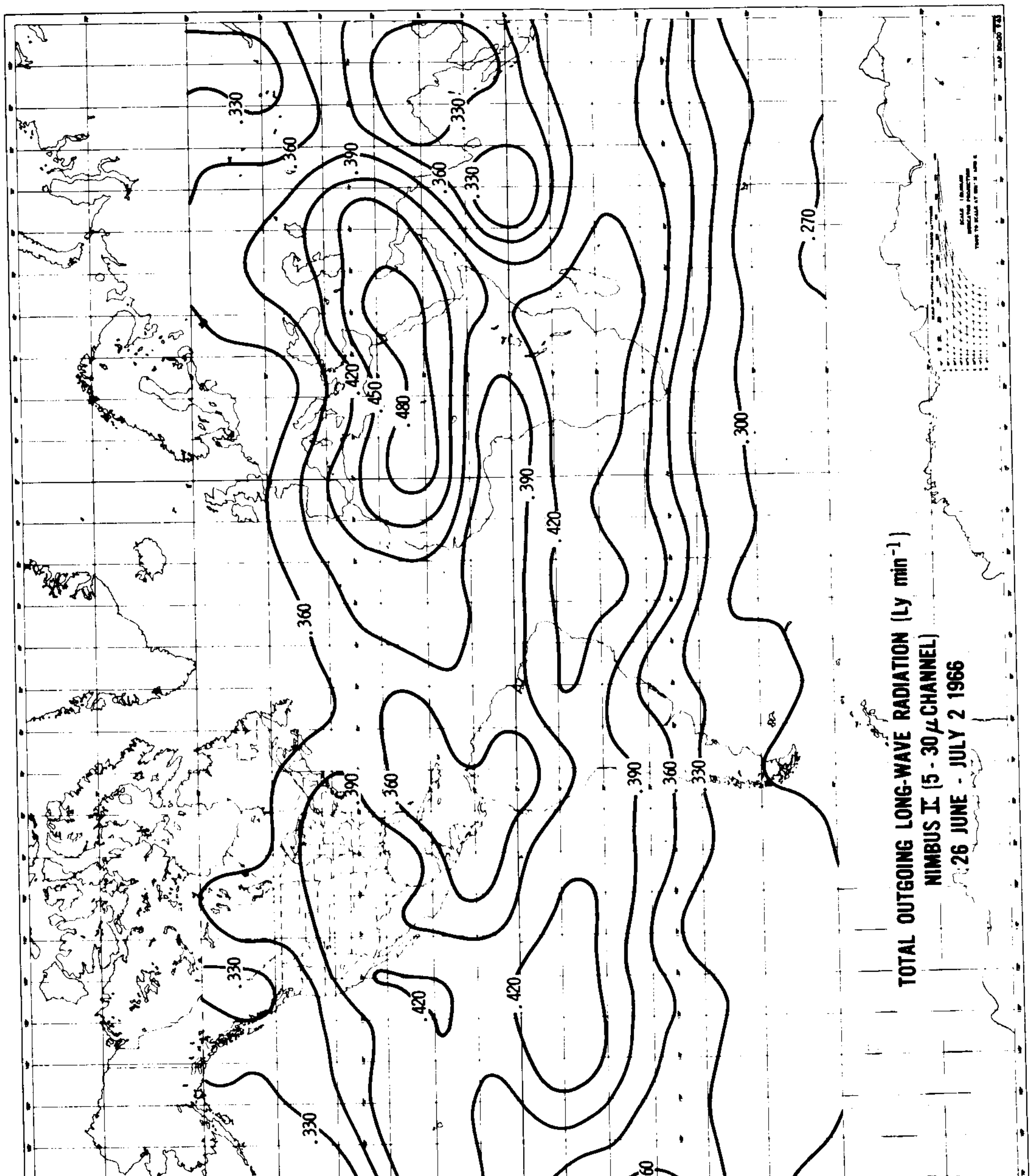

TOTAL OUTGOING LONG-WAVE RADIATION (Ly min^{-1})
NIMBUS II (5 - 30μ CHANNEL)
26 JUNE - JULY 2 1966

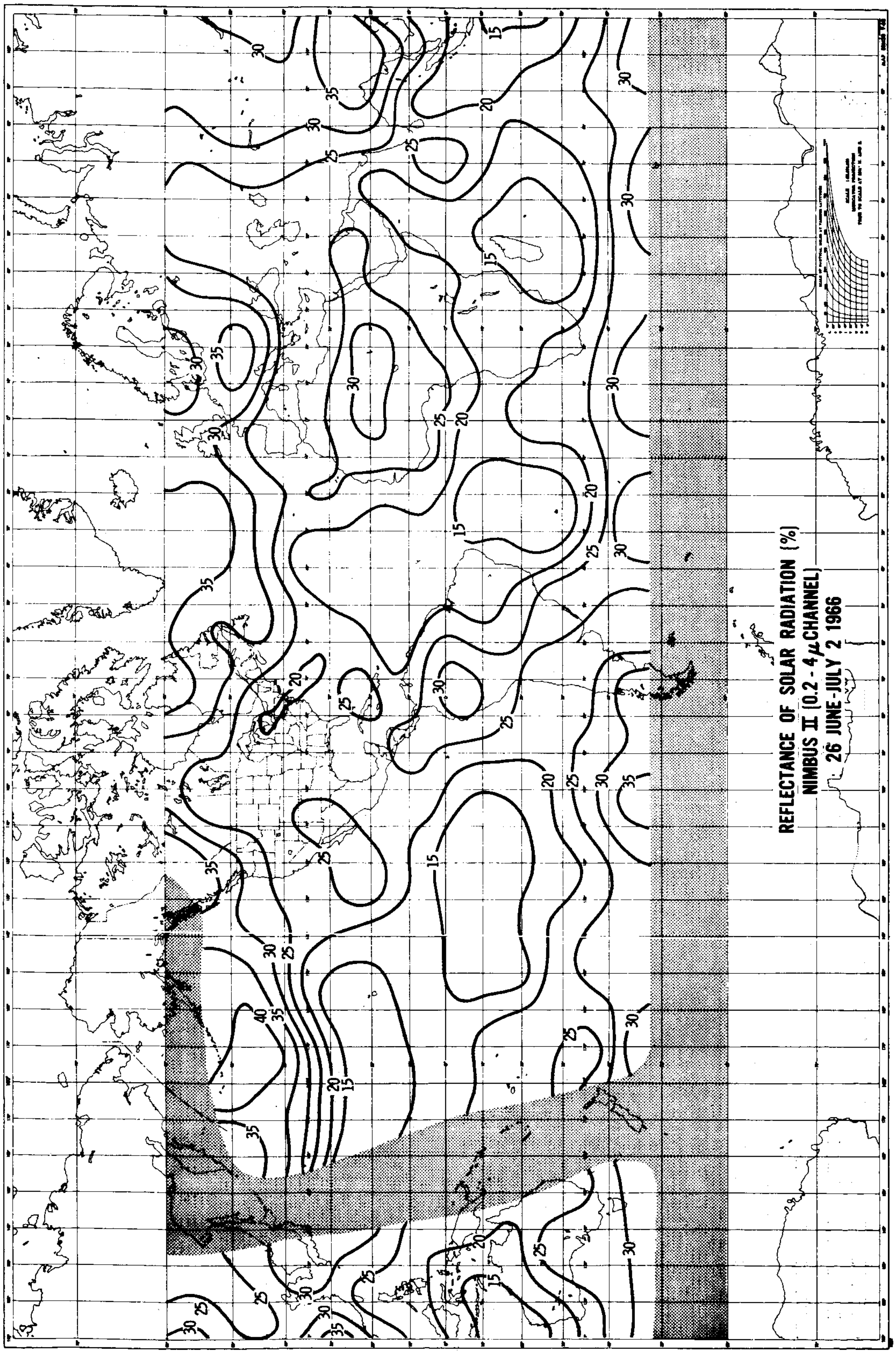

REFLECTANCE OF SOLAR RADIATION (%)
NIMBUS II (0.2 - 4 μ CHANNEL)
26 JUNE-JULY 2 1966

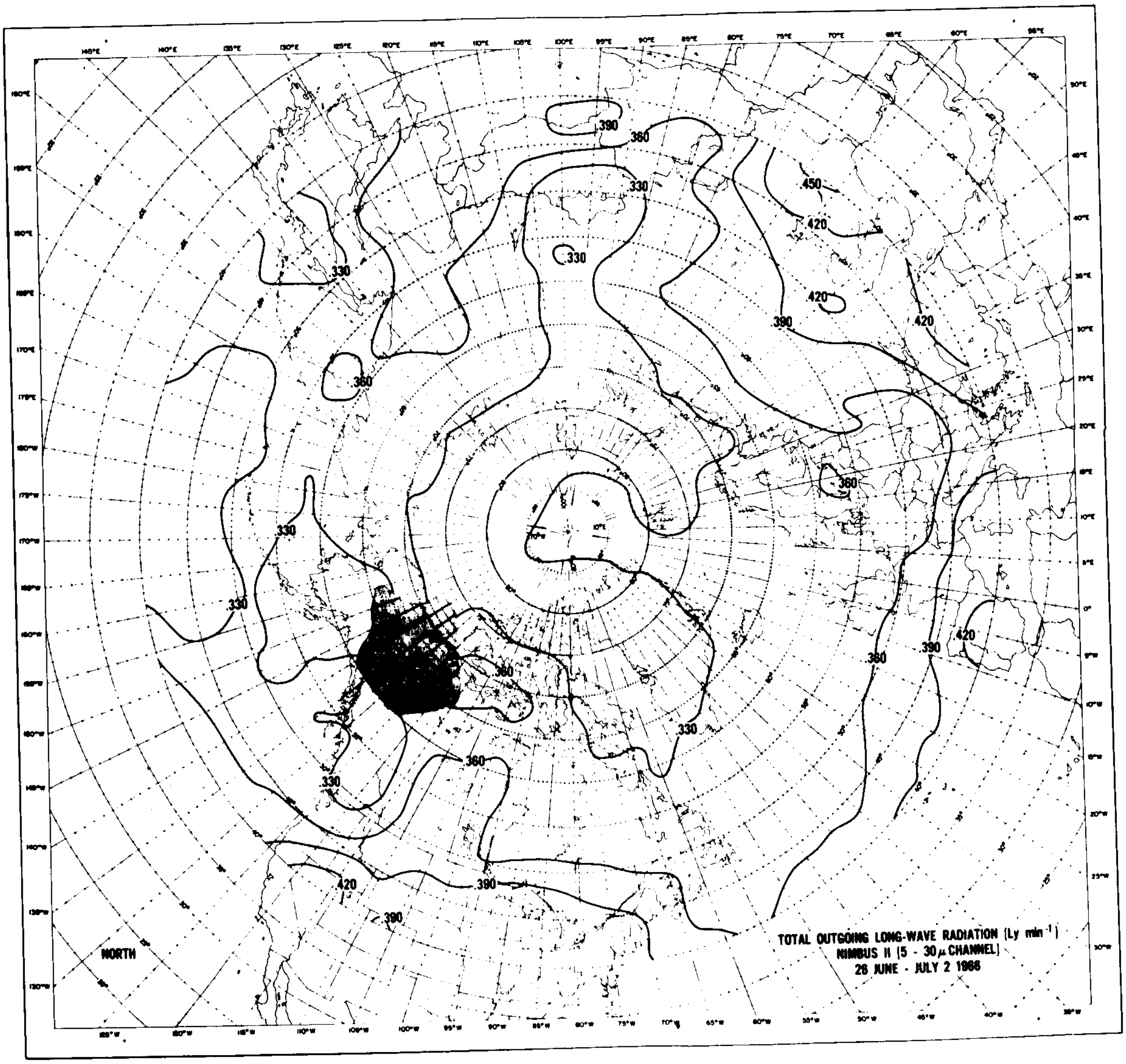

TOTAL OUTGOING LONG-WAVE RADIATION (Ly min^{-1})
NIMBUS II (5 - 30 µ CHANNEL)
28 JUNE - JULY 2 1966
NORTH

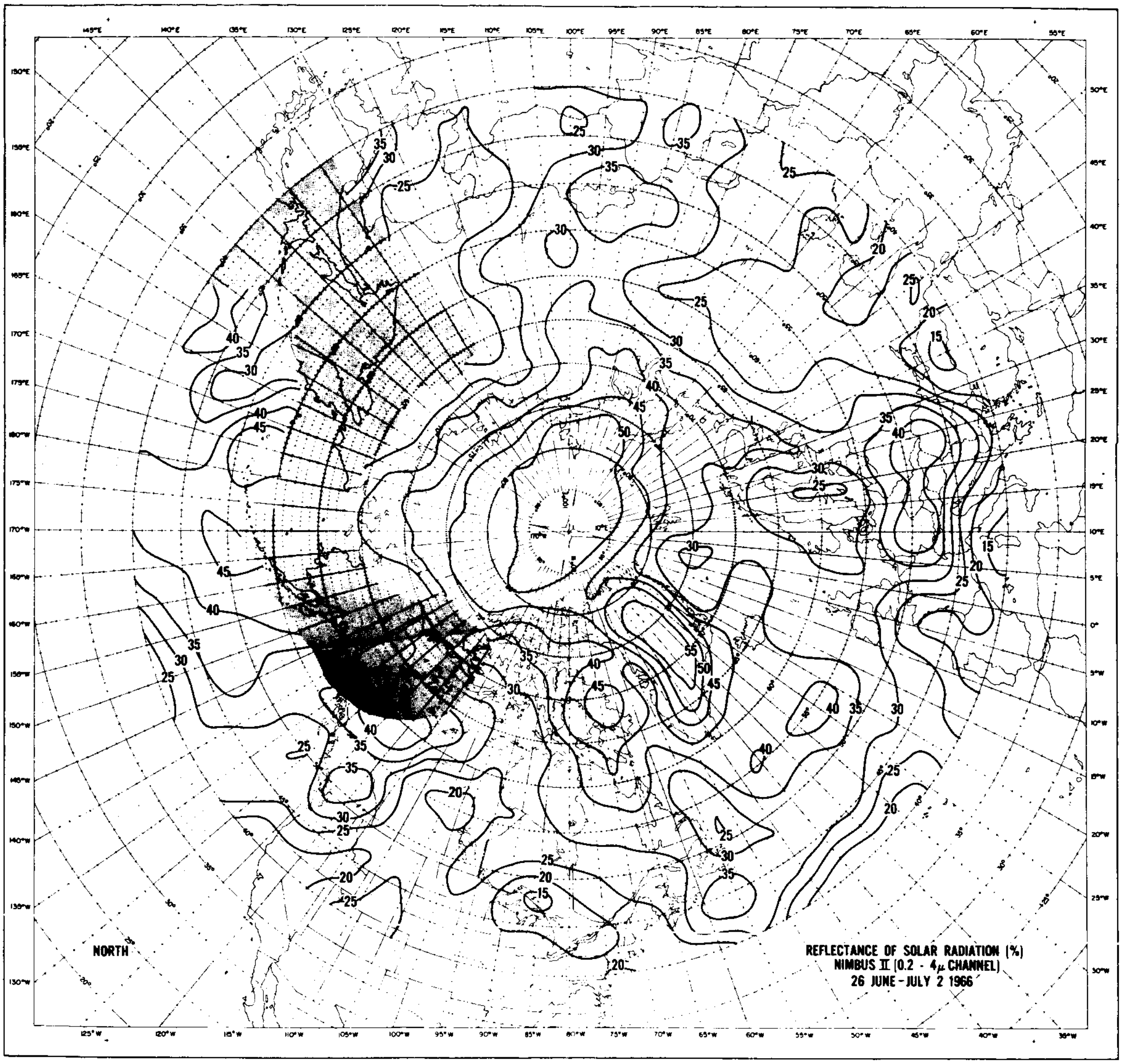
NORTH
REFLECTANCE OF SOLAR RADIATION (%)
NIMBUS II (0.2 - 4μ CHANNEL)
26 JUNE - JULY 2 1966

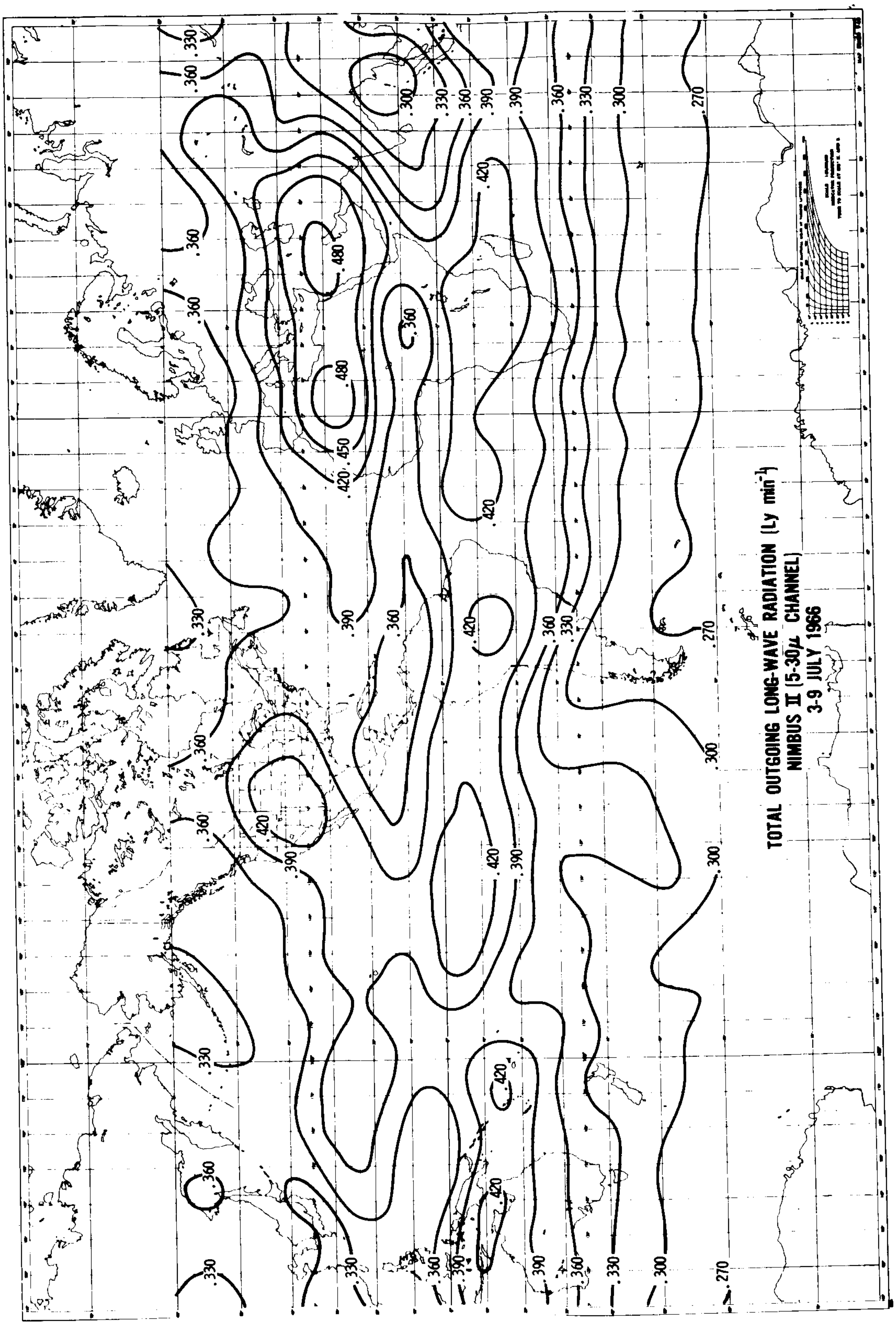

TOTAL OUTGOING LONG-WAVE RADIATION (Ly min^{-1})
NIMBUS II (5-30μ CHANNEL)
3-9 JULY 1966

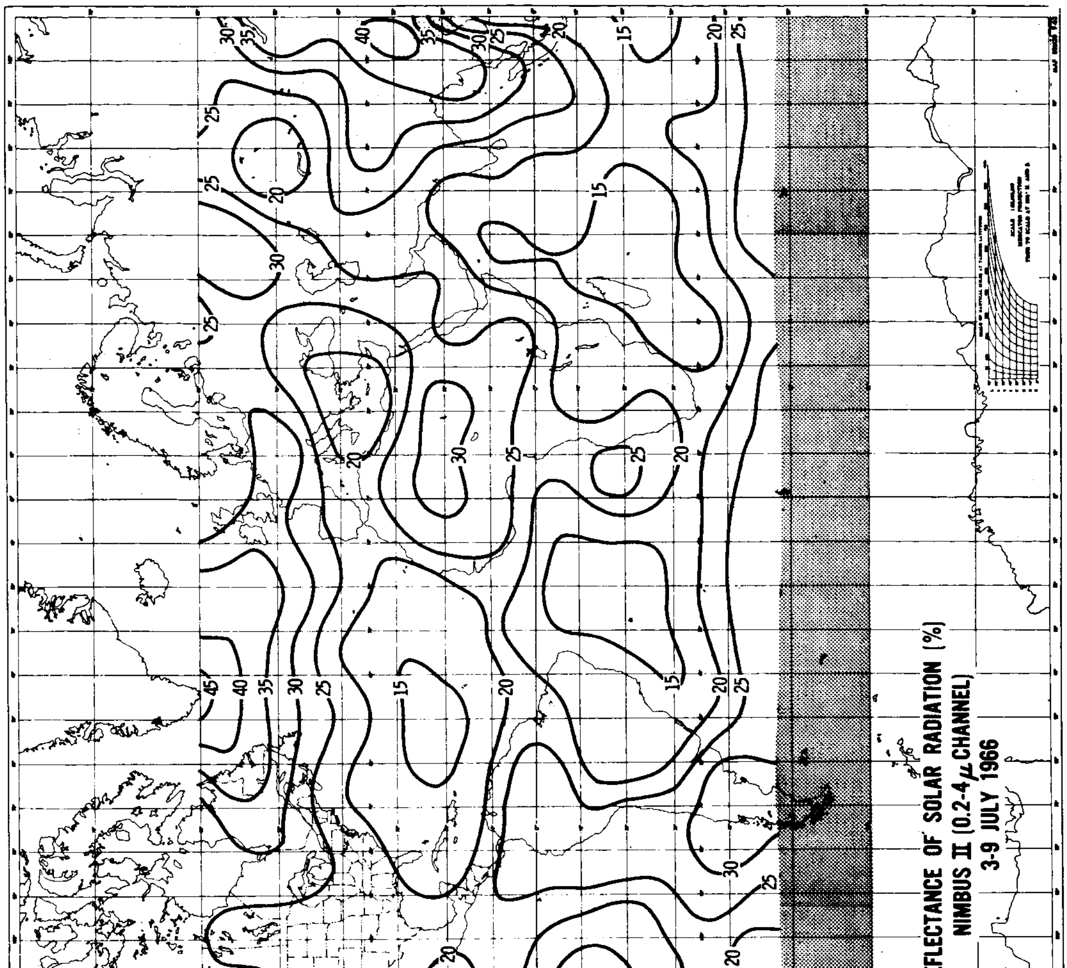

REFLECTANCE OF SOLAR RADIATION (%)
NIMBUS II (0.2-4 μ CHANNEL)
3-9 JULY 1966

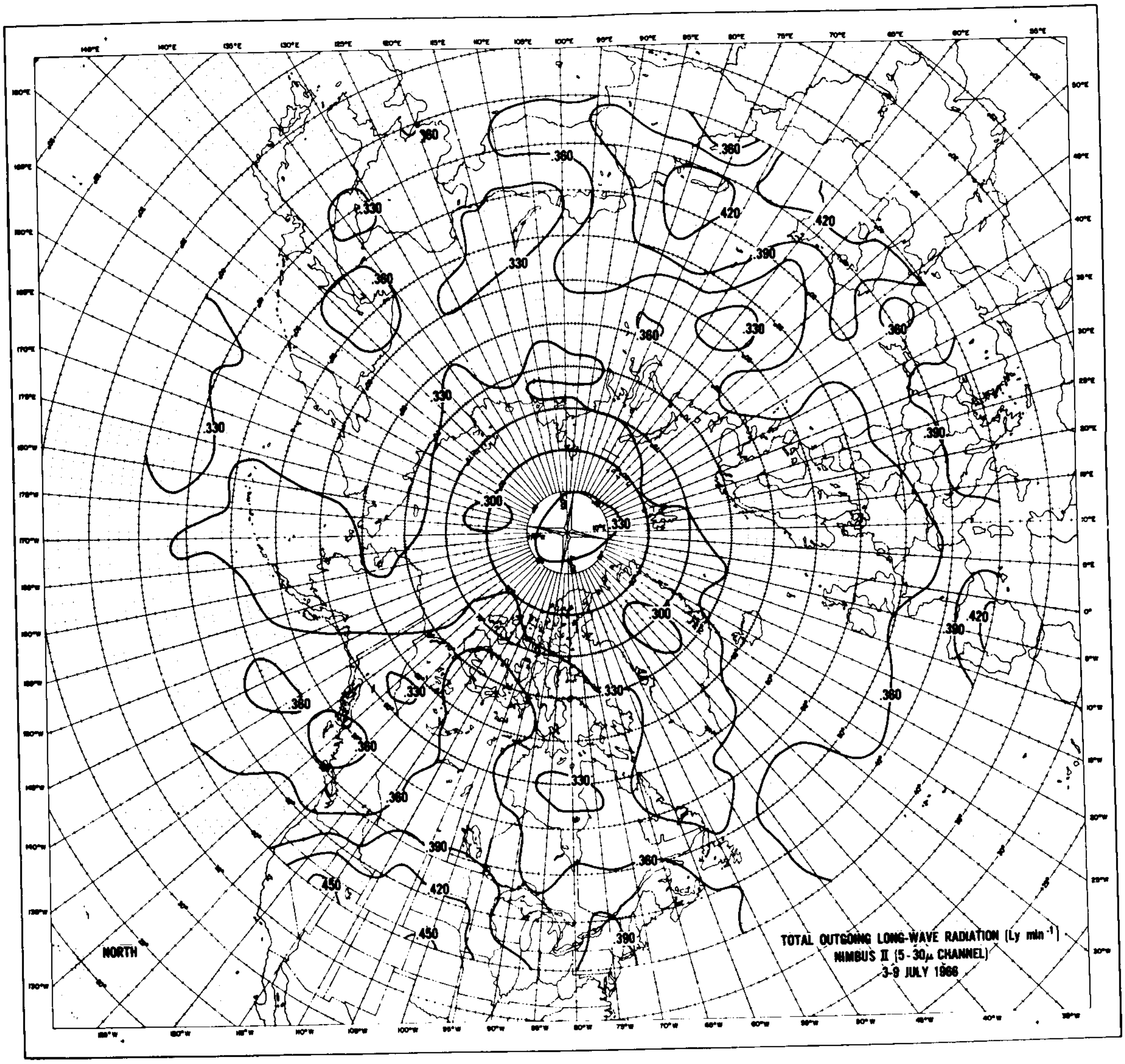
TOTAL OUTGOING LONG-WAVE RADIATION (Ly min^{-1})
NIMBUS II (5-30μ CHANNEL)
3-9 JULY 1966
NORTH
.300
.330
.360
.390
420
.450

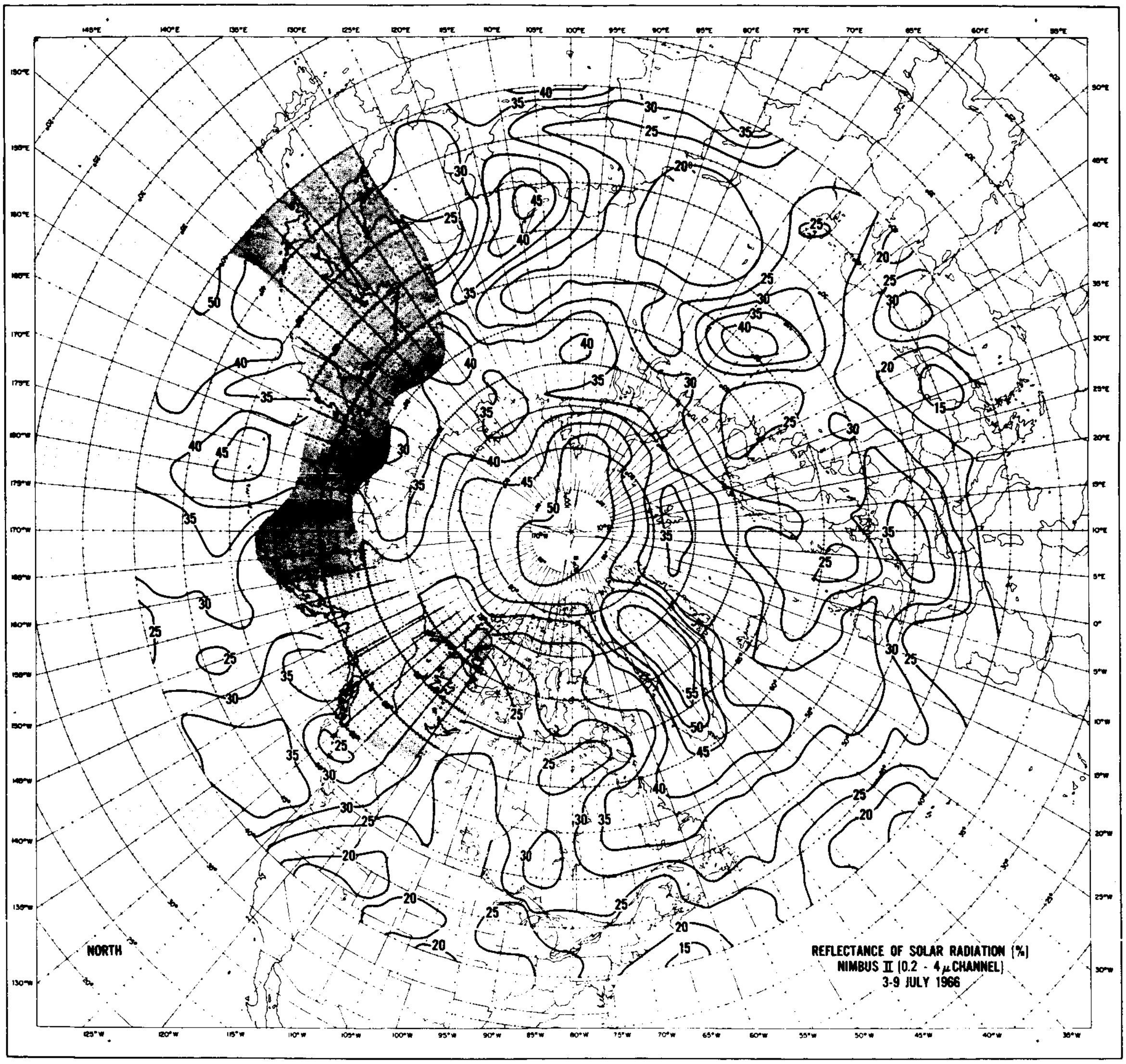
NORTH
REFLECTANCE OF SOLAR RADIATION (%)
NIMBUS II (0.2 - 4 μ CHANNEL)
3-9 JULY 1966

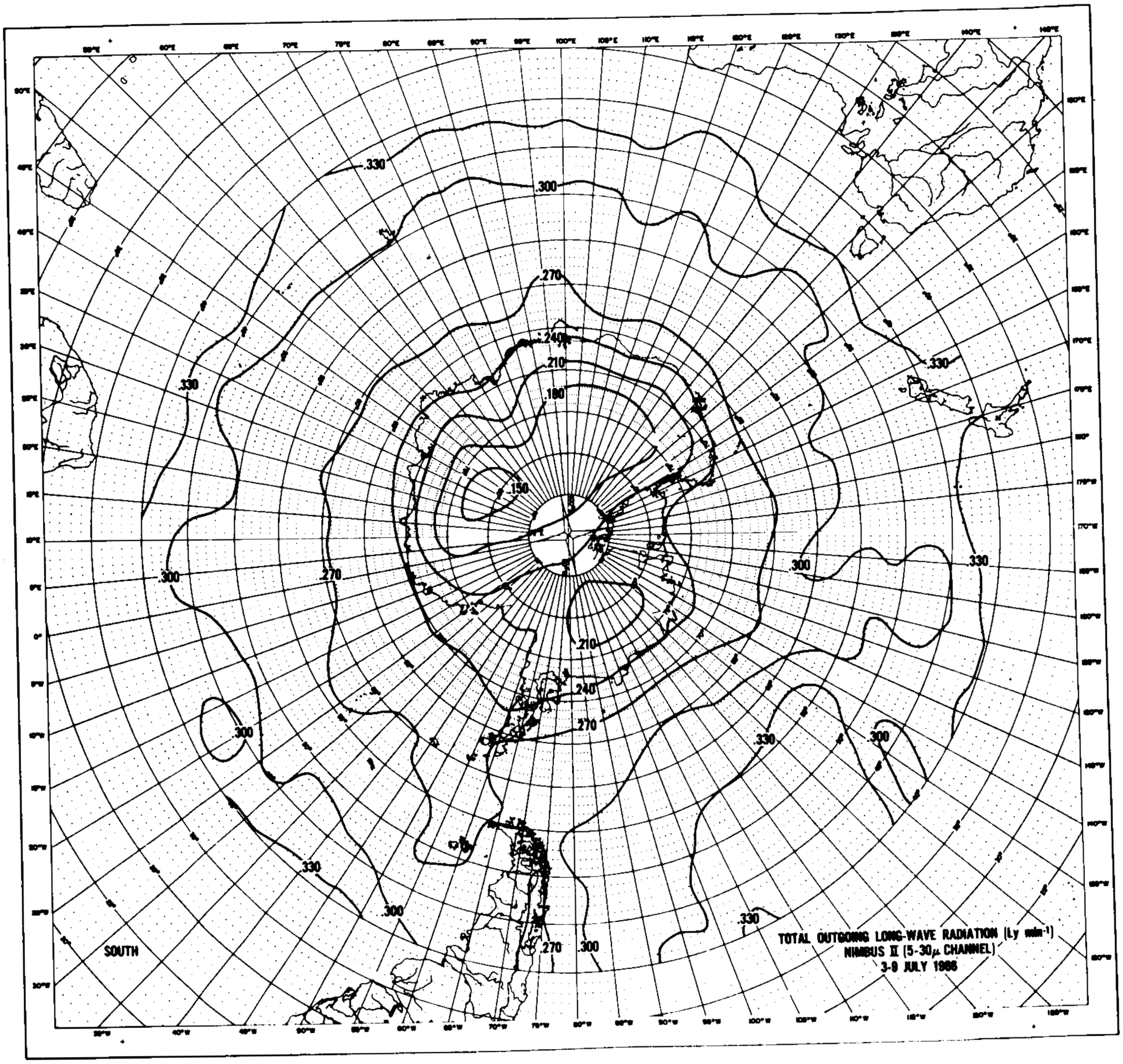
TOTAL OUTGOING LONG-WAVE RADIATION (Ly min-1)
NIMBUS II (5-30μ CHANNEL)
3-9 JULY 1966
SOUTH
.330
.300
.270
.240
.210
.180
.150

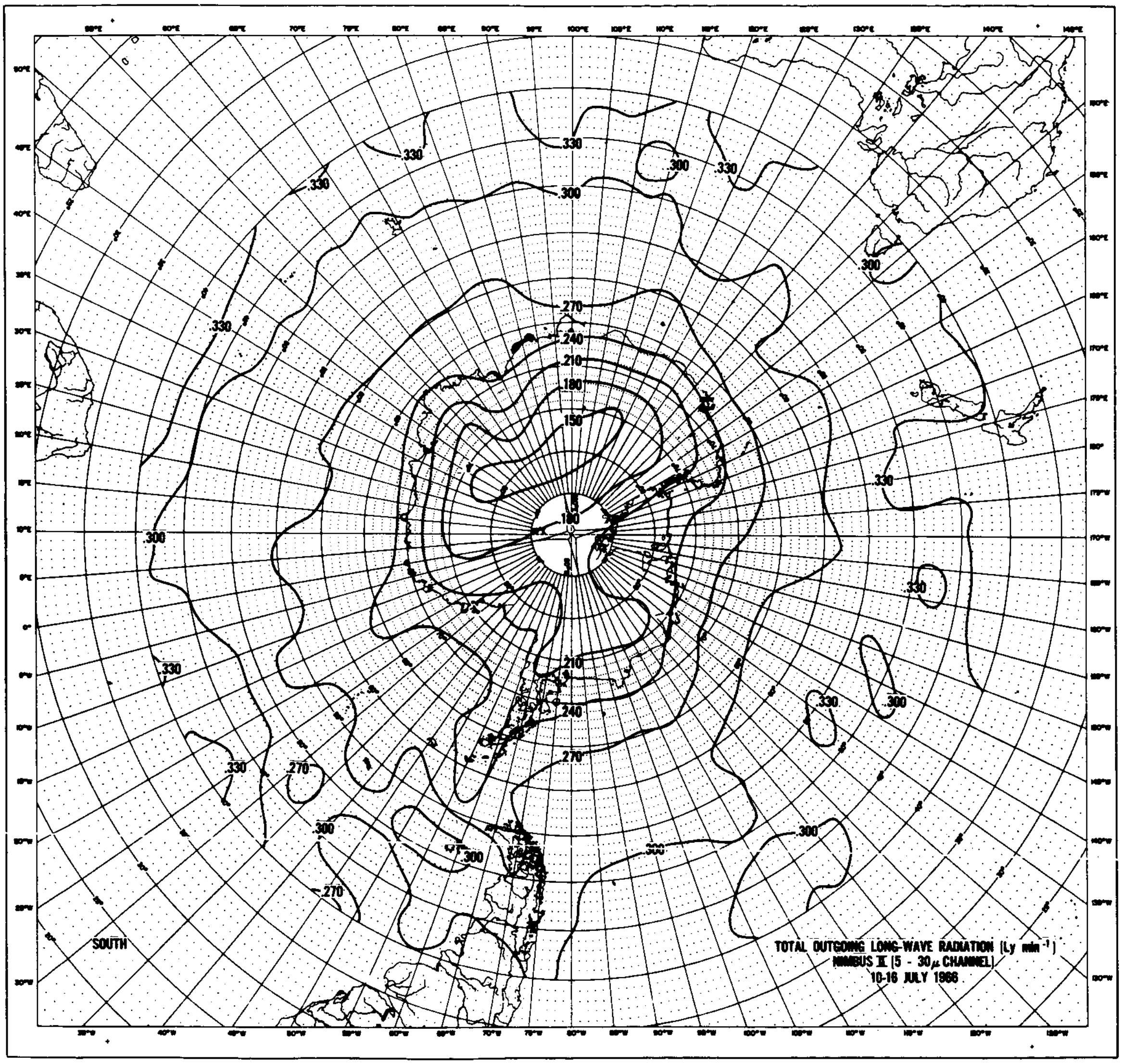

SOUTH
TOTAL OUTGOING LONG-WAVE RADIATION (Ly min⁻¹)
NIMBUS II (5 - 30μ CHANNEL)
10-16 JULY 1966

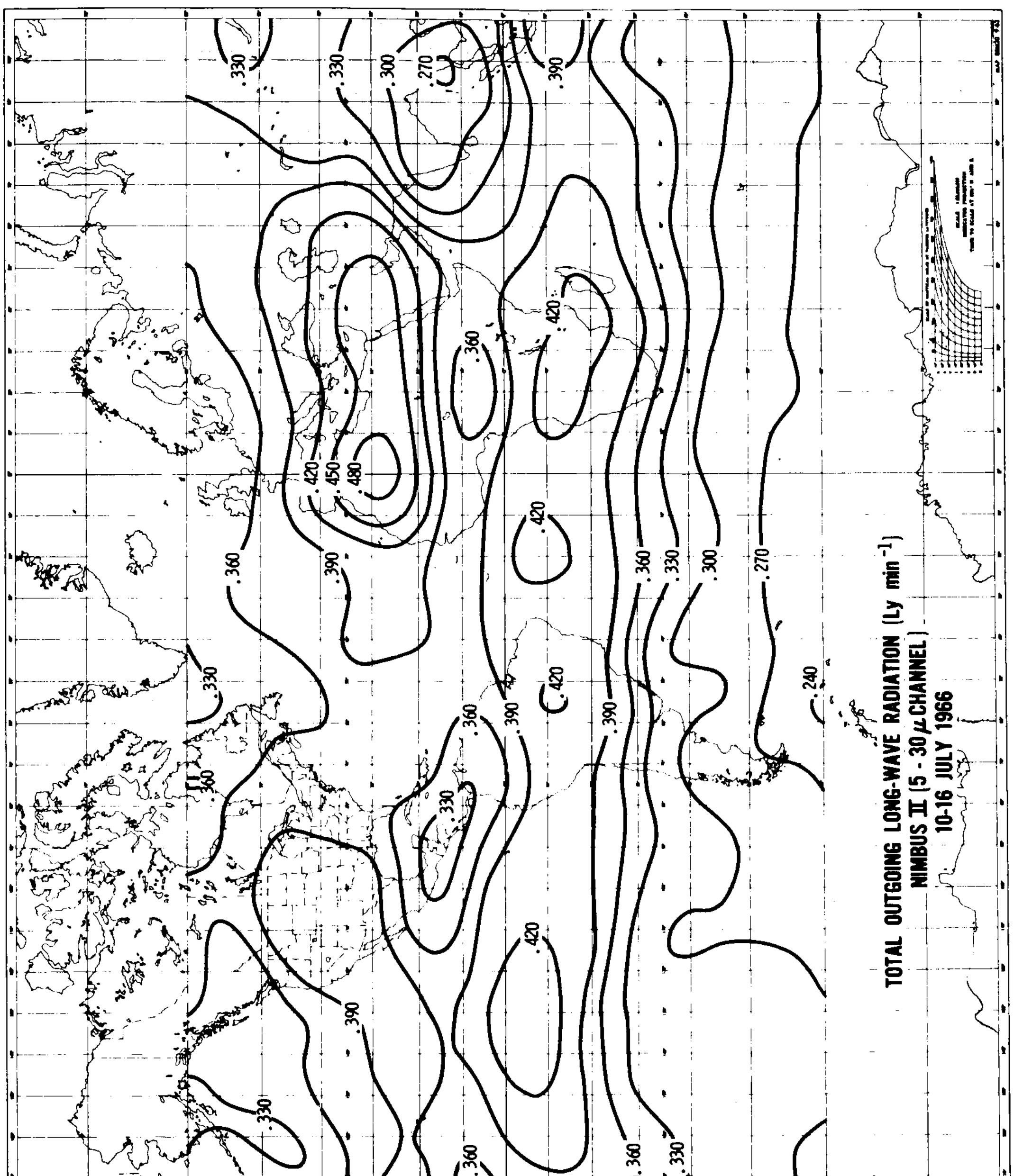

TOTAL OUTGOING LONG-WAVE RADIATION (Ly min^{-1})
NIMBUS II (5 - 30 μ CHANNEL)
10-16 JULY 1966

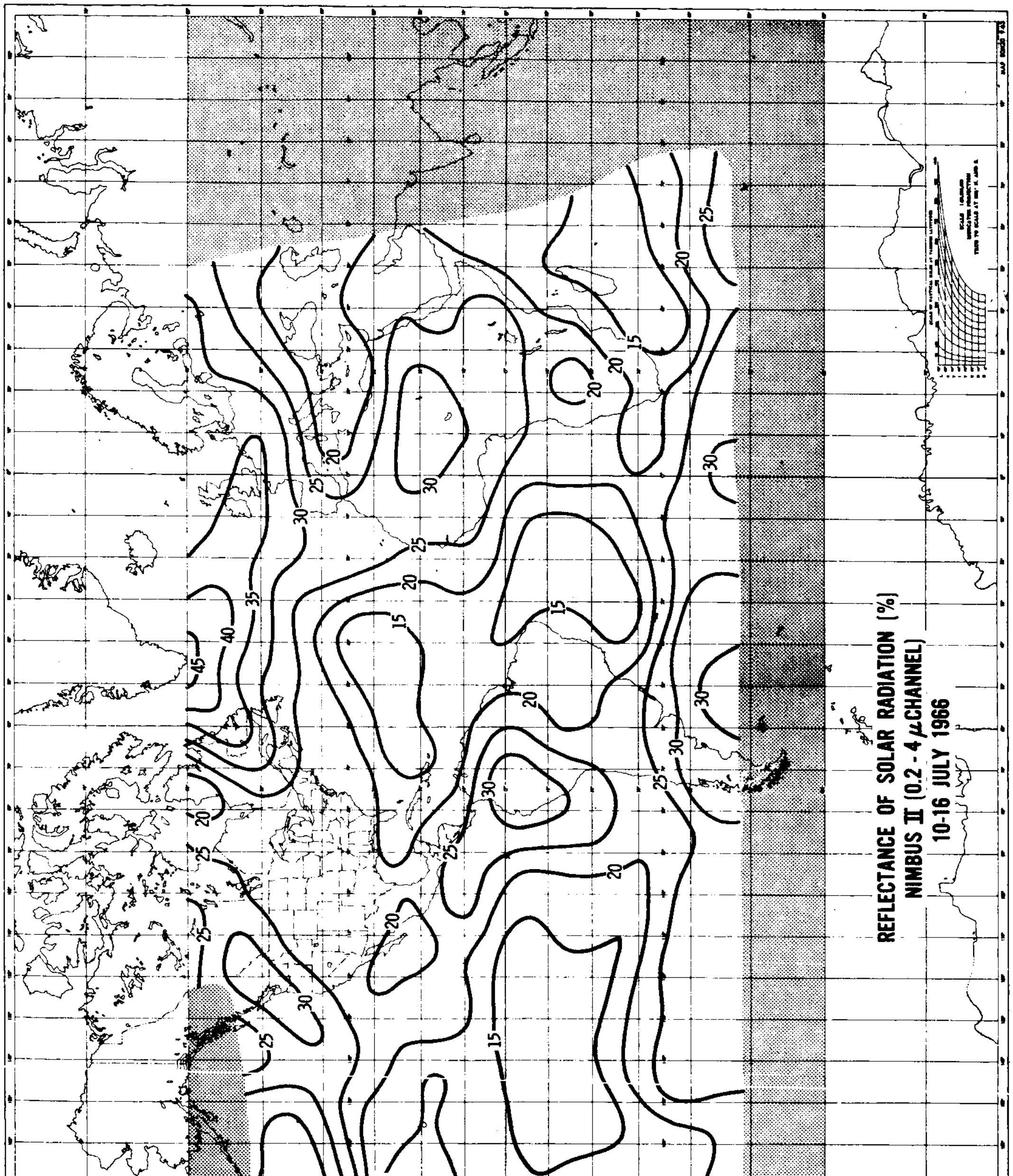

REFLECTANCE OF SOLAR RADIATION (%)
NIMBUS II (0.2 - 4 μ CHANNEL)
10-16 JULY 1966

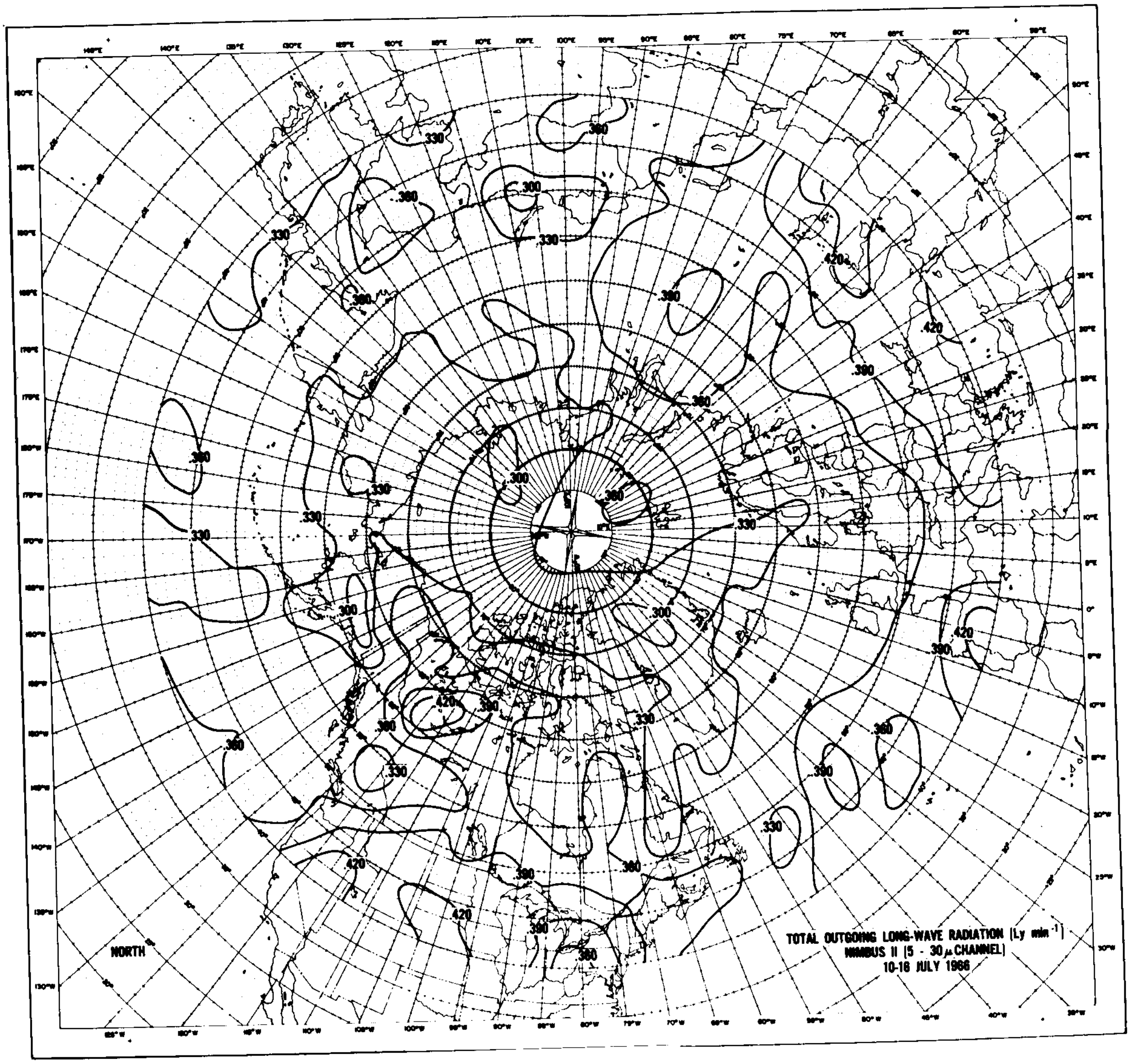
NORTH
TOTAL OUTGOING LONG-WAVE RADIATION (Ly min⁻¹)
NIMBUS II (5 - 30μ CHANNEL)
10-16 JULY 1966

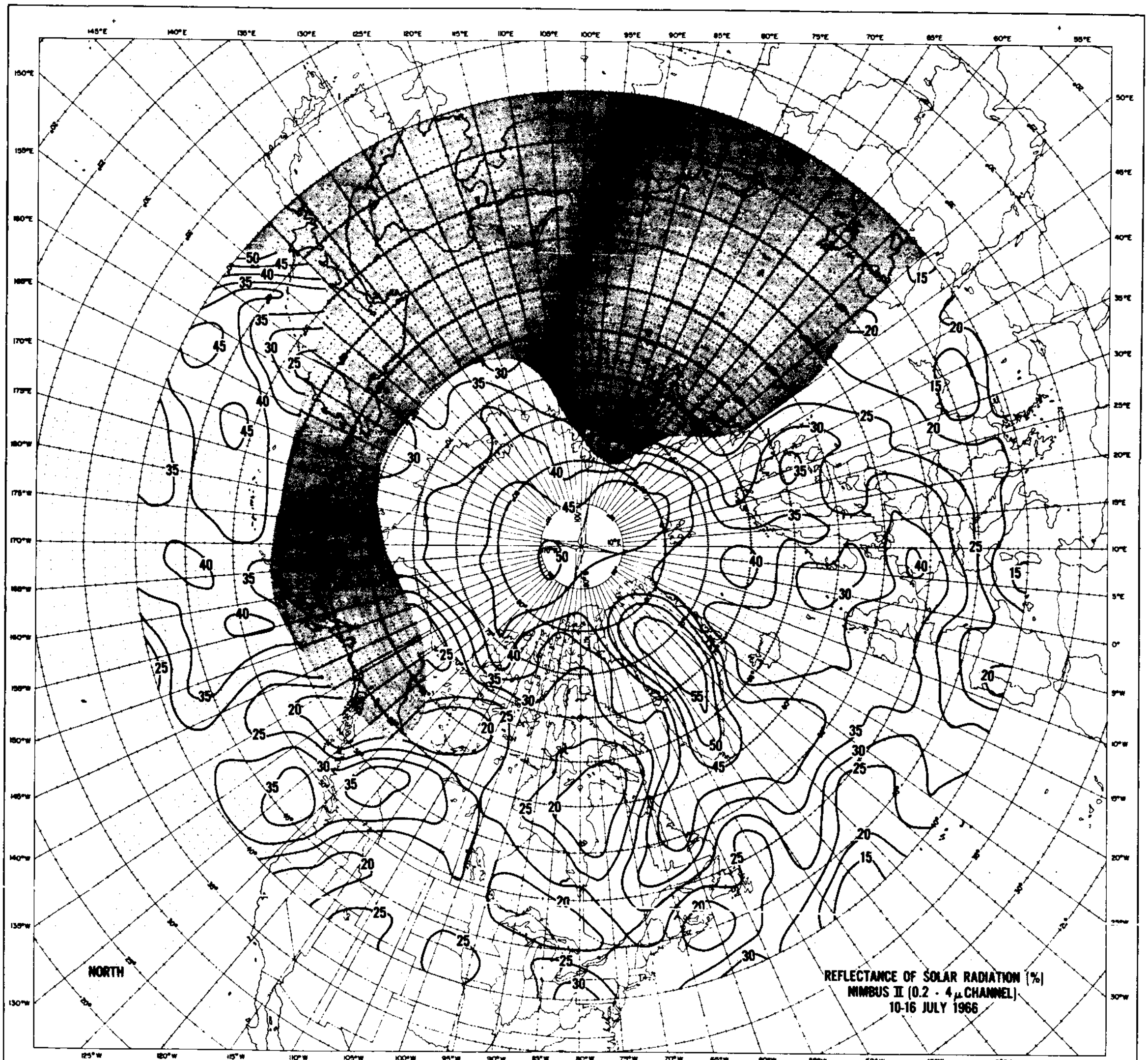
NORTH
REFLECTANCE OF SOLAR RADIATION (%)
NIMBUS II (0.2 - 4 μ CHANNEL)
10-16 JULY 1966

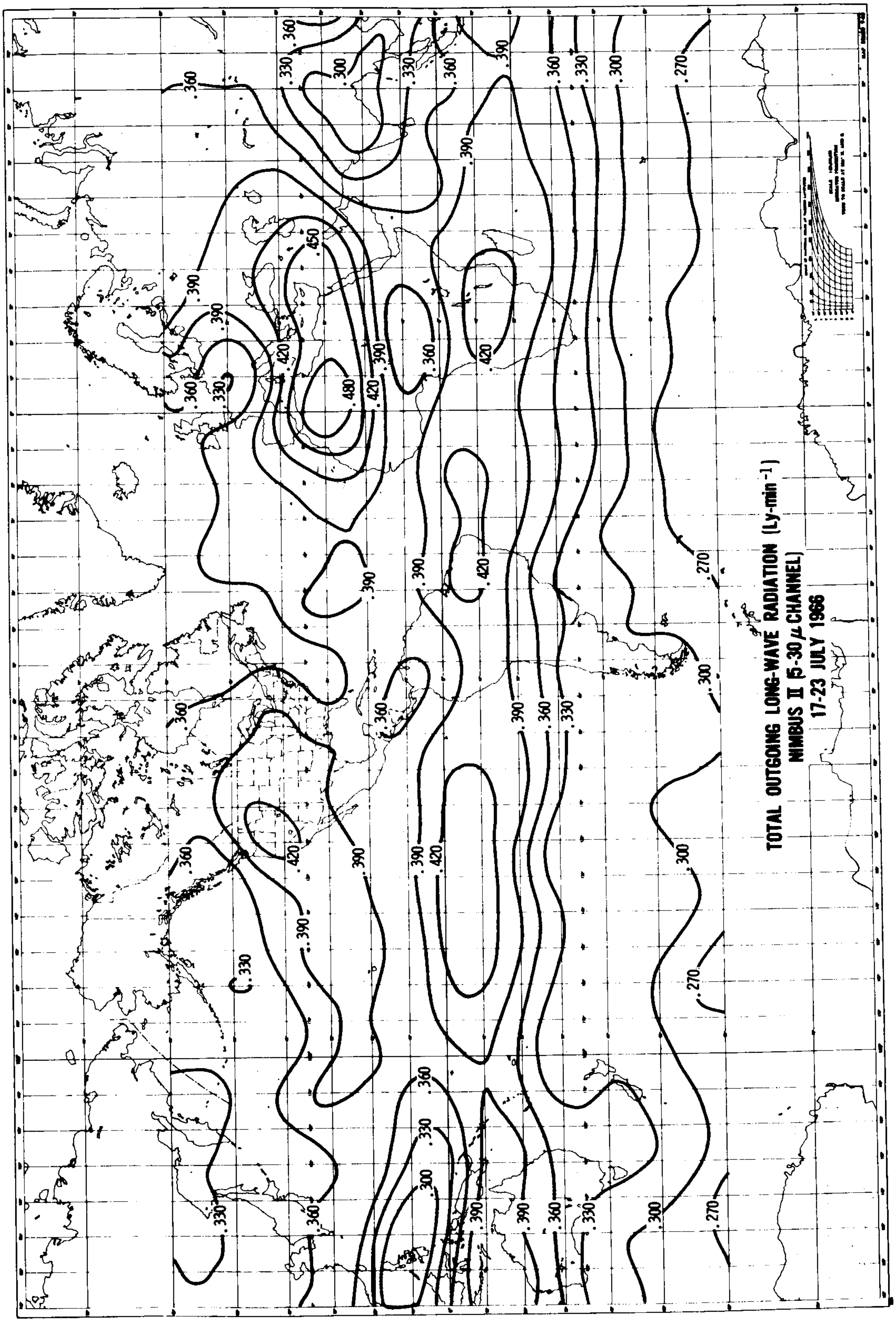

TOTAL OUTGOING LONG-WAVE RADIATION (Ly-min^{-1})
NIMBUS II (5-30 μ CHANNEL)
17-23 JULY 1966

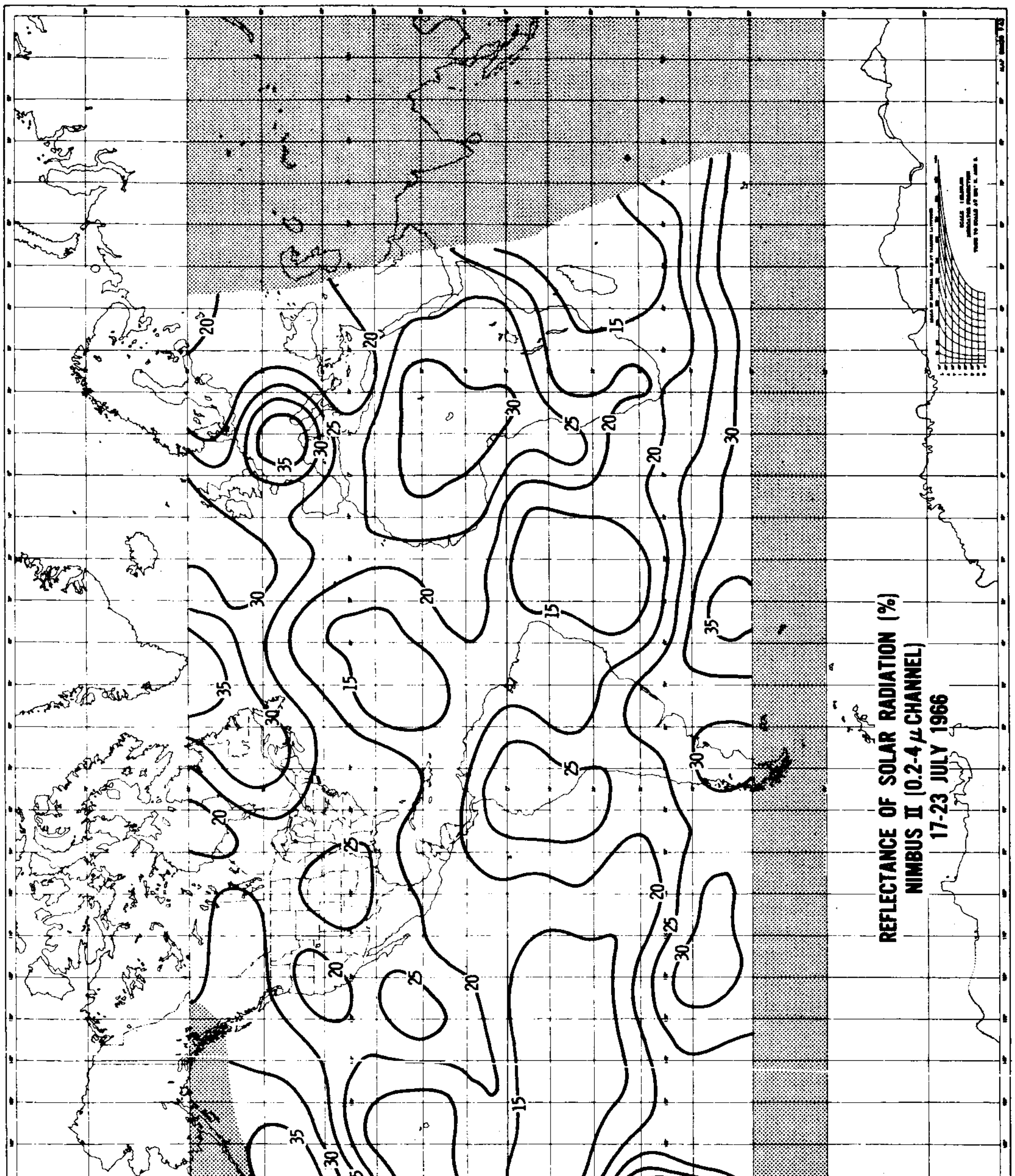

REFLECTANCE OF SOLAR RADIATION (%)
NIMBUS II (0.2-4 μ CHANNEL)
17-23 JULY 1966

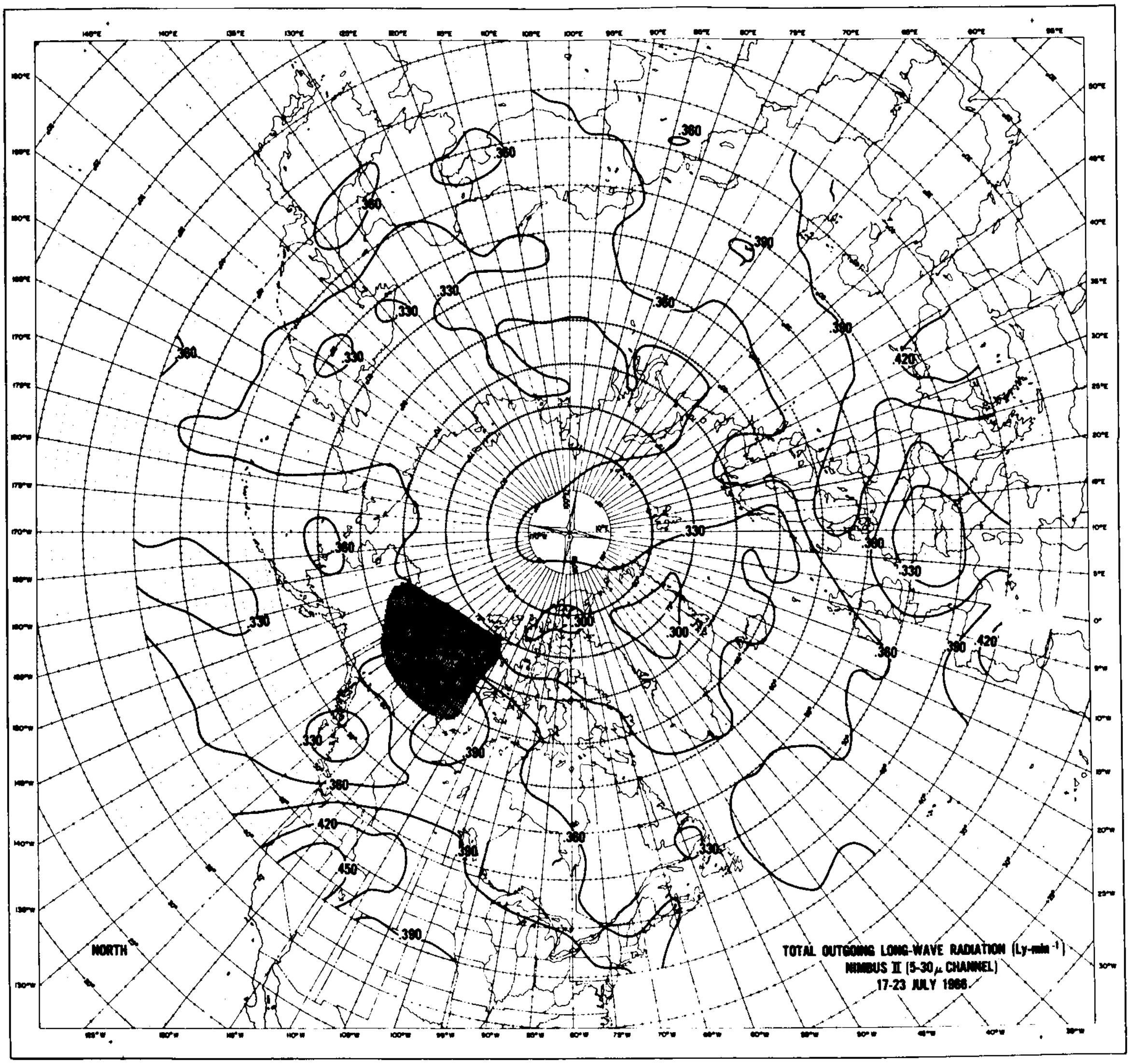
NORTH
TOTAL OUTGOING LONG-WAVE RADIATION (Ly-min⁻¹)
NIMBUS II (5-30μ CHANNEL)
17-23 JULY 1966

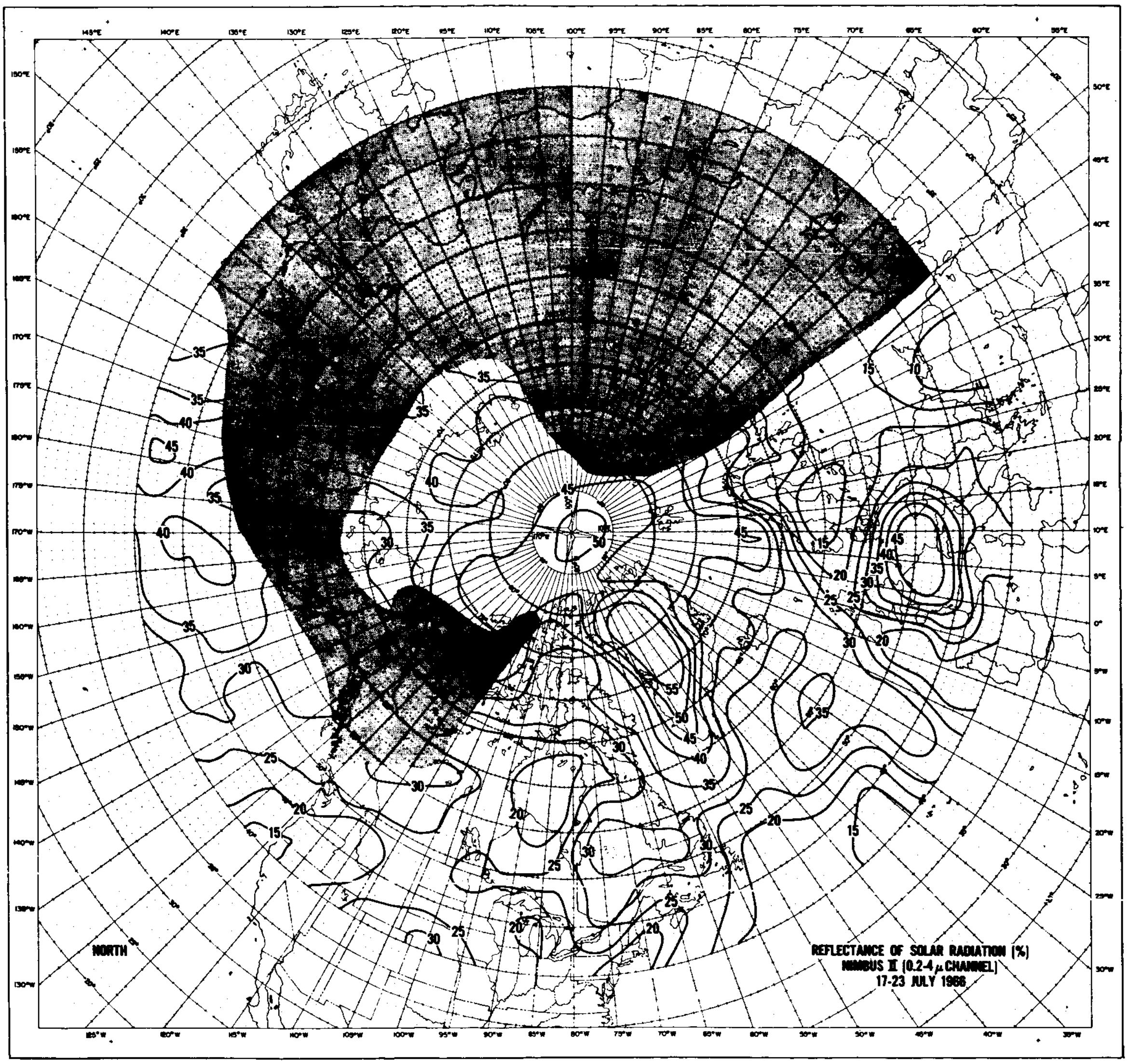
NORTH
REFLECTANCE OF SOLAR RADIATION (%)
NIMBUS II (0.2-4 μ CHANNEL)
17-23 JULY 1966

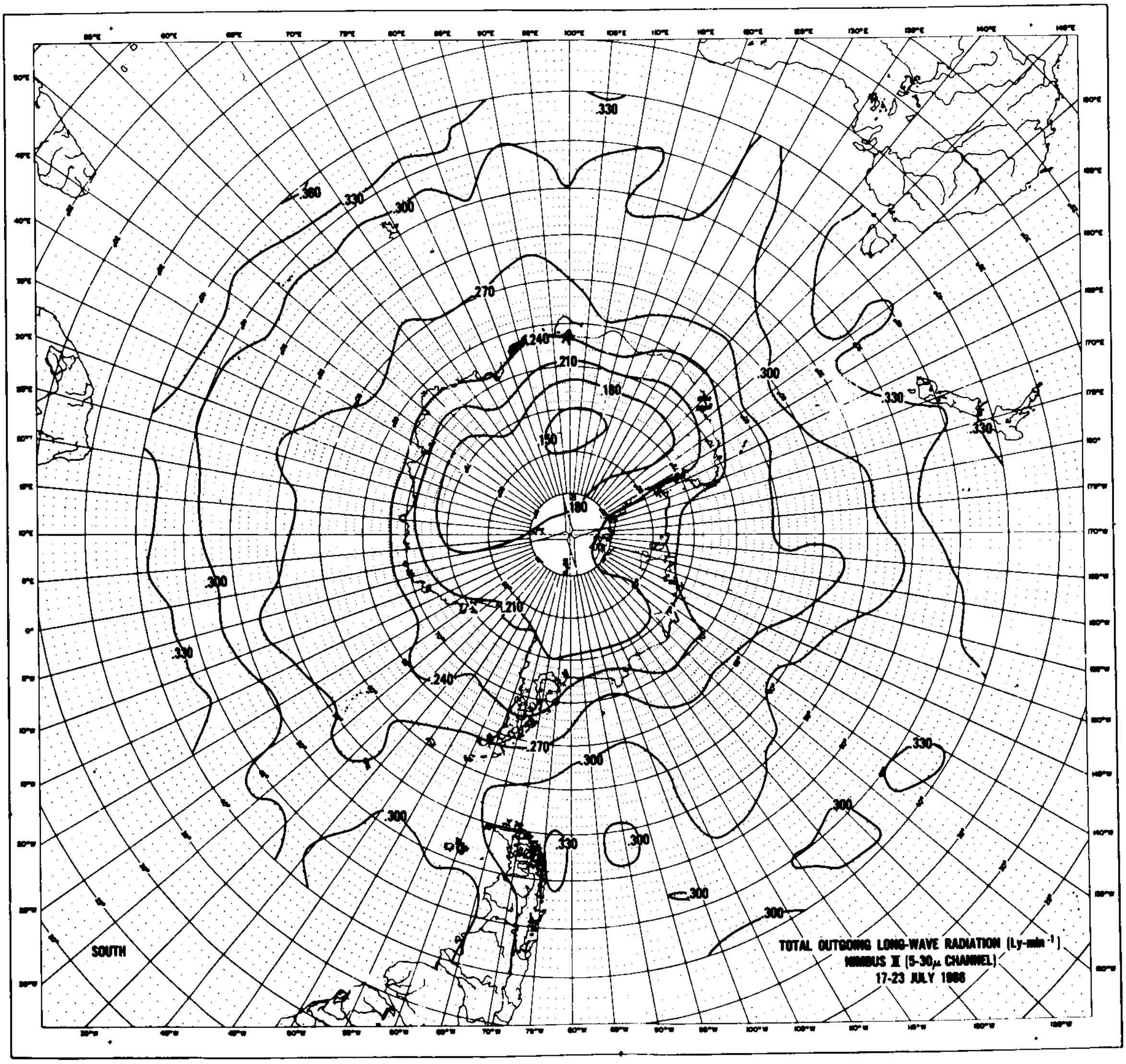

TOTAL OUTGOING LONG-WAVE RADIATION (Ly-min⁻¹)
NIMBUS II (5-30μ CHANNEL)
17-23 JULY 1966
SOUTH
.330
.300
.270
.240
.210
.180
.150

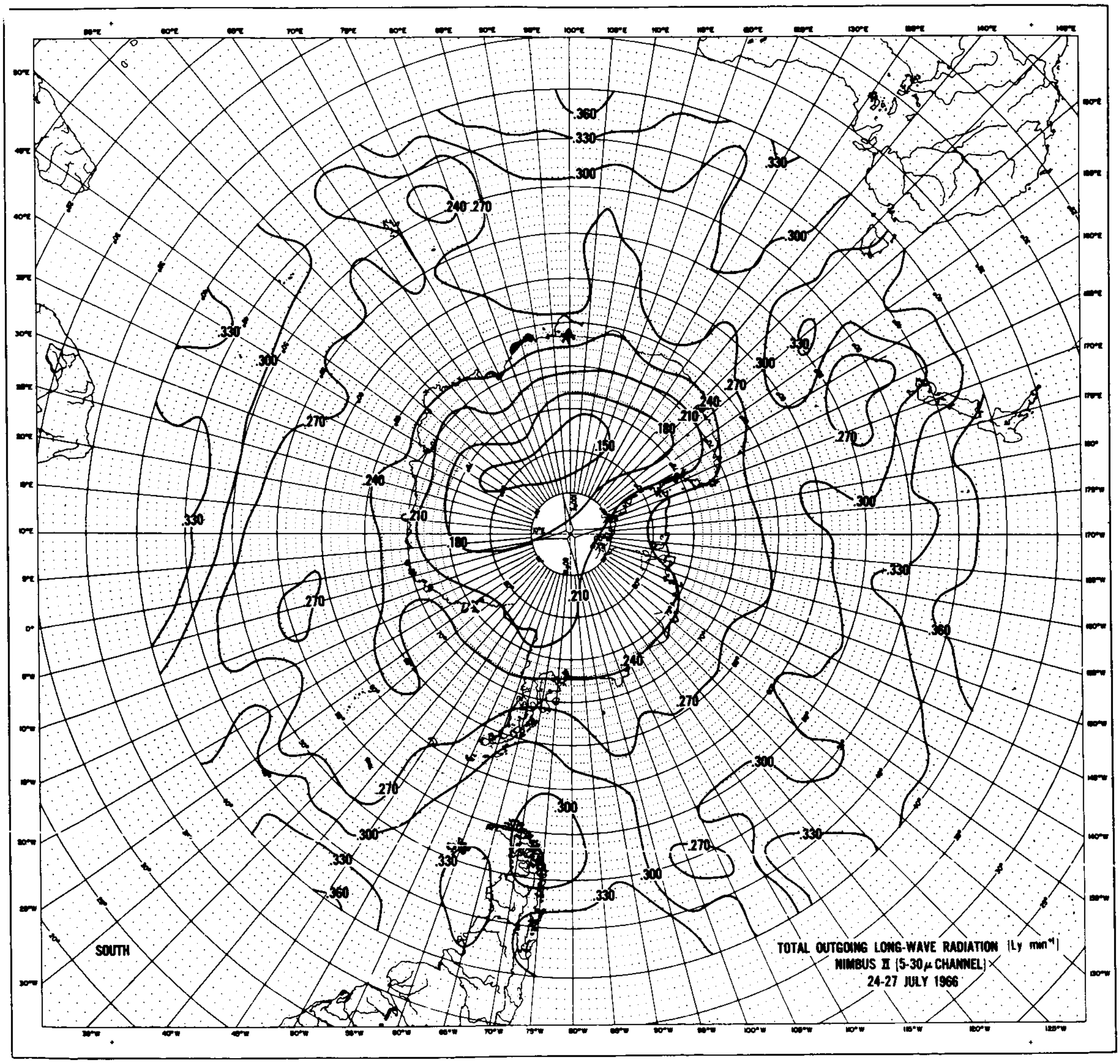
.360
.330
.300
240
.270
.150
.180
.210
.240
SOUTH
TOTAL OUTGOING LONG-WAVE RADIATION (Ly min⁻¹)
NIMBUS II (5-30μ CHANNEL)
24-27 JULY 1966

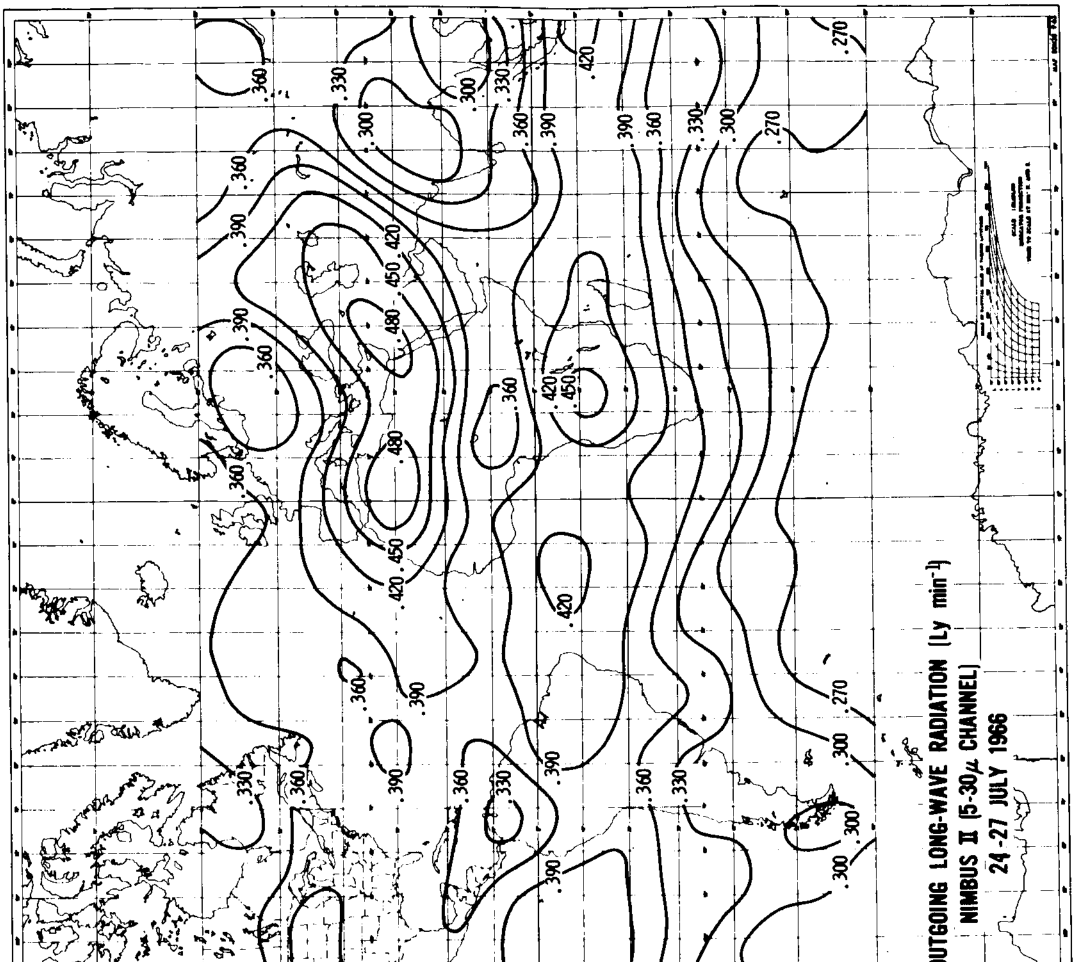

TOTAL OUTGOING LONG-WAVE RADIATION (Ly min^{-1})
NIMBUS II (5-30μ CHANNEL)
24-27 JULY 1966

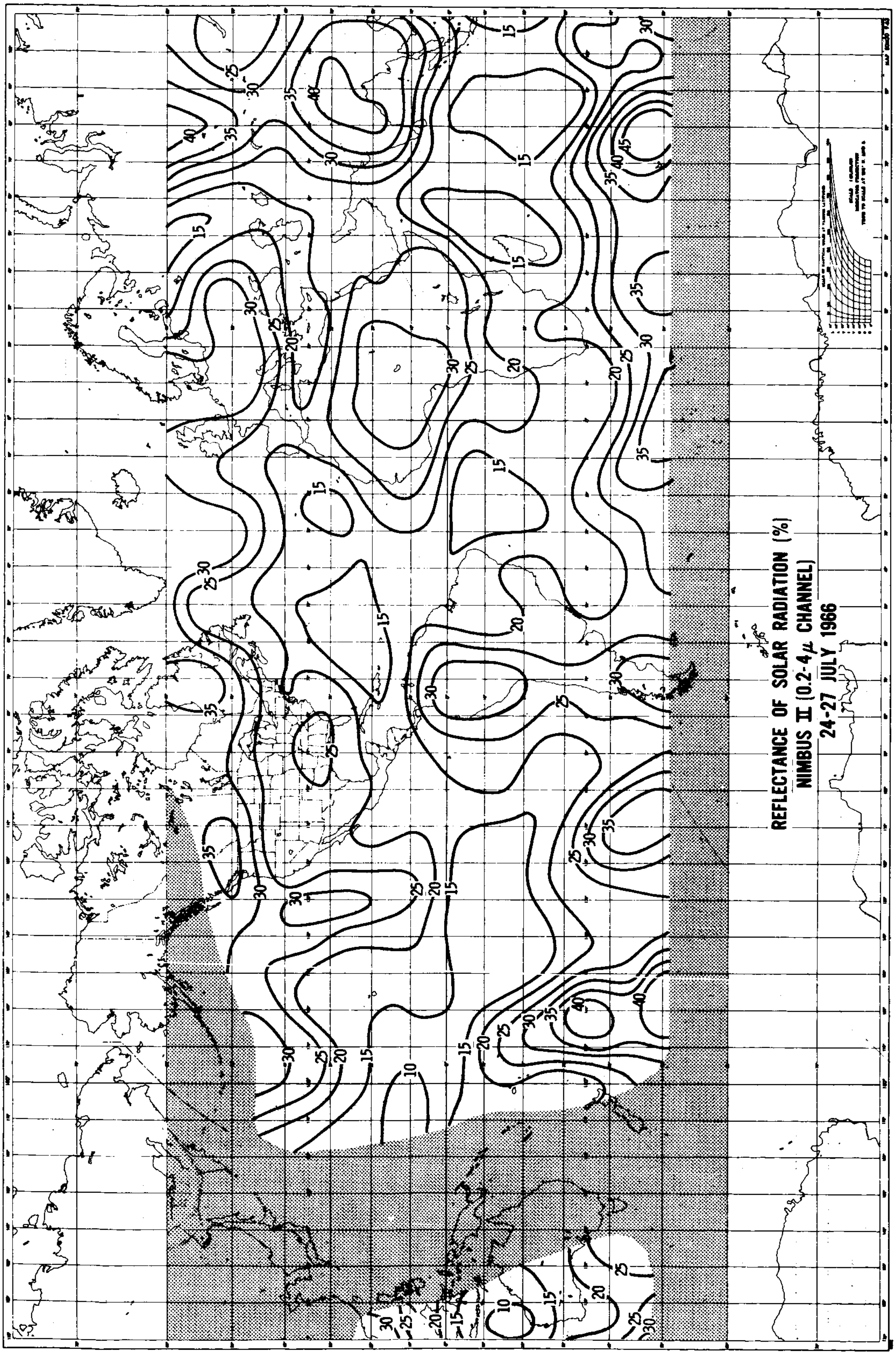

REFLECTANCE OF SOLAR RADIATION (%)
NIMBUS II (0.2-4μ CHANNEL)
24-27 JULY 1966

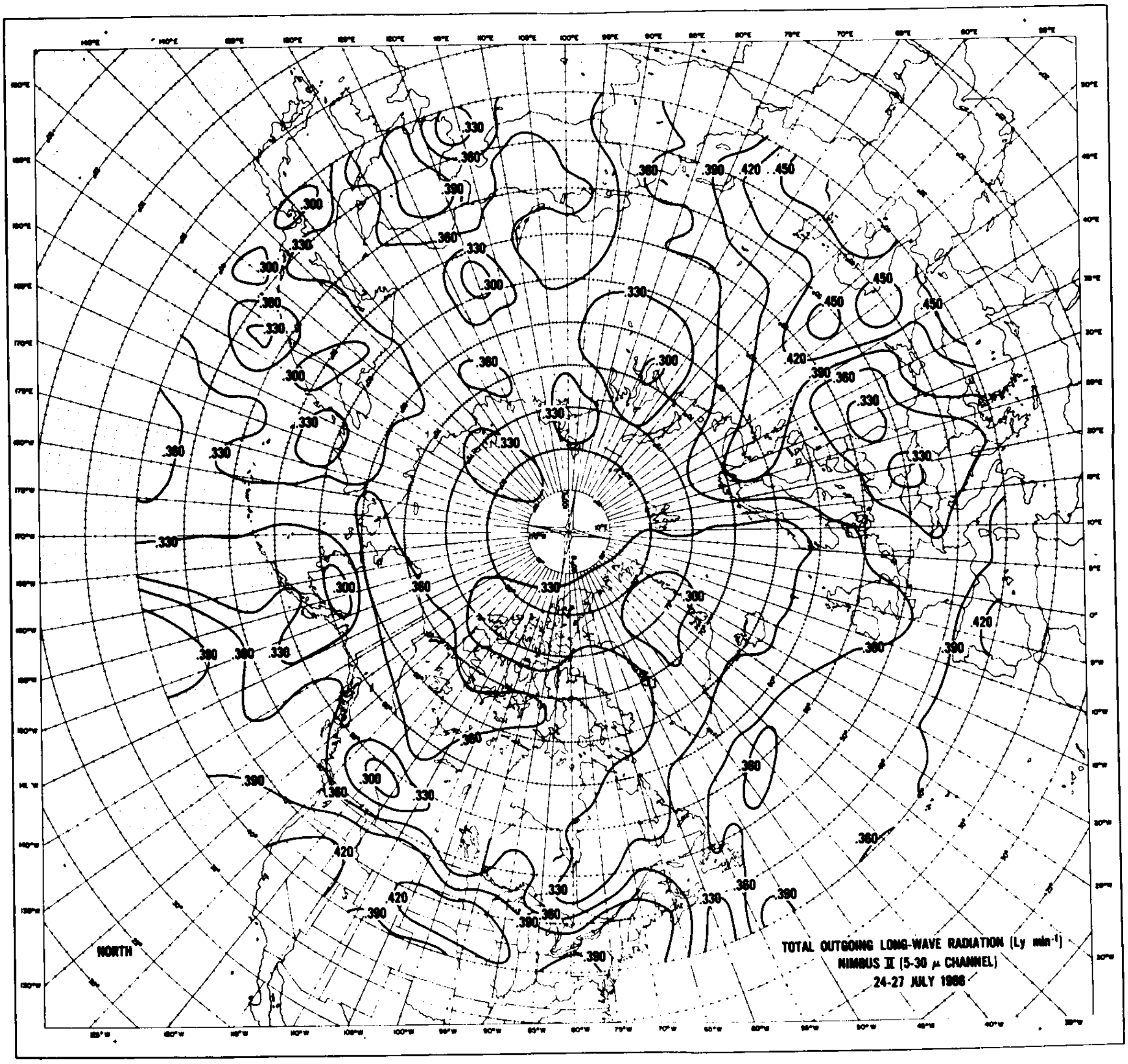
NORTH
TOTAL OUTGOING LONG-WAVE RADIATION (Ly min-1)
NIMBUS II (5-30 μ CHANNEL)
24-27 JULY 1966

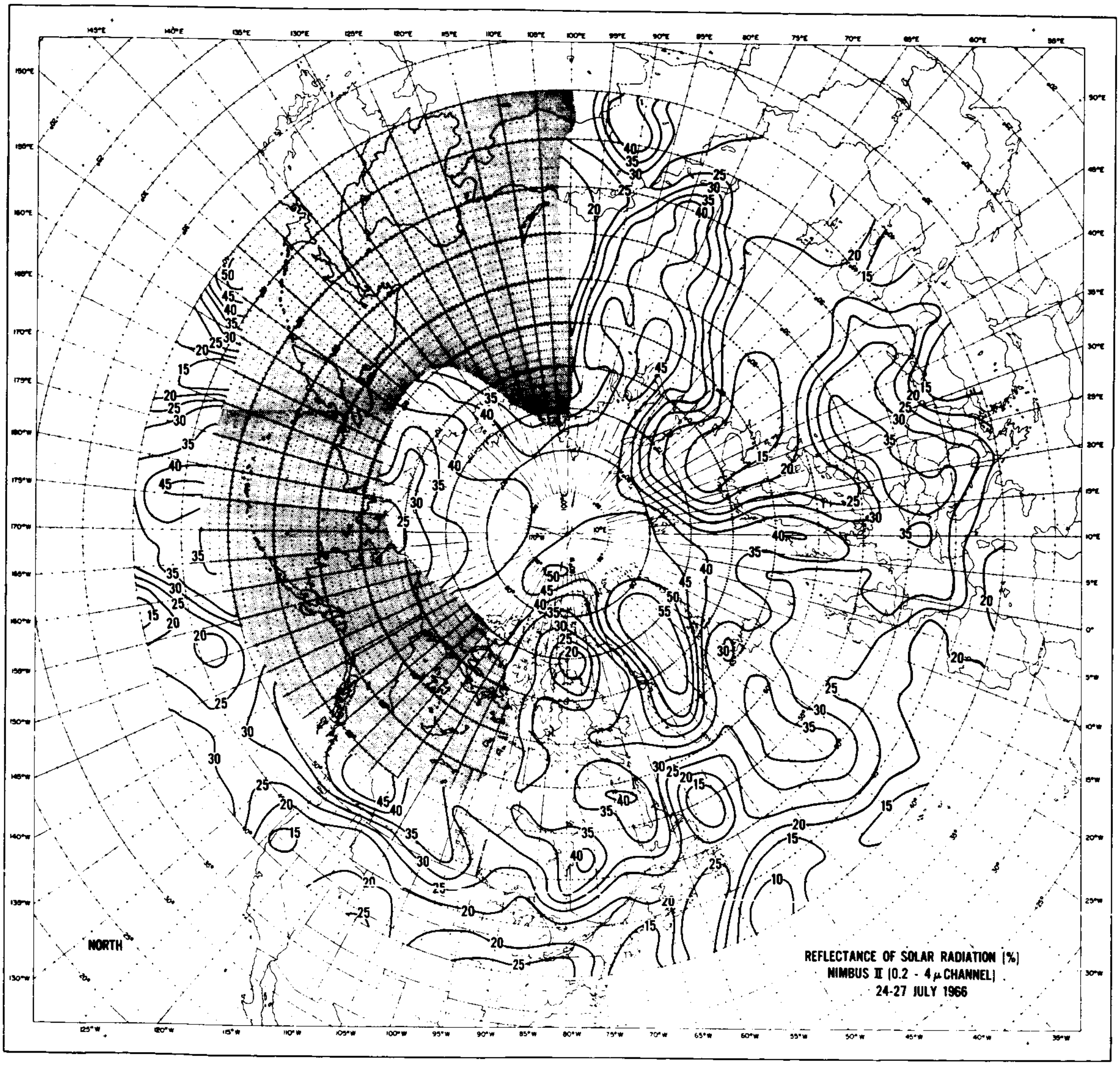
NORTH
REFLECTANCE OF SOLAR RADIATION (%)
NIMBUS II (0.2 - 4 μ CHANNEL)
24-27 JULY 1966